



HAL
open science

Sensorimotor integration in the moving spinal cord

Steven Knafo

► **To cite this version:**

Steven Knafo. Sensorimotor integration in the moving spinal cord. *Neurons and Cognition [q-bio.NC]*. Université Pierre et Marie Curie - Paris VI, 2015. English. NNT : 2015PA066559 . tel-01330942

HAL Id: tel-01330942

<https://theses.hal.science/tel-01330942>

Submitted on 13 Jun 2016

HAL is a multi-disciplinary open access archive for the deposit and dissemination of scientific research documents, whether they are published or not. The documents may come from teaching and research institutions in France or abroad, or from public or private research centers.

L'archive ouverte pluridisciplinaire **HAL**, est destinée au dépôt et à la diffusion de documents scientifiques de niveau recherche, publiés ou non, émanant des établissements d'enseignement et de recherche français ou étrangers, des laboratoires publics ou privés.

Université Pierre et Marie Curie
Ecole doctorale Cerveau Cognition Comportement (ED3C)

Institut du Cerveau et de la Moelle épinière (ICM)
Equipe du Dr. C. Wyart

Sensorimotor integration in the moving spinal cord

Intégration sensorimotrice dans la moelle épinière en mouvement

Steven KNAFO

Thèse de doctorat de Neurosciences

Présentée et soutenue publiquement le 29 septembre 2015

Directeur de thèse : Pr Hugues Pascal-Mousselard (PU-PH, UPMC)

Chef d'équipe : Dr Claire Wyart (CR1, Inserm)

Rapporteur : Dr Florian Engert (Professor, Harvard University)

Rapporteur : Dr Wenchang Li (Research fellow, University of St Andrews)

Examineur : Pr Fabrice Parker (PU-PH, Université Paris Sud)

Examineur : Pr Philippe Cornu (PU-PH, UPMC)



Except where otherwise noted, this work is licensed under
<http://creativecommons.org/licenses/by-nc-nd/3.0/>

Remerciements / Acknowledgments

Au terme de ce travail, je souhaiterais remercier tous ceux qui ont permis sa réalisation, et en premier lieu le Pr Hugues Pascal-Mousselard et le Dr Claire Wyart qui ont soutenu et accompagné ce projet depuis le départ. Merci Hugues pour ta curiosité, ta simplicité, pour toujours trouver un moment pour discuter malgré tes responsabilités hospitalières. Claire, ton dévouement au quotidien pour ton équipe, ta bonne humeur et ta capacité à gérer tant de choses à la fois m'impressionnent chaque jour : bravo d'avoir réussi à construire ce labo où chacun peut s'épanouir, c'est un plaisir de voir chaque projet éclore au fur et à mesure...

I would also like to thank the members of my jury, and in particular Dr Florian Engert and Dr Wenchang Li for accepting to report on the thesis and to come to Paris for the defense: your research papers have been a source of inspiration and challenge throughout my PhD journey. Je remercie aussi les Pr Fabrice Parker et Philippe Cornu pour avoir encouragé mes projets de recherche tout au long de mon internat de neurochirurgie, pour leur ouverture d'esprit et leur écoute attentive.

Merci à tous les membres du labo qui ont rendu ce travail possible en y contribuant de près ou de plus loin : Charlie, for your dedication from the very first day until the last, I'm sure you'll make a great doctor and researcher! – Alexandre, pour ton dynamisme, ta curiosité, et tes bonnes idées – Kevin, pour tes conseils avisés et pour m'avoir laissé gagner au *Killer* ;-)) – Andy, for your molecular biology recipes but even more for being patient enough to walk me through them (several times!) – Urs, for your amazing geeky skills and for being the perfect bedmate (several times!) – Lydia, pour ton écoute, ta patience et ton t-shirt Bob l'éponge – Kris, for your permanent joy of life and for making me watch GoT – Jeff, for demonstrating that one can love guns and be so relax – Jenna, for putting Chopin in the spinning room instead of Kevin's Maroon 5 – Pierre-Luc, pour écouter France Culture en compagnie de bons fromages – Laura, pour toujours savoir où ça se trouve dans le freezer – Sophie, pour ta boîte à kiwi et ton étui à banane – Natalia et Bogdan, pour décapsuler avec le sourire malgré l'odeur – et à tous ceux qui rendent l'ICM tellement plus accueillant que le reste de l'hôpital...

Enfin, merci à ma famille de m'avoir accompagné à chaque instant : à mes grands-parents pour leur modestie et gentillesse, pour m'avoir demandé « comment vont tes petits poissons » chaque semaine, à mes parents pour m'avoir éduqué dans le plaisir du travail, à ma sœur et mes frères pour leur sagacité de tous les instants.

À Delphine, surtout, qui réalise chaque jour notre promesse d'avenir de la plus belle des façons.

Résumé

Certaines observations suggèrent que les afférences méchano-sensorielles peuvent moduler l'activité des générateurs centraux du rythme locomoteur (ou *Central Pattern Generators*, CPGs). Cependant, il est impossible d'explorer les circuits neuronaux sous-jacents chez l'animal en mouvement à l'aide d'enregistrements électrophysiologiques lors d'expériences de locomotion dite « fictive ». Dans cette étude, nous avons enregistré de façon sélective et non-invasive les neurones moteurs et sensoriels dans la moelle épinière pendant la locomotion active en ciblant génétiquement le senseur bioluminescent GFP-Aequorin chez la larve de poisson zèbre. En utilisant l'imagerie calcique à l'échelle des neurones individuels, nous confirmons que les signaux de bioluminescence reflètent bien le recrutement différentiel des groupes de motoneurones spinaux durant la locomotion active. La diminution importante de ces signaux chez des animaux paralysés ou des mutants immobiles démontre que le retour méchano-sensoriel augmente le recrutement des motoneurones spinaux pendant la locomotion active. En accord avec cette observation, nous montrons que les neurones méchano-sensoriels spinaux sont en effet recrutés chez les animaux en mouvement, et que leur inhibition affecte les réflexes d'échappement chez des larves nageant librement. L'ensemble de ces résultats met en lumière la contribution du retour méchano-sensoriel sur la production locomotrice et les différences qui en résultent entre les locomotions active et fictive.

Mots-clés :

GFP-Aequorin, bioluminescence, intégration sensori-motrice, locomotion, moelle épinière, poisson-zèbre

Abstract

There is converging evidence that mechanosensory feedback modulates the activity of spinal central pattern generators underlying vertebrate locomotion. However, probing the underlying circuits in behaving animals is not possible in “fictive” locomotion electrophysiological recordings. Here, we achieve selective and non-invasive monitoring of spinal motor and sensory neurons during active locomotion by genetically targeting the bioluminescent sensor GFP-Aequorin in larval zebrafish. Using GCaMP imaging of individual neurons, we confirm that bioluminescence signals reflect the differential recruitment of motor pools during motion. Their significant reduction in paralyzed animals and immotile mutants demonstrates that mechanosensory feedback enhances the recruitment of spinal motor neurons during active locomotion. Accordingly, we show that spinal mechanosensory neurons are recruited in moving animals and that their silencing impairs escapes in freely behaving larvae. Altogether, these results shed light on the contribution of mechanosensory feedback to motor output and the resulting differences between active and fictive locomotion.

Keywords:

GFP-Aequorin, bioluminescence, sensorimotor integration, locomotion, spinal cord, zebrafish

Outline

**Part A. Sensorimotor integration in the spinal cord, from behaviors to circuits:
new tools to close the loop?p.7**

Abstract

- 1 A closed-loop approach to sensorimotor behaviors.....p.9
 - 1.1. Defining sensorimotor behaviors
 - 1.1.1. Eliciting sensory input
 - 1.1.2. Measuring motor output
 - 1.2. Modulating sensorimotor behaviors
 - 1.2.1. Sensory feedback
 - 1.2.2. Neuromodulation
 - 1.3. Modeling sensorimotor behaviors
 - 1.3.1. Behavioral computations
 - 1.3.2. Circuits computations

- 2 An open-loop access: sensorimotor circuits in the spinal cord across
vertebrates.....p.17
 - 2.1. Extrinsic inputs to spinal sensorimotor circuits
 - 2.1.1. Descending motor control
 - 2.1.2. Ascending sensory feedback
 - 2.2. Intrinsic spinal sensorimotor circuitry
 - 2.2.1. Sensorimotor interneuronal networks
 - 2.2.2. Spinal central pattern generator
 - 2.3. Dynamic spinal sensorimotor interactions
 - 2.3.1. Modulation of spinal circuitry from extrinsic inputs
 - 2.3.2. Implications for plasticity after spinal cord injury

- 3 Closing the loop? Optogenetic manipulation of spinal sensorimotor circuits in
zebrafish.....p.31
 - 3.1. Genetic targeting of spinal sensorimotor circuits in zebrafish

- 3.1.1. Identified sensorimotor neurons in the zebrafish spinal cord
- 3.1.2. A genetic toolbox for targeting populations of neurons
- 3.2. Optogenetic tools for monitoring and breaking neural circuits
 - 3.2.1. Reporters: monitoring neural circuits
 - 3.2.2. Actuators: breaking neural circuits
- 3.3. The escape response as a model for sensorimotor integration
 - 3.3.1. The escape response and its supraspinal control
 - 3.3.2. Monitoring spinal neurons during active locomotion

Part B. Mechanosensory neurons enhance motor output in the zebrafish spinal cord during active locomotion.....p.51

Abstract

- 1 Introduction.....p.52
- 2 Results.....p.53
 - 2.1. Bioluminescence signals reflect the level of recruitment of motor neurons during movement
 - 2.2. Spinal motor neurons recruitment is enhanced in the presence of mechanosensory feedback
 - 2.3. Mechanosensory neurons are recruited during active but not fictive locomotion
 - 2.4. Silencing mechanosensory neurons impairs escape responses
- 3 Discussion.....p.66
 - 3.1. Investigating sensorimotor integration in the spinal cord during ongoing locomotion
 - 3.2. Non-invasive bioluminescence monitoring of genetically targeted neurons in motion
 - 3.3. A closed-loop circuit within the spinal cord for mechanosensory integration
- 4 Methods.....p.68

- 4.1. Zebrafish care and strains
- 4.2. Generation of transgenic lines
- 4.3. Immunohistochemistry for GFP-Aequorin and quantification of muscle fibers
- 4.4. Monitoring of neuronal activity with GFP-Aequorin bioluminescence
- 4.5. High-speed behavior recording
- 4.6. Bioluminescence analysis
- 4.7. Kinematics analysis
- 4.8. Calcium imaging of spinal motor neurons
- 4.9. Ventral nerve root recording (VNR)
- 4.10. Calcium imaging of spinal sensory neurons
- 4.11. Behavioral analysis of freely moving BoTxLCB larvae
- 4.12. Statistical analysis

Part C. From spatial to genetic targeting: a paradigm shift for neurosurgery.....p.77

Abstract

- 1 Introduction.....p.78
- 2 How we moved to genetically targeted neurosciences.....p.78
 - 2.1. From morphological to genetic identification of neurons
 - 2.2. Genetic targeting of neurons in tractable animal models
 - 2.3. A toolbox for manipulating genetically identified neurons
- 3 Moving toward genetically targeted neurosurgery.....p.83
 - 3.1. Candidate diseases for genetically targeted neurosurgery
 - 3.2. Genetic identification and cellular targeting in the human brain
 - 3.3. Genetically targeted neuromodulation and neuroablation in patients
- 4 Two challenges for a paradigm shift.....p.88
- References.....p.93**

Figures

Part A.

Figure 1. Closed-loop sensorimotor behaviors versus open-loop access to neural circuitry

Figure 2. Descending and ascending inputs to spinal circuits involved in sensorimotor reflexes

Figure 3. Neural substrates of spinal sensorimotor integration across vertebrates

Figure 4. Monitoring and breaking neural circuits with genetically encoded reporters and actuators

Figure 5. Monitoring the activity of spinal neurons during active escape responses in zebrafish

Part B.

Figure 1. Bioluminescence monitoring of spinal motor neurons during active locomotion discriminates distinct behaviors

Figure 2. Calcium imaging of spinal motor neurons during fictive locomotion reveals specific patterns of recruitment for escape and slow swims

Figure 3. Spinal motor neurons recruitment is enhanced in the presence of mechanosensory feedback

Figure 4. Mechanosensory neurons are recruited during active but not fictive locomotion

Figure 5. Calcium imaging of spinal mechanosensory neurons shows enhanced activation during motion

Figure 6. Silencing mechanosensory neurons impairs escape responses

Supp. Figure 1. Bioluminescence and kinematic parameters measured during active locomotion.

Supp. Figure 2. Calcium imaging of spinal motor neurons and fictive locomotion of ventral nerve root recording

Supp. Figure 3. Calcium imaging of trigeminal neurons in active and paralyzed *Tg(Isl2b:Gal4, cmlc2:eGFP, UAS:mRFP, UAS:GCaMP5)* larvae

Part C.

Figure 1. Genetic targeting of neurons in tractable animal models.

Figure 2. A toolbox for manipulating genetically identified neurons.

Figure 3. Moving toward genetically targeted neurosurgery.

Part A.

Sensorimotor integration in the spinal cord, from behaviors to circuits: new tools to close the loop?

Abstract

Sensorimotor behaviors are by definition “closed-loop” processes in which sensory feedback modulates behavioral output. Sensory feedback can be provided by visual, auditory and vestibular inputs or direct proprioceptive inputs from muscle contraction. Although sensory feedback is not necessary for oscillation underlying locomotion to occur, there is evidence in the cat that sensory feedback can initiate locomotion (Lundberg, 1979) or reset the rhythm (Schomburg et al., 1998). The contribution of sensory feedback to active locomotion is however difficult to estimate for technical reasons. Indeed most physiological studies of spinal circuits involved in sensorimotor integration rely on preparations where muscles are paralyzed or dissected out, and are therefore deprived of sensory feedback. In this chapter, we will first explain closed-loop processes, and we will review the precious information obtained using “open-loop” experimental paradigms on how spinal neurons generate the neural rhythms that are at the basis of locomotion (Grillner et al., 2008). Optical and genetics techniques offer today alternatives to electrophysiology for monitoring neuronal activity from genetically defined populations of spinal neurons. We will then discuss how innovative tools for monitoring and manipulating neural activity, together with conducting sophisticated behavioral analysis, have provided exciting opportunities for “closing the loop” in genetically accessible model organisms with a special emphasis on zebrafish.

Introduction

The transformation of a sensory input into a motor output is a fundamental computation process, which is carried out by the brain and the spinal cord itself. Sensorimotor integration occurs when a set of neurons detect a sensory stimulus and process it to generate a behavioral output. Classic physiological approaches aim to record neurons specifically activated during sensorimotor integration, and to dissect the causative links by manipulating the activity of these neurons.

Sensorimotor behaviors are by definition “closed-loop” processes in which sensory feedback modulate the behavioral output. “Circuit dissection” experiment requires the experimenter to elicit a given sensory input and to quantitatively assess its behavioral output. In addition, it requires the determination of modulatory components such as systemic and local neuromodulators, or multiple sensory inputs.

Studies of spinal sensorimotor integration are mainly based on preparations of isolated spinal cord, and therefore deprived of descending and ascending inputs to the spinal cord. Such “open-loop” experimental paradigms have proved extremely valuable in understanding how spinal neurons generate neural rhythms that are at the basis of locomotion (Grillner et al., 2008). They might however not be optimal for studying spinal sensorimotor integration in a dynamic fashion.

In recent years, innovative tools for monitoring and manipulating neural activity in genetically accessible model organisms has provided alternative opportunities for “closing the loop”. By monitoring targeted populations of spinal neurons while the animal is fictively or actively performing a sensorimotor task, optogenetics offer new means to selectively study the role of a given class of neurons, without discarding sensory or neuromodulatory inputs.

Probing neural activity of targeted sensorimotor circuits during active locomotion will also open new paths to study how spinal circuits can reconfigure after removal of supraspinal inputs. This could shed light on intriguing results observed in spinal cord injured rodents (Edgerton et al., 2008), and eventually provide new means to exploit

plasticity of spinal sensorimotor circuits in pathological conditions.

1 A closed-loop approach to sensorimotor behaviors

1.1. Defining sensorimotor behaviors

1.1.1. Eliciting sensory input

Even a behavior as simple as a fly approaching an odorant fruit while flying is nothing but a trivial sensorimotor task (Seelig and Jayaraman, 2011): the fly must first detect the odor (Budick and Dickinson, 2006), extract information regarding its environmental relevance, and adapt its locomotor course to approach the fruit. All those steps have to be achieved while the animal is moving, thus adjusting its locomotor output to a changing visual, olfactory and mechanosensory feedback (Frye, 2010). Combining multiple sensory modalities (visual, olfactory, mechanosensory), and their closed-loop feedbacks, is critical to adapt to a noisy sensory environment and enhances the robustness of the behavioral output (Frye, 2010). Multisensory processing relies on interdependent sensory signals, allowing for increased efficiency during sensorimotor tasks compared to unimodal sensory stimuli (Loquet, 2013).

In mammals, it has long been demonstrated that “high-level” cortical areas, such as parietal and prefrontal cortices, were able to integrate multiple sensory modalities, increasing evidence suggests that multisensory integration also occurs in “low-level” cortices that were previously thought to be unisensory (Ghazanfar and Schroeder, 2006; Schroeder and Foxe, 2005). Studying sensorimotor integration, even at a relatively low-level, thus requires to reproduce a behaviorally relevant multisensory environment. However, experimental conditions often allow investigating only one sensory modality at a time.

One solution proposed by the field of neuroethology (Dickinson and Moss, 2012) is to consider that neural circuits can be experimentally understood in the context of the animal’s natural behavior. By focusing on innate behaviors in which the animal extracts critical sensory inputs to produce a behaviorally meaningful

locomotor output, neuroethology has provided important models for sensorimotor integration. For instance, escape behaviors, by which an animal escapes from its predator, are the perfect example of sensorimotor tasks that are crucial for the animal survival, and therefore are stereotyped. Interestingly, escape responses can be found in many species, including *Drosophila* (Card, 2012), *C. elegans* (Pirri and Alkema, 2012) and several fish species (Schuster, 2012), allowing for comparative studies of sensorimotor integration across taxa.

Determining the sensory stimulus to control experimentally is a critical step of sensorimotor studies. We cannot reproduce the highly variable and multidimensional sensory inputs from the animal's natural environment, but we should at least choose a stimulus that replicates the minimum set of sensory cues necessary to elicit a behaviorally relevant and consistent motor output (Clark et al., 2013). We also need to reliably record and quantify the locomotor output elicited by this sensory input.

1.1.2. Measuring motor output

The behavioral output of a sensorimotor transformation can be measured at different spatial and temporal scales: from the migration of an entire population of animals over several days to the analysis of single muscle fibers at millisecond timescale (Clark et al., 2013). Choosing the right scale for addressing the sensorimotor process of interest is not trivial.

At one extremity of this scale, "Taxis" behaviors, such as chemotaxis in *Drosophila* (Gao et al., 2013) or rheotaxis in zebrafish (Suli et al., 2012), examine the cumulative change in spatial position of a group of animals over a relatively long period of time. It is also possible to look at the level of an individual in order to identify sequences of stereotyped behaviors such as mating in *C. elegans* (Liu and Sternberg, 1994). Sequential analysis of canonical behaviors allow the constitution of a detailed locomotor repertoire for a given specie, such as zebrafish (Budick and O'Malley, 2000). Lastly, a more detailed kinematics analysis could measure the

movements of individual joints, coupling this analysis with muscle activity recordings in rodents (Courtine et al., 2009a).

With the refinement of locomotor analysis, and the increasing set of kinematics parameters measured simultaneously, automated tracking programs have become crucial to reliably quantify behaviors. Such programs have been successfully applied to track individuals and classify behaviors in *C. elegans* (Baek et al., 2002), *Drosophila* (Fry et al., 2008) or zebrafish (Mirat et al., 2013). Interestingly, such automated tracking programs can also be used to identify interactions between populations of multiple animals (Branson et al., 2009; Mirat et al., 2013), characterize mutants behaviors and build behavioral phenotypes databases (Yemini et al., 2013), and might lead to high-throughput drug screening (Mirat et al., 2013).

Analyzing complex datasets with multiple levels of kinematics parameters per animal and several animals interacting simultaneously raises important technical challenges. Reducing the dimensionality of the behavioral dataset can be achieved either by arbitrarily focusing on a restricted number of kinematic parameters or through statistical dimensionality reduction as in principal component analysis (PCA) (Musienko et al., 2011). The main issue with dataset reduction is to determine and preserve the behavioral output related to the sensory stimulus of interest. This can be achieved by computing the level of prediction or correlation between the sensory input and motor output (Briggman et al., 2006).

Although sensory input and motor output are the two ends and most accessible parts of a sensorimotor circuit, they are not sufficient to apprehend sensorimotor neural computation. Modulating inputs related to “top-down” afferents or “bottom-up” feedback also heavily influence sensorimotor processing.

1.2. Modulating sensorimotor behaviors

1.2.1. Sensory feedback

In real world, sensorimotor integration is a dynamic process where the animal is constantly updating its sensory inputs according to their behavioral output: as the fly is approaching the fruit, odorant and visual stimuli are continuously modified, allowing the fly to adjust its flight to reach the target (Frye, 2010). In experimental setting, the animal must often be restrained or paralyzed to allow for recording of neuronal activity. Such preparations are called “open-loop” because the motor output does not influence subsequent sensory input. But one might hypothesize that neuronal activity is not the same in the absence of sensory feedback.

“Closed loop” experiments, where new sensory information is acquired as the motor output is produced, can be obtained mainly through two complementary approaches: by attaching a miniaturized device onto a freely moving animal interacting with a controlled environment, or by providing some simulated sensory inputs to a restrained animal. The developing field of brain-machine interfaces has provided numerous studies in which cortical activity is recorded through chronically implanted electrode arrays, and decoded in real-time to control a motor effector, such as prosthetic limb (Carmena et al., 2003). It has also been possible to restore tactile sensation using a “brain-machine-brain interface”, by providing a way to produce a virtual motor output and to generate the corresponding sensory feedback (O’Doherty et al., 2012) (Tabot et al., 2013).

Such tools make it possible to monitor neuronal activity while the animal is freely behaving, but they don’t provide precise control over its sensory inputs. Virtual reality environments (Dombeck and Reiser, 2012) reproduce a simulated sensory environment that is continuously updated based on the animal behavior. Besides providing a better-controlled sensory input, virtual environments most importantly enables simultaneous neural recording by allowing the animal to perform a closed loop sensorimotor task while being physically restrained.

Combined with electrophysiology or genetically encoded calcium imaging, virtual environments have been applied in mice (Harvey et al., 2010), drosophila (Seelig et al., 2010) and zebrafish (Ahrens et al., 2012; Portugues, 2011). Notably, the zebrafish studies have showed that larvae were able to quickly modify their motor

output in response to an unexpected visual feedback (Portugues, 2011), and that this adaptive behavior correlated with state-dependent neural activity in a subset of brain areas identified using brain-wide calcium imaging (Ahrens et al., 2012).

1.2.2. Neuromodulation

State-dependent sensorimotor processing, in which the activity of a given population of neurons differs according to the behavioral state of the animal, are investigated within the larger framework of neuromodulation of neural circuits.

The core hypothesis underlying the concept of “multifunctional circuits” is that a given neural circuit should not be considered as a hard-wired diagram, activated during discrete states, but rather as a distributed network that is able to switch continuously between a variety of dynamical states to produce different patterns of activity, and eventually different behaviors (Briggman and Kristan, 2008). In a multifunctional sensorimotor circuit, a given neuron can be active during multiple locomotor behaviors (Sankrithi and O'Malley, 2010), producing different patterns of activity based on its modulatory inputs (Briggman and Kristan, 2008). External parameters, such as neuromodulatory substances (Marder, 2012) or synaptic input, e.g. sensory afferents (Latorre et al., 2013), can control the transitions between these different phases.

The neuromodulatory functions of monoaminergic substances have been extensively studied in invertebrates' sensorimotor models such as the crustacean somatogastric ganglion (STG) (Marder, 2012). The central pattern generator circuit can generate fictive locomotor patterns and is modulated by numerous substances, from neurotransmitters released locally by projecting sensory neurons to diffused hormones released at distance by secretory structures (Blitz and Nusbaum, 2011). In spinal cord injured rats, the role of monoaminergic (in particular serotonergic and dopaminergic) substances in modulating spinal locomotor circuits have been well documented (Musienko et al., 2011). Pharmacological manipulation, together with electrical spinal cord stimulation, could restore some locomotion independently of supraspinal inputs regeneration (Courtine et al., 2009b). Such neuromodulatory-

mediated functional recovery is also phase-dependent, suggesting that different interventions facilitate distinct phases of the locomotor pattern (Edgerton et al., 2008). This observation is in line with a multifunctional framework for the spinal sensorimotor circuits driving locomotion in spinal cord injured rats.

Intrinsic sensory states, i.e. neural dynamics that are not directly affected by an external physical stimulus, can also modulate multifunctional sensorimotor networks. One interesting example is the dual role of the gravimetric organ of the mollusk *Clione limacina*, which can switch between two very different rhythmic patterns, and behavioral output, depending on whether the animal is under control of a “hunting neuron” (Latorre et al., 2013). Another example of intrinsic sensory modulation is the feeding behavior of the *Aplysia californica*, where the same neurons drive both ingestion and rejection of food, but are differentially modulated by the coupling between the mouth muscles (Ye et al., 2006).

1.3. Modeling sensorimotor behaviors

1.3.1. Behavioral computations

Analyzing sensorimotor transformations is more complicated than just correlating an observed motor output with an experimentally elicited sensory input. Therefore, computational models for sensorimotor integration have proven more and more helpful as the number of measured variables increased with the improvement of experimental techniques.

For any sensorimotor task, the underlying computation is complex and can be modeled on a coarse behavioral scale, or on a more refined circuitry scale. Both approaches are complementary and have so far mostly been developed independently. The long-term objective is to map those behavioral computations on neural circuits models.

One major issue when dealing with sensorimotor computation is that our motor system is highly nonlinear (Franklin and Wolpert, 2011). In a linear system, one can easily predict the behavioral response to a multisensory stimulus by calculating the sum of the motor outputs for each individual sensory stimulus. However, the force developed by a muscle in response to its nervous input largely depends on other variables such as muscle length, velocity, tendons, joints positions, among others. (Zajac, 1989). Similarly, multiple sensory input creates multimodal sensory representations that are more than merely the sum of unimodal sensory inputs (Green and Angelaki, 2010).

Besides nonlinearity, many other issues increase the complexity computations of sensorimotor behaviors. For instance, noise is limiting our ability to perceive accurately sensory inputs (e.g.: estimating the location of the fruit on the table for our approaching fly) and carry out motor outputs precisely (e.g.: adjusting speed by modifying wings movements to reach the target) (Rohrseitz and Fry, 2010). Other issues include redundancy, i.e. the fact that multiple combinations of motor sequences can achieve the same behavioral task; nonstationarity, i.e. the fact that sensory and motor systems are modified throughout development and aging; uncertainty arising from noise, sensory ambiguity, partial information; and even multiple and variable delays, whether due to sensory or motor processing (Franklin and Wolpert, 2011).

One approach to resolve such complex sensorimotor computations is Bayesian decision theory (Wolpert, 2007). Bayesian decision theory aims to produce, using a probabilistic reasoning, optimal inferences based on uncertain inputs by combining prior beliefs and multiple sensory modalities. Based on these inferences, decision theory is subsequently used to decide which action is more likely to achieve the task objectives (Franklin and Wolpert, 2011). In a Bayesian system, the probability of a sensory state being true (named “posterior”) is produced by combining the probability of receiving the sensory information if that state were true (named “likelihood”) with the prior probability of that state (named “prior”) (Körding and Wolpert, 2006).

Such Bayesian sensorimotor computation can be easily tested using a simple task where a subject is asked to reach a cursor in a virtual-reality environment. The

discrepancy is introduced between the subject's actual and displayed hand position (Körding and Wolpert, 2004). The “prior” distribution can be experimentally changed by varying the size of the discrepancy, while the sensory feedback “likelihood” is adjusted by varying the degree of visual blur controls. Using this approach, the authors showed that subjects combined prior statistical distribution with sensory feedback likelihood in a Bayesian manner to optimize their performance during sensorimotor learning.

1.3.2. Circuits computations

Mapping behavioral sensorimotor computations onto identified neural circuits requires knowing how do those circuits process sensory inputs to produce a motor output at a cellular scale.

One important challenge for computing sensorimotor transformations, whether on a behavioral or cellular scale, is that they are mostly nonlinear, i.e. their motor output cannot be written as the weighted sum of its sensory inputs plus a constant. Geometrically, this means that modeling any neural network underlying a sensorimotor process requires at least a three-layers transformation, with an intermediate layer (referred to as “hidden layer”) used to recode sensory inputs before they are transformed into motor output. Such non-linear transformations can be approximated using a linear combination of “basis functions” (such as sine and cosine functions in a Fourier transform) as the intermediate layer: this is called the “basis function approach” (Pouget et al., 2002). This basis function approach is particularly relevant in the context of sensorimotor transformations. For instance, if a subject wants to reach toward a visual target as in the previously described experiment, the basis function approach postulates that the motor command can be approximated by the weighted sum of several non-linear basis functions of the visual and postural inputs (Pouget and Snyder, 2000). On a cellular scale, this ‘intermediate layer’ would be constituted by neurons whose firing properties, or “tuning curve”, can be described as a basis function for both visual and postural sensory inputs. Such neurons whose gain is modulated by visual and postural inputs can actually be found in the parietal

(Andersen et al., 1985), occipital (Trotter and Celebrini, 1999) and prefrontal (Boussaoud et al., 1993) cortices.

Besides nonlinearity, another major concern when looking at sensorimotor transformations is variability. Indeed, most experiments whether looking at sensorimotor processes or not, rely on mean statistics calculated from populations. However, it has been repeatedly shown that multiple solutions can produce similar circuit outputs (Marder, 2011). Even the most stereotyped motor behaviors such as rhythms generated by central pattern generators can be highly variable across animals (Marder and Taylor, 2011). The variability of the behavioral output to similar sensory inputs is well known, although not always documented. Most studies describe the “typical” behavior of the system by a single model. One attempt to take into account variability in sensorimotor circuits models would be to construct of population of models reproducing the actual behavioral data rather than trying to use a single model to reproduce the generic behavior (Marder and Taylor, 2011).

2. An open-loop access: sensorimotor circuits in the spinal cord across vertebrates

In the particular case of spinal sensorimotor circuits, a great wealth of anatomical and electrophysiological data has been accumulated over the years. However, being able to elaborate broader models in order to fit those data onto observed behaviors still remains a challenge, largely due to the fact that available techniques have prevented monitoring sensory inputs concomitantly with motor outputs until recently.

2.1. Extrinsic inputs to spinal sensorimotor circuits

2.1.1. Descending motor control

Located in the periphery of the spinal cord, white matter tracts comprise both ascending fibers, mainly located dorsally and laterally, carrying sensory information, and descending axons, mainly located ventrolaterally and laterally, carrying motor information (Figure 2A).

Descending motor tracts mainly include corticospinal tracts, which forms monosynaptic connections between motoneurons located in the primary motor cortex and spinal motoneurons located in the anterior horn of the grey matter at each segment. 80 to 90% of the corticospinal axons decussate to the contralateral side at the pyramid level in the medulla oblongata (hence the name “pyramidal tracts”), and travels in the dorsolateral funiculus (Guertin, 2013). Corticospinal tracts are mostly involved in voluntary skilled movements.

Other descending motor tracts originate mainly in subcortical nuclei in the brainstem, and in particular the reticular formation, and are called “extra-pyramidal tracts” by opposition to the corticospinal (pyramidal) tract. Extra-pyramidal tracts are composed of the rubrospinal (located along the corticospinal tract in the dorsolateral funiculus), vestibulospinal, tectospinal and reticulospinal tracts (all three located in the ventrolateral funiculus) (Bican et al., 2013) (Rossignol and Frigon, 2011).

Those descending inputs are mainly involved in autonomic functions, postural control and locomotion. More specifically: they facilitate contralateral upper limbs flexion (rubrospinal tract), neck and head motor control (tectospinal tract), autonomic functions (reticulospinal tract) and facilitating ipsilateral extensors and antigravity muscles to control tone and posture (vestibulospinal tract) (Guertin, 2013). Extra-pyramidal tracts project mainly on premotor lamina (lamina VI to VIII) of the spinal cord grey matter at each segment (Bican et al., 2013).

In particular, the role of reticulospinal pathways originating from the brainstem in the initiation and control of locomotion have been extensively studied, leading to the concept that, while the spinal central pattern generator produces the basic locomotor rhythm (see section 2.2.1), brainstem structures are necessary to activate and regulate this spinal central pattern generator (Jordan et al., 2008a; Whelan, 1996).

Numerous studies, mainly using decerebrate cat preparations, have identified several areas within the brainstem that can lead to the production of locomotion when

activated, whether chemically or electrically. The mesencephalic locomotor region (MLR), first identified by Shik et al (Shik et al., 1969), receives inputs from both the basal ganglia, the limbic system and the frontal cortex, and projects to neurons of the medial medullary reticular formation (MRF), and then on to interneurons in the spinal cord (Whelan, 1996). When stimulated electrically in decerebrate cats, the MLR can generate different gait patterns (walking, trotting, galloping) depending on the strength of the electrical stimulus (Rossignol et al., 2006). Interestingly, after its initial description in cats, homologous areas of the MLR have been described in many vertebrate species, including the rat (Garcia-Rill et al., 1990), lamprey (McClellan and Grillner, 1984) and monkey (Eidelberg et al., 1981).

Other areas in the midbrain, such as the medial MLR, the pontomedullary locomotor strip (PLS) or areas in the subthalamic nucleus (subthalamic locomotor region), have been shown to be involved in the control of locomotion by projecting onto spinal circuits through reticulospinal pathways in rodents (Whelan, 1996). More recently, isolated spinal cord preparations from neonatal rats and mice have allowed the identification of various neurotransmitters (N-methyl-D-aspartate, 5-hydroxytryptamine, dopamine, noradrenaline) that can elicit locomotor rhythmic activity by stimulating the spinal CPG through descending reticulospinal pathways (Jordan et al., 2008b).

In non-mammalian vertebrates, the descending control of locomotion has been particularly documented in the lamprey (Dubuc et al., 2008). Trigeminal relay cells activate reticulospinal neurons in a “all-or-nothing” fashion to elicit escape responses in response to a mechanical cutaneous stimulus (Viana Di Prisco et al., 1995). On the contrary, MLR inputs to reticulospinal neurons initiate locomotion in a graded fashion through monosynaptic cholinergic and glutamatergic inputs, with the middle rhombencephalic reticular nucleus (RRN) being activated for low intensity stimulation, and the posterior RRN being activated for as the stimulation strength increases (Wannier et al., 1998) (Figure 3A).

2.1.2. Ascending sensory feedback

While descending inputs schematically provide the motor command to spinal sensorimotor circuits, ascending afferents to the spinal cord mainly provide sensory information. In mammalian vertebrates, ascending sensory inputs include proprioceptive inputs (group Ia and II afferents from, respectively, primary and secondary endings of muscles spindles, and Ib afferents from Golgi tendon organs), cutaneous inputs (chemosensitive group III/A δ and group IV/C fibers from nociceptive receptors). They have been extensively studied in the context of local spinal reflex pathways (Knikou, 2008; Rossignol et al., 2006) (Figure 2B).

The simplest, and fastest, somatic reflex is the monosynaptic pathway between primary sensory afferents from primary muscle spindles (Ia) and homonymous alpha motoneurons in the ventral horn of the corresponding segment grey matter. This is the basic myotatic reflex that is elicited by a muscle stretch due to a tendon tap, but is also involved in tonus and postural adjustments (Guertin, 2013). The experimental analog of the Ia reflex, the Hoffman reflex (H-reflex), where the mechanical stretch is replaced by a sub-threshold electrical stimulation of the afferent nerve, has been extensively used to investigate spinal sensorimotor circuits, and in particular presynaptic and reciprocal inhibition (Jankowska, 1992; Knikou, 2008), see (section 2.2.1).

Golgi tendon organs are force-sensitive receptors located at the muscle-tendinous junction, that are activated by passive and active muscle force. The Ib reflex arc, also known as the “inverse myotatic reflex”, is a disynaptic pathway by which group Ib sensory afferents from Golgi tendon organs inhibit alpha-motoneurons. This is the reflex arc responsible for the abrupt termination of the myotatic reflex, the well-known “clasp-knife” phenomenon (Hultborn, 2006). Although stimulating the Golgi tendon organs at rest cannot induce any movement, the Ib reflex has been suggested to be important for regulating muscle stiffness (Knikou, 2008).

While group Ib afferents from Golgi tendon organs provide information about the tension developed during muscle contraction, and group Ia afferents from primary muscle spindles inform spinal circuits about the dynamic of changes in muscle length, group II afferents from muscle spindle secondary endings provide information of muscle length itself (Jankowska and Edgley, 2010). Group Ia, Ib and II muscle afferents taken together constitute what is generally termed the “proprioception” input. Together with cutaneous afferents from nociceptors (A δ and C fibers) and other muscle afferents (thinly myelinated group III and unmyelinated group IV fibers), group II muscle afferents constitute the flexion reflex afferents (FRA) involved in the withdrawal reflex, by which a painful stimulus lead to withdrawal of the limb through ipsilateral flexion and contralateral extension (Eccles and Lundberg, 1958). This sensorimotor reflex, more sophisticated than the “myotatic” and “inverse myotatic” reflexes, involves at least to two interneurons to either activate or inhibit the ipsilateral flexor or extensor alpha-motoneurons over several spinal segments (Guertin, 2013).

Sensory feedback pathways in non-mammalian vertebrates still remain unclear. Indeed, there is no clear equivalent to mammalian peripheral proprioceptive receptors in swimming vertebrates. However, in the lamprey, intra-spinal mechanosensitive receptors called the “edge cells” (Grillner et al., 1984) might provide movement-related sensory feedback (Di Prisco et al., 1990). Interestingly, it has recently been proposed that edge cells could be modulated by GABAergic cerebrospinal fluid contacting neurons (CSFns) (Jalalvand et al., 2014). Similar CSFns, called “Kolmer-Agduhr” cells, have been described in the zebrafish, and were able to trigger slow swim upon optical activation (Wyart et al., 2009). Another sensory feedback pathway in larvae and adult zebrafish is the lateral line system (Ghysen and Dambly-Chaudière, 2007). Mechanosensory hair cells in the lateral line neuromasts provide information about the water flow, contributing to orientating the fish against the water, a behavior called rheotaxis (Olszewski et al., 2012; Suli et al., 2012) (Figure 3C).

2.2. Intrinsic spinal sensorimotor circuitry

2.2.1. Sensorimotor interneuronal networks

Presynaptic inhibition

As we have seen, spinal circuits are continuously provided with multiple ascending sensory inputs from various sources. This sensory feedback needs to be controlled to allow for the proper execution of a motor task (Knikou, 2008). One way to control this sensory input is through presynaptic inhibition of muscle afferents on alpha-motoneurons through GABAergic axo-axonic synapses (Rudomin and Schmidt, 1999) (Figure 2B). A similar control can be achieved through primary afferent depolarization (PAD), and the two phenomena are now actually considered to be mediated by the same interneurons (Jankowska, 1992).

Initially described in relation to group Ia afferents from primary endings of muscle spindles (Frank and Fuortes, 1959), presynaptic inhibition through GABAergic interneurons has more recently also been described for group Ib and group II muscle afferents, as well as cutaneous and articular afferents (Rudomin, 2009). Although it has traditionally been considered that different subgroups of interneurons were mediating PAD of distinct muscle sensory afferents (Jankowska, 1992), it has also been demonstrated that the same interneurons, located within Rexed's laminae VI-VII of the spinal cord grey matter (*intermediate zone*), could be co-excited by group Ia and group Ib afferents (Fetz et al., 1979). More surprisingly, even group Ib and group II inputs can be integrated by a common pool of interneurons, located within laminae V-VII (Bannatyne et al., 2009). These results led some authors to consider all those subpopulations of interneurons (groups Ia, Ib and II) may actually operate as a single functional population with multisensory inputs from both several types of afferents and several muscles (Jankowska and Edgley, 2010). (Figure 2 B1)

Reciprocal Ia inhibition

Considered that the same Ia muscle afferents innervate motoneurons belonging to many different motor pools, it has long been postulated that a neural pathway involving Ia afferents allowed for inhibition of alpha-motoneurons controlling antagonist muscles. The reciprocal Ia inhibition is mediated by a single glycinergic inhibitory interneuron activated by Ia afferents from a given flexor muscle, which in turn inhibits alpha-motoneurons controlling the antagonistic extensor muscle (Eccles et al., 1957a; Jankowska, 1992). As for PAD interneurons, it has later been showed that these reciprocal Ia inhibitory interneurons, located dorsomedially to the motor nuclei in the ventral horn, actually also receives convergent inputs, both excitatory and inhibitory, from multiple descending and ascending sources, including Renshaw cells (see below) (Hultborn, 1972) (Figure 2 B2).

Non-reciprocal Ib inhibition

Group Ib sensory afferents from Golgi tendon organs inhibit motoneurons projecting to synergist muscles and facilitate motoneurons projecting to antagonist muscles through di- or tri-synaptic pathways involving respectively one or two inhibitory glycinergic interneurons (Eccles et al., 1957b; Jankowska, 1992). As for Ia interneurons mediating reciprocal inhibition, Ib inhibitory interneurons exhibit a wide convergence of inputs from both descending inputs (excitatory corticospinal, rubrospinal and inhibitory reticulospinal afferents) and ascending inputs (excitatory group Ia and Ib muscle afferents, as well as cutaneous and joint afferents) (Hultborn, 2006) (Figure 2 B3).

Recurrent inhibition

Lastly, another sensorimotor interneuronal pathway involving an inhibitory interneuron is the one formed by Renshaw cells, located in the ventral horn (next to Ia reciprocal inhibitory interneurons) (Renshaw, 1946). Renshaw cells are excited by cholinergic axonal collaterals from alpha-motoneurons and provide glycinergic

recurrent inhibition to the same or synergistic muscles (Eccles et al., 1956). Again, as for other sensorimotor interneurons, Renshaw cells also receive inputs from other afferents, including ipsilateral group II and III muscle afferents, cutaneous afferents, and descending motor afferents, and project themselves not only to alpha-motoneurons but also to gamma-motoneurons, Ia reciprocal inhibitory interneurons and other Renshaw cells within the same spinal segment (Windhorst, 2007).

2.2.2. Spinal central pattern generator across vertebrates

Along with this complex interplay between sensory afferents and sensorimotor interneuronal networks, a large amount of work has converged toward the identification of a spinal network able to generate the elementary patterns and rhythms of locomotion: the spinal central pattern generator (CPG). First postulated from studies of decerebrated cats more than a century ago (Brown, 1911), extensive research in non-mammalian vertebrate species such as the lamprey (Grillner, 2003) and the *Xenopus* tadpole (Roberts et al., 2009) have provided many insights into the swimming CPG and its cellular mechanisms, leading to rapid advances in the understanding of the mammalian walking CPG (Kiehn, 2006).

Homology across vertebrates

Interestingly, new insights into the genetic profiles of spinal interneurons have allowed direct comparison between different classes of interneurons across all vertebrates (Goulding, 2009). Based on the dynamic expression pattern of transcription factors, five major subclasses of spinal ventral interneurons have been described, called V0, V1, V2, V3 and Hb9 interneurons (Figure 3). Each class being characterized by a specific transcription factor, such “molecular code” opens the way for functional investigation of genetically targeted, rather morphologically or electrophysiologically identified, spinal interneurons within the CPG (Figure 3B).

Excitatory rhythm-generating circuits

Several lines of evidence suggest that the rhythmogenic neurons of the CPG are glutamatergic excitatory neurons projecting ipsilaterally onto inhibitory left-right and flexor-extensor coordinating neurons at each spinal segment (Kiehn et al., 2008). Indeed, blocking inhibitory commissural or ipsilateral interneurons does not prevent rhythm generation, whether in the lamprey (Cangiano, 2005), rodent (Bonnot et al., 2002) or cat (Kato, 1987), therefore discarding the “half-center model” for CPG rhythm generation (Kiehn, 2006). Various putative candidates for the role of “pacemakers” neurons have been recently investigated (Kiehn, 2011): among them, Hb9-expressing interneurons (Tazerart et al., 2008) and V2a-Chx10 expressing interneurons (Hägglund et al., 2010) have been shown to have rhythmogenic properties in neonatal mouse models. Morphological homologs in the lamprey (Grillner, 2003) and tadpole (Li et al., 2010), and molecular homologs in zebrafish (McClean et al., 2007) support the hypothesis of a glutamatergic ipsilateral drive to the spinal CPG.

Flexor-extensor coordination

Ipsilateral-projecting glycinergic inhibitory interneurons are known to be involved in alternation of extensor and flexor muscles activation for a long time, since flexor-extensor coordination is suppressed when glycinergic transmission is blocked but can persist in hemisected spinal preparations (Bonnot et al., 2002). Putative candidate interneurons include Ia inhibitory interneurons and Renshaw cells (see section 2.2.1), as both have been shown to fire rhythmically during locomotion and in opposing phases in respect to their flexor/extensor afferents (McCrea et al., 1980).

However, a recent study challenged this assumption (Gosgnach et al., 2006). V1-derived interneurons expressing the transcription factor *Engrailed-1* (En1) are inhibitory ipsilaterally projecting interneurons that give rise to Renshaw cells and Ia inhibitory interneurons. Genetic knock out of En1-expressing neurons induced slower locomotor activity and increased step cycle, but did not suppress flexor-extensor coordination. This suggests the existence of other ipsilateral inhibitory interneurons, that might be specific to mammalian locomotor CPG (Kiehn, 2006).

Left-right coordination

Coordination of left-right activity during locomotion is mainly achieved through commissural interneurons that are crossing the midline via the ventral commissure (Kiehn, 2006). Experiments in mice have revealed a dual system for left/right coordination: 1) during alternative walking, contralateral motoneurons inhibition is achieved either through mixed glycinergic and GABAergic inhibitory commissural interneurons projecting monosynaptically to contralateral motoneurons, or excitatory commissural interneurons projecting onto contralateral inhibitory premotor interneurons; 2) during synchronous “hopping”, contralateral motoneurons excitation is achieved through glutamatergic commissural interneurons (Quinlan and Kiehn, 2007).

Candidate commissural interneurons for this left/right dual model are derived from Dbx1 positive neurons from the V0 transcription domain (Lanuza et al., 2004), in which about one third of commissural interneurons are glutamatergic (Evx-1-positive, V0_v interneurons) and two thirds are inhibitory (Evx1-negative, V0_D interneurons) (Moran-Rivard et al., 2001). A recent study (Talpalari et al., 2013) confirmed and further refined this hypothesis by showing that V0-ablated mice exhibited a hopping gait at all frequencies, while selective ablation of inhibitory V0 interneurons (V0_D) led to a lack of left-right alternation only at low frequencies whereas selective ablation of excitatory V0 interneurons (V0_v) led to similar hopping gait but only at medium and high frequencies.

Neurons participating to the left-right alternation spinal network have also been identified in non-mammalian vertebrates. In the *Xenopus* tadpole, inhibitory glycinergic commissural interneurons are responsible for mid-cycle reciprocal inhibition and are driven by descending glutamatergic interneurons (Roberts et al., 2009). In the lamprey, both inhibitory and excitatory commissural interneurons have been described with left-right alternating pattern of activity (Grillner, 2003). Lastly, similar glycinergic inhibitory and glutamatergic excitatory commissural interneurons have been identified in the zebrafish, sharing molecular markers with the mouse V0

neurons, although the network details have not yet been worked out (Fetcho and Mclean, 2010).

2.3. Dynamic spinal sensorimotor interactions

2.3.1. Modulation of spinal circuitry from extrinsic inputs

Both descending motor inputs and ascending sensory feedback can modulate the activity of the spinal CPG. Indeed, if the CPG is able to generate the basic locomotor patterns, dynamic sensorimotor interactions with both supraspinal and peripheral inputs continuously modulate these patterns to achieve a flexible adaptation to the environment. Such interactions take place in a phase-dependent (swing/stance) and state-dependent (forward/backward) manner, that is extrinsic inputs will result in different modulations depending on the ongoing phase of the locomotor cycle (Rossignol et al., 2006).

As discussed in section 2.1.1, supraspinal pathways, such as the MLR and its projections through the reticulospinal tract, can induce locomotion in “fictive preparations”, i.e. isolated spinal cord or decerebrated adult cat preparations. However, descending pathways, whether carrying sensory or motor information, can also modulate ongoing locomotion. Such modulation can be achieved either through modulation of brainstem command circuitry, or through direct modulation of spinal circuitry (McCrea, 2001).

Vestibular inputs (relaying information about balance and posture) modulate the activity of reticulospinal neurons with a phasic pattern during fictive locomotion in lampreys, thereby avoiding a counteractive drive from reticulospinal neurons during ongoing locomotion (Bussi eres and Dubuc, 1992). A recent study in zebrafish larvae suggested that vestibular inputs are able to differentially recruit dorsal and ventral premotor spinal microcircuits during postural correction, possibly prefiguring the mammalian modular organization of spinal flexor/extensor microcircuits (Bagnall and McLean, 2014). The influence of visual feedback on the control of locomotion

can be experienced on a daily basis when one needs to anticipate and adjust his gait to avoid an obstacle (Rossignol, 1996). New experimental paradigms, such as the optomotor response in zebrafish (Orger et al., 2008), have started to shed light on the neural circuitry responsible for visually induced locomotion.

Besides descending inputs, ascending sensory feedback, from either proprioceptive or cutaneous inputs, can also modulate the activity of the spinal CPG. Cutaneous inputs (C and A fibers, see section 2.1.2) are mainly involved in correcting the steps in response to external perturbations, such as an uneven floor, during the different phases of the step cycle (McCrea, 2001; Rossignol et al., 2006). Interestingly, the same cutaneous stimulus can lead to responses in flexor or extensor muscles depending on the initial position of the limb, therefore behaving as excitatory inputs to a given muscle group in one locomotor phase, and excitatory to the antagonist muscles in the opposite phase, a phenomenon termed “reversal” (Rossignol and Gauthier, 1980).

Proprioceptive feedback also has an important role in modulating ongoing locomotion, in particular by adjusting the duration of, and facilitating the switch between, the different phases of the step cycle, therefore setting the frequency of locomotion (Rossignol et al., 2006). For instance, in decerebrate cats preparations, stimulation of group Ib afferents from Golgi tendon organs of extensor muscles can reset the locomotor cycle by abruptly terminating the ongoing fictive flexor activity and initiating a new burst in the extensor recording (Conway et al., 1987). Similarly, stretch-evoked Ia inputs can increase the duration of the stance phase, but only when stimulated during flexor activity (Guertin et al., 1995).

Therefore, patterns of fictive locomotion produced by the spinal CPG should not be considered as a fixed output of a hard-wired circuit, but should be viewed rather as a dynamic multimodal process whose output is modulated by the various supraspinal and peripheral sensory inputs.

2.3.2. Implications for plasticity after spinal cord injury

The emerging concept that intrinsic spinal circuits can produce adaptive locomotion with modulation by sensory feedback, independently, at least to some extent, from supra-spinal inputs, bears important consequences for new neurorehabilitative strategies after spinal cord injury.

Experimental paradigms with adult cats walking on a treadmill have demonstrated that neither bilateral lesion of the dorsolateral spinal cord (interrupting cortico- and rubrospinal tracts) (Jiang and Drew, 1996), nor bilateral lesion of the ventrolateral spinal cord (interrupting vestibulo- and reticulospinal tracts) (Brustein and Rossignol, 1998), could permanently suppress quadrupedal locomotion. However, after unilateral complete hemisection at the lower thoracic (T13) level, interrupting both dorsal and ventral descending pathways, cats showed a complete paralysis of the ipsilateral hindlimb during the first three days, followed by a progressive recovery over the following three weeks (Rossignol and Frigon, 2011). Interestingly, this recovery was accompanied by a modification of the step cycle, forelimb/hindlimb and left/right coordination (Martinez et al., 2012). These results suggest that the intrinsic spinal circuitry is able to produce locomotion even after removal of all supraspinal inputs, and that this recovery is underpinned by extensive reorganization of the spinal sensorimotor network (Martinez and Rossignol, 2013). They also suggest that treadmill-induced locomotor training, by providing sensory feedback, is crucial to drive the reorganization of spinal circuits (Rossignol and Frigon, 2011).

To test this hypothesis of a plastic spinal CPG, Rossignol et al. designed a dual-lesion paradigm in which a first hemisection performed at the T10/T11 spinal level is followed, after several weeks of locomotor training and complete recovery, by a complete spinal transection at the T13 level (Barrière et al., 2008; Martinez and Rossignol, 2013). The major finding was that cats regained full locomotor performance after only 24 hours, without any training or pharmacological intervention (Barrière et al., 2008), therefore indicating that intrinsic changes within the spinal

CPG had indeed occurred during the rehabilitation period, and could be retained after the complete removal of supraspinal inputs.

Similar results have been obtained recently in rodents (Edgerton et al., 2008), in which recovery of coordinated hindlimbs locomotion on a treadmill could be achieved only one-week after complete thoracic (T7) spinal transection when combined lumbosacral electrical epidural stimulation (EES) and systemic application of serotonergic agonists were applied (Courtine et al., 2009a). Interestingly, removing peripheral sensory inputs by unilateral dorsal rhizotomy prevented EES-facilitated locomotor recovery after complete spinal transection, but only on the deafferented side, thereby confirming the hypothesis that sensory feedback drives the reorganization of intrinsic spinal circuitry (Lavrov et al., 2008).

However, those results only concerned treadmill-induced “automatic” locomotion. To which extent can we exploit the plasticity of spinal sensorimotor circuits to induce restoration of voluntary locomotion? This question was investigated by a recent study (Brand et al., 2012), in which the authors used a simultaneous dual hemisection paradigm in adult rats together with a so-called “electrochemical neuroprosthesis” (i.e. the combination of lumbosacral epidural electrical stimulation together with systematic administration of a cocktail of monoaminergic agonists). They observed that rats trained with a robotic postural interface encouraging supraspinally mediated locomotion could regain voluntary control through remodeling of corticospinal projections. A similar approach have even been used successfully in a paraplegic human subject, who could regain some voluntary control of one of his lower extremity after intensive rehabilitation and electrical epidural stimulation, although this recovery was very limited and observed in a single individual only (Harkema et al., 2011).

These results have raised hopes that clinically significant locomotor recovery can be achieved through reorganization of intrinsic sensorimotor circuitry, facilitated by intensive training and electrical and/or chemical manipulation. However, one major issue of such studies is that they can probe changes in spinal circuitry only in a very indirect manner.

Indeed, until now, one had to choose whether to be able to access spinal circuitry in open-loop “fictive” preparations, discarding the sensory feedback but being able to identify and record from neurons within the spinal cord, or to preserve active locomotion and sensory feedback but having only a limited and indirect access to spinal circuits. However, new tools and animal models might change this conundrum in a near future.

3. Closing the loop? Optogenetic manipulation of spinal sensorimotor circuits in zebrafish

3.1. Genetic targeting of spinal sensorimotor circuits in zebrafish

3.1.1. Identified sensorimotor neurons in the zebrafish spinal cord

As in any other vertebrates, neurons in the zebrafish spinal cord can be broadly divided between motoneurons, sensory neurons, and interneurons (Lewis and Eisen, 2003). Recent developments of genetic tools allowing specific targeting of subtypes of neurons has allowed marked progress in our understanding of their functional roles, and has led to a refined classification.

Sensory neurons within the spinal cord mainly include mechanosensitive Rohon-Beard neurons, of which homologs can be found in most anamniote vertebrate, such as *Xenopus* tadpoles and lampreys (Reyes et al., 2003). Rohon-Beard neurons are derived from the same neural plate domain that generates neural crest cells, and presumably die during development to be replaced by dorsal root ganglion cells in adult zebrafish (Lewis and Eisen, 2003). When stimulated optically, Rohon-Beard neurons are able to trigger escape responses (Douglass et al., 2008; Wyart et al., 2009), through either direct excitation of reticulospinal cells (Douglass et al., 2008) or activation of CoPA interneurons (Pietri et al., 2009).

In larvae, both primary and secondary motoneurons (together with oligodendrocytes) are derived from the pMN transcription domain in the ventral

spinal cord, are positive for *olig2* expression and persist through adulthood (Kimmel et al., 1994; Lewis and Eisen, 2003). Primary motoneurons are located more dorsally (with subtypes according to their position from caudal to rostral: CaP, MiP, RoP), innervate fast muscles, and are involved in fast swimming and startle response, while secondary motoneurons, located more ventrally, innervate both slow and fast muscles, and are also involved in slow swim (Lewis and Eisen, 2003).

To explore the differences between slow swim and escape spinal networks, Ritter et al. used a head-embedded preparation in which they could elicit either slow swim by illuminating the head with a fiber optic, or escapes by tapping the head with a piezoelectric actuator. They simultaneously monitored the activity of morphologically identified interneurons in the embedded part of the tail using calcium imaging, and recorded the movements of the caudal tail using a high-speed camera (Ritter et al., 2001). They showed that “circumferential ipsilateral descending” (CiDs) interneurons were activated during escapes but not during slow swim movements, while excitatory glutamatergic “multipolar commissural and descending” (MCoDs) interneurons were, on the contrary, activated during swimming but not during escapes (Ritter et al., 2001).

A subsequent study from the same group (Bhatt et al., 2007) combining calcium imaging and paired patch recording, confirmed that CiDs were responsible for motoneurons excitation during escapes, and showed that stronger escapes elicited by a head tap were associated with the recruitment of a larger number of CiDs than delayed escapes elicited by a tail tap, thereby apparently contradicting previous results about differential descending control from the hindbrain (Bhatt et al., 2007; Liu and Fetcho, 1999). Interestingly, the same authors also demonstrated that reinnervation of CiDs by regenerating Mauthner axon, following injection of cAMP, was associated with improved locomotor performances (Bhatt et al., 2004).

Using isolated spinal cord from larvae zebrafish, a “topographic map” of recruitment for premotor interneurons has been documented (McClean et al., 2007; 2008). MCoDs interneurons, located in the ventral spinal cord, provided a phasic drive to a subset of ventral contralateral motoneurons during slow swimming patterns.

On the other hand, when the swimming frequency was increased, MCoDs were inhibited through glycinergic synapses, while CiDs interneurons became activated, providing a glutamatergic excitatory drive to ipsilateral motoneurons, with the more dorsal CiDs being activated for the faster swimming speeds (McLean et al., 2008). Of interest is the fact that CiDs interneurons are the fish homologs of the mouse V2a interneurons (Kimura, 2006; Kimura et al., 2013) (see section 2.2.2).

Interestingly, it has also been shown in adult zebrafish that different motoneurons pools exhibited different patterns of recruitment, with slow, intermediate and fast secondary motoneurons being recruited progressively as the fictive locomotion frequency increased, while fast primary motoneurons were recruited only during presumed escapes. Moreover the distribution of these different motoneurons pools also followed a ventro-dorsal gradient, from slow secondary motoneurons to fast primary motoneurons (Ampatzis et al., 2013; Gabriel et al., 2011).

Apart from premotor interneurons, other populations of interneurons are also rhythmically activated during fictive locomotion. Glycinergic “circumferential ascending (CiA) interneurons, that are *Engrailed-1* positive interneurons derived from the V0 transcription domain, monosynaptically inhibit “commissural primary ascending” (CoPA) interneurons during swimming (Higashijima et al., 2004). Remarkably, CoPA interneurons are glutamatergic interneurons relaying excitation from Rohon-Beard sensory neurons, therefore providing a connectivity pattern that would be consistent with a homologous sensorimotor gating pathway observed in the *Xenopus* tadpole (Li et al., 2002; 2004).

“Commissural local” (CoLo) interneurons are inhibitory glycinergic interneurons driven by gap junctional inputs from reticulospinal cells (Mauthner cells, see section 3.3) that have been shown to exert monosynaptic inhibition on contralateral primary motoneurons during fast swimming, thereby enhancing the efficiency of the escape responses (Satou et al., 2009). Lastly, Kolmer-Agduhr interneurons, which are GABAergic cells located next to the central canal and have cilia extending into the cerebrospinal fluid, have been shown to be able to trigger slow swim when optically stimulated (Wyart et al., 2009).

Many other subtypes of spinal interneurons have been identified and classified, mainly according to their morphology and neurotransmitter phenotype (Hale et al., 2001; Satou et al., 2013), but their implication into sensorimotor circuits remains to be elucidated.

3.1.2. A genetic toolbox for targeting populations of neurons

Considering the large number of cells involved into spinal sensorimotor circuits, even in a simple vertebrate such as the zebrafish, one crucial requirement to investigate their functional role is to be able to specifically target the neural subpopulation of interest. Rather than relying on morphological cues, identification of specific promoters, and new tools to efficiently generate and screen transgenic lines, have recently allowed researchers to take full advantage of the optical and genetic accessibility of the zebrafish model.

The most straightforward approach to target a given neuronal population is to identify a specific gene with selective expression in the population of interest, isolate its promoter sequence and generate a bacterial artificial chromosome (BAC) incorporating the putative promoter, the gene and an attached reporter such as GFP. The plasmid is then microinjected into embryos at the single-cell stage for homologous recombination to occur, and injected zebrafish are subsequently screened for fluorescence in order to establish the transgenic line (Asakawa et al., 2013). Such approach have been successfully used to produce transgenic lines labeling cranial motoneurons or trigeminal/Rohon-Beard sensory neurons under control of the *Islet-1* promoter (Higashijima et al., 2000). This transgenic line was then used to investigate the role of Rohon-Beard and trigeminal neurons in the sensorimotor escape circuitry (Douglass et al., 2008).

This BAC approach can be combined with the bipartite Gal4/UAS system, widely used in *drosophila*, which relies on the specific expression of the yeast Gal4 transcriptional activator to drive the expression of the reporter gene placed under the control of repetitive Gal4-responsive upstream activator sequences (UAS) (Asakawa

and Kawakami, 2009; Davison et al., 2007). Enhanced reporter expression can be obtained using Gal4-VP16 (Koster and Fraser, 2001) or Gal4FF (Asakawa and Kawakami, 2009) fusion sequences and multiple (14X) repeats of the UAS. Stable zebrafish transgenic lines using the Gal4/UAS system has been achieved using *Tol2*-mediated transposition: a plasmid carrying the *Tol2* element is injected in zebrafish embryos with the *Tol2* transposase mRNA, generating genome-wide insertions in the zebrafish genome (Asakawa et al., 2008; Kawakami et al., 2000). *Tol2*-mediated Gal4-UAS transgenesis has been used to successfully generate wide enhancer-trap screens, leading to identification of a large number of stable transgenic lines selectively labeling subsets of spinal neurons (Abe et al., 2011; Asakawa and Kawakami, 2009; Satou et al., 2013; Scott et al., 2007).

Another recent approach for genetic targeting of neurons in zebrafish is to combine viral gene delivery, using for instance rabies or sindbis viruses, together with the Tet system (Zhu et al., 2009). The Tet system works in a similar fashion to the Gal4/UAS system, with the transactivator (tTA) binding to the tTA-responder element (Ptet) to drive transcription of the downstream gene (Gossen and Bujard, 1992). However, the Tet system has the advantage of being able to be regulated with doxycycline, which binds to tTA and dramatically reduces its affinity to Ptet, turning off the expression of the gene of interest (Zhu et al., 2009). Interestingly, such silencing could also be used to generate sparse labeling in pan-neuronal *HuC* transgenic lines (Zhu et al., 2009). Combining the Tet and Gal4 systems provide exciting opportunities for combinatorial gene targeting of several neuronal populations of interest in zebrafish.

3.2. Optogenetic tools for monitoring and breaking neural circuits

3.2.1. Reporters: monitoring neural circuits

Monitoring neural activity can be indirectly achieved by measuring the intracellular level of calcium, since electrical activity of neurons lead to a calcium influx through voltage dependent calcium channels (Grienberger and Konnerth, 2012). This strategy has led to the elaboration of number of chemical calcium

indicators and genetically encoded calcium indicators (GECI) that have been successfully used in many different mammalian and non-mammalian animal models (Nakai et al., 2001; Tian et al., 2009) (Figure 4A). GECIs consist in engineered fluorescent proteins having two key features: their emission properties are modified depending upon the intracellular level of calcium, and their pattern of expression can be restricted using the above mentioned genetic toolbox. They include either permuted single fluorescent proteins whose fluorescence properties are modified when calcium is binding to Ca^{2+} recognition elements (Nagai et al., 2001), or pairs of fluorescent proteins in which conformational change induced by calcium binding leads to FRET (Förster Resonance Energy Transfer) mediated modification of fluorescence (Miyawaki et al., 1997)

The transparency of the zebrafish larva and its genetic accessibility make it an ideal model to use such optical tools for monitoring neural activity. In the first zebrafish study using a GECI (*cameleon*), expressed under the *islet-1* promoter (Higashijima et al., 2000) (see section 3.1.2), calcium transients could be observed within the spinal cord, in Rohon-Beard neurons activated by electrical cutaneous stimulation, and in motoneurons and CiD interneurons during escapes triggered by a mechanical head tap (Higashijima et al., 2003). Since this first study, GECIs have been extensively used in zebrafish to monitor neural activity in various behavioral paradigms, including investigating the role of the optic tectum in prey capture (Del Bene et al., 2010), performing brain-wide monitoring of neural dynamics in a sensorimotor virtual environment (Ahrens et al., 2012) or testing neural coding of odors by the olfactory bulb (Blumhagen et al., 2012). Targeted mutagenesis and high-throughput screening have led to the continuous improvement of GECIs such as the single fluorophore GCaMP family by optimizing their calcium affinity, kinetics and dynamic range (Akerboom et al., 2012; Muto et al., 2011; Nakai et al., 2001; Tian et al., 2009). From the first GCaMP (Nakai et al., 2001) to the current GCaMP6 (Chen et al., 2013), and including the generation of multi-color variants (Akerboom et al., 2013), the always improving GECIs arsenal now allow for monitoring of neural activity over a wide range of firing rates.

One major limitation of GECIs such as GCaMP, regarding in particular investigation of closed-loop sensorimotor behaviors *in vivo*, is the need for providing focal excitation to the fluorescent proteins. Indeed, this limitation implies constraining the neurons of interest to a given focal plane, either by partially embedding and/or paralyzing the animal. One alternative approach is to use the bioluminescent protein *aequorin-GFP*, derived from the jellyfish *Aequorea victoria* (Shimomura et al., 1962a). ApoAequorin, the naturally occurring complex of aequorin with GFP, binds to its substrate coelenterazine, which is then oxidized in the presence of calcium leading to the emission of a green photon by the GFP through chemiluminescence resonance energy transfer (CRET) (Baubet et al., 2000). Bioluminescence assays based on aequorin-GFP have been used for non-invasive monitoring of neural activity *in vitro* (Rogers et al., 2005), but also in restrained flies (Martin et al., 2007) and freely behaving mice (Rogers et al., 2007).

Taking advantage of this bioluminescence approach, monitoring of neural activity in freely behaving zebrafish larvae has been achieved by genetically targeting the expression of aequorin-GFP in a specific subset of neurons and simultaneously counting the number of photons emitted over time while recording the locomotor activity using a high-frequency camera (Naumann et al., 2010). Remarkably, the author could monitor the activity of a small group of hypocretin-positive neurons in the hypothalamus over several days, or combine a gated photomultiplier tube with stroboscopic illumination to record visually evoked behaviors (Naumann et al., 2010). While the aequorin allows for non-invasive monitoring of an entire population of neurons in a moving animal, it does not provide any spatial information, thus making the specificity of the genetic targeting a crucial limitation.

3.2.2. Actuators: breaking neural circuits

Besides monitoring neural activity, the optical and genetic accessibility of the zebrafish larva also constitute an optimal playground for optogenetic actuators, making it possible to selectively activate or inhibit genetically targeted neurons (Del Bene and Wyart, 2012; Portugues et al., 2013; Zhang et al., 2007a) (Figure 4B). Channelrhodopsin-2 (ChR2) is a light-gated channel derived from the unicellular alga

Chlamydomonas reinhardtii allowing non-specific influx of cations when illuminated with blue light (Li et al., 2005; Nagel et al., 2003). ChR2 can therefore be used to control a genetically targeted neuronal population with a millisecond timescale precision in a dynamic and reversible manner (Boyden et al., 2005). First tested in zebrafish to trigger escape responses by photo-activating Rohon-Beard neurons (Douglass et al., 2008), ChR2 has subsequently been used to investigate diverse behaviors such as the optokinetic response (Schoonheim et al., 2010) or odor responses modulation (Bundschuh et al., 2012). Synthetic excitatory actuators, obtained by combining a chemical ligand to a ionic channel, such as the light-gated ionotropic glutamate receptor (LiGluR, (Gorostiza et al., 2007; Szobota et al., 2007)) and the light-gated metabotropic glutamate receptor (LimGluR2, (Levitz et al., 2013)) have been successfully used to trigger neural activity in zebrafish. For instance, the potential role of Kolmer-Agduhr interneurons in modulating slow locomotion could be investigated by combining LiGluR activation and Gal4/UAS enhancer-trap transgenics (Wyart et al., 2009).

Optogenetics have also been used to selectively silence genetically targeted neurons in zebrafish, using the light-gated chloride pump halorhodopsin (NpHR), derived from the archaeobacterium *Natronomonas pharaonis* (Schobert and Lanyi, 1982; Slimko et al., 2002). NpHR hyperpolarizes neurons by pumping chloride ions upon activation with yellow light, leading to optical silencing. Interestingly, optical silencing with NpHR, and its improved variant eNpHR (Gradinaru et al., 2008), can be combined with photo-activation using ChR2 to provide a versatile optogenetic toolbox to dissect circuits within the same animal (Zhang et al., 2007b).

Such combined strategy has been successfully used in zebrafish to identify neurons in the hindbrain able to initiate locomotion through a rebound activity after eNpHR silencing (Arrenberg et al., 2009), or dissecting the mechanism of eye saccades during optokinetic response (Schoonheim et al., 2010). In those two studies, light was delivered using optic fibers to achieve a high spatial selectivity regarding the stimulated area. However, new microscopic techniques relying on light patterning with multi-mirror devices (Blumhagen et al., 2012; Martial and Hartell, 2012) or temporal focusing of two-photon excitation (Papagiakoumou et al., 2010) should

allow for more complex 2D stimulation patterns. Lastly, 3D optical stimulation with a high spatiotemporal resolution could be achieved by combining digital holography and temporal focusing (Oron et al., 2012), opening the way for simultaneous imaging and neural manipulation in multiple planes in vivo (Portugues et al., 2013).

3.3. The escape response as a model for sensorimotor integration

3.3.1. The escape response and its supraspinal control

The “escape response” is a stereotyped sensorimotor behavior whereby the animal aims to escape an approaching predator, which has been extensively described in many teleost fish species, including the goldfish and zebrafish (Eaton et al., 1977), but also in other anamniotic vertebrates such as the lamprey (Currie, 1991) or the *Xenopus* tadpole (Roberts et al., 2009). Escape responses in zebrafish can be elicited by several types of sensory stimuli, such as touch to the head or the tail (Bhatt et al., 2007), a water jet to the otic vesicle (Kohashi et al., 2012) or an auditory-vestibular stimulus produced by a sound vibration for instance (Satou et al., 2009). In the zebrafish larvae aged 6 to 9 days post-fertilization (dpf), it typically consists in an initial fast “C-shaped” bend, followed by a counter-bend in the opposite direction, and lastly a burst swim (Budick and O'Malley, 2000). Typical kinematics parameters for escapes in zebrafish larvae are: a mean angular velocity of $21.2^\circ/\text{ms}$, a mean duration until completion of the first bend of 10.4 ms, a mean counter-bend angle of 125.1° (Budick and O'Malley, 2000).

The role of reticulospinal neurons, and in particular the so-called “Mauthner cell” (M-cell), in the initiation of escape responses have been extensively documented, initially in the goldfish (Eaton et al., 2001; Korn and Faber, 2005). The M-cell and its homologs MiD2cm and MiD3cm are paired reticulospinal neurons, located respectively in hindbrain rhombomeres 4 to 6, sending their descending axons to the contralateral spinal cord. The M-cells receive excitatory inputs from the auditory and vestibular branches of the VIII nerve, the posterior lateral line, and the optic tectum (Nakayama and Oda, 2004).

In zebrafish larvae that were head-embedded in agar with the tail free to move, monitoring of neural activity in reticulospinal cells by calcium imaging has demonstrated that, while M-cells were activated by both head and tail mechanical stimuli, its homologs MiD2cm and MiD3cm were only activated by head taps (O'Malley et al., 1996). Ablation studies confirmed this differential descending control, showing that laser ablation of the whole array led to delayed escape responses elicited from both head and tail touch stimuli, while ablation of the M-cell only increased the latency of tail-induced escapes only (Liu and Fetcho, 1999). These results suggest that the Mauthner homologs can drive escape responses induced by mechanical head stimuli without the need for the M-cell. Remarkably, even ablation of the whole M-array was not sufficient to completely suppress the escape responses.

Recent studies by the group of Oda (Kohashi and Oda, 2008; Kohashi et al., 2012; Nakayama and Oda, 2004) further refined our understanding of the descending control of this multimodal sensorimotor behavior. Using simultaneous calcium imaging of reticulospinal neurons and high-speed video recording of actual escapes elicited by a water jet to the otic vesicle, the authors demonstrated that activation of the Mauthner cell led to fast-onset (4-8 ms) escapes while activity in the MiD3cm homolog gave rise to delayed escapes (8-12 ms), and that these activation were mutually exclusive (Kohashi and Oda, 2008). Interestingly, the authors subsequently showed that: 1) before 75 hours post-fertilization (hpf), suppression of auditory-vestibular inputs by selective ablation of the otic vesicle did not increase escapes latency, whereas ablating the trigeminal ganglia responsible for relaying tactile input did; 2) after 90 hpf, eliminating auditory-vestibular inputs increased escapes latency, whereas suppressing tactile input did not. These results therefore suggest a dual control of the escape behavior, switching during development from a preferentially tactile-driven, long-latency, non-M escape to a preferentially auditory-vestibular driven, short-latency, M-dependent pathway (Kohashi et al., 2012).

3.3.2. Monitoring spinal neurons during active locomotion

The ability to simultaneously record active locomotor behavior and monitor neural activity in partially restrained zebrafish has proven very valuable to dissect the descending motor and sensory control of escape responses. Similar head-embedded experimental paradigms have also been used to investigate the recruitment of spinal interneurons during active locomotion (Bhatt et al., 2007; Ritter et al., 2001) (see section 3.1.1). Although studies based on calcium imaging of either hindbrain or spinal neurons in partially restrained animals has been an important step forward in the study of sensorimotor behaviors such as the escape response, they did not provide information about neural activity in the moving tail of the fish, therefore discarding segmental sensory feedback due to locomotion itself.

Even though an attempt to indirectly monitor neural circuits involved underlying escape responses in freely swimming zebrafish larvae has been reported using electric field potentials recordings (Issa et al., 2011), this technique did not provide specific information about the nature of the neurons involved.

However, new techniques such as bioluminescent monitoring of genetically targeted neurons with aequorin-GFP (see section 3.2.1) could prove helpful in providing specific monitoring of neural activity in actively moving animals, whether head-restrained or freely swimming. Indeed, using an experimental setup adapted from Naumann et al. (2010) in which escape responses were elicited in head-embedded zebrafish larvae either by a water jet to the otic vesicle or an auditory-vestibular sound stimulus, we can simultaneously record detailed quantitative kinematics parameters and count photons emitted by the aequorin-GFP. Taking advantage of the Gal4/UAS system to restrict the expression of aequorin-GFP to motoneurons, we could obtain bioluminescence signals following the recruitment of spinal motoneurons (Figure 5, Knafo et al. *unpublished*). This approach could prove particularly useful to investigate the recruitment of sensory spinal neurons during active locomotion, and question whether sensory feedback from the moving part of the tail does actually modulate locomotion.

Conclusion

The ability to monitor active behaviors in vivo with precise kinematics also provides a new framework in which results obtained from fictive recordings could be validated in order to confirm their environmental relevance. Moreover, the variability observed in real-world locomotor behaviors also questions whether “hard-wired” connectivity diagrams are actually the most suitable mean of modeling sensorimotor integration (Marder and Taylor, 2011). The emergence of multifunctional neuronal populations, i.e. neurons that are recruited during multiple behaviors (Liao and Fetcho, 2008), as opposed to specialized neurons that are only active for a given motor output (Satou et al., 2009), will also benefit from in vivo studies involving active locomotion, in which multiple behaviors can be tested within the same animal (Briggman and Kristan, 2008).

The advances in genetic targeting and the identification of molecular markers to classify homologous populations of spinal neurons have allowed bringing together results obtained across animal models. However, the extent to which the walking CPG of mammalian vertebrates (such as rodents and cats) and the swimming CPG of non-mammalian vertebrates (such lampreys, zebrafish or tadpoles) can mutually inform each other remains unclear. In this regard, amphibian metamorphosis, during which the swimming CPG of a tadpole is transformed into a frog walking CPG, could provide an intriguing and unique model (Sillar et al., 2008).

Sensorimotor behaviors are inherently a closed-loop process, where sensory feedback heavily influence the motor output. Although spinal networks do integrate this sensory information to modulate locomotion, detailed access to spinal sensorimotor circuitry has so far been only possible in open-loop preparations, where the sensory feedback was not taken into account. New tools, such as optogenetic reporters and actuators, combined to genetically accessible animal models, such as zebrafish, should provide bright opportunities for monitoring targeted spinal sensorimotor neurons in actively moving animals, and, possibly, closing the loop.

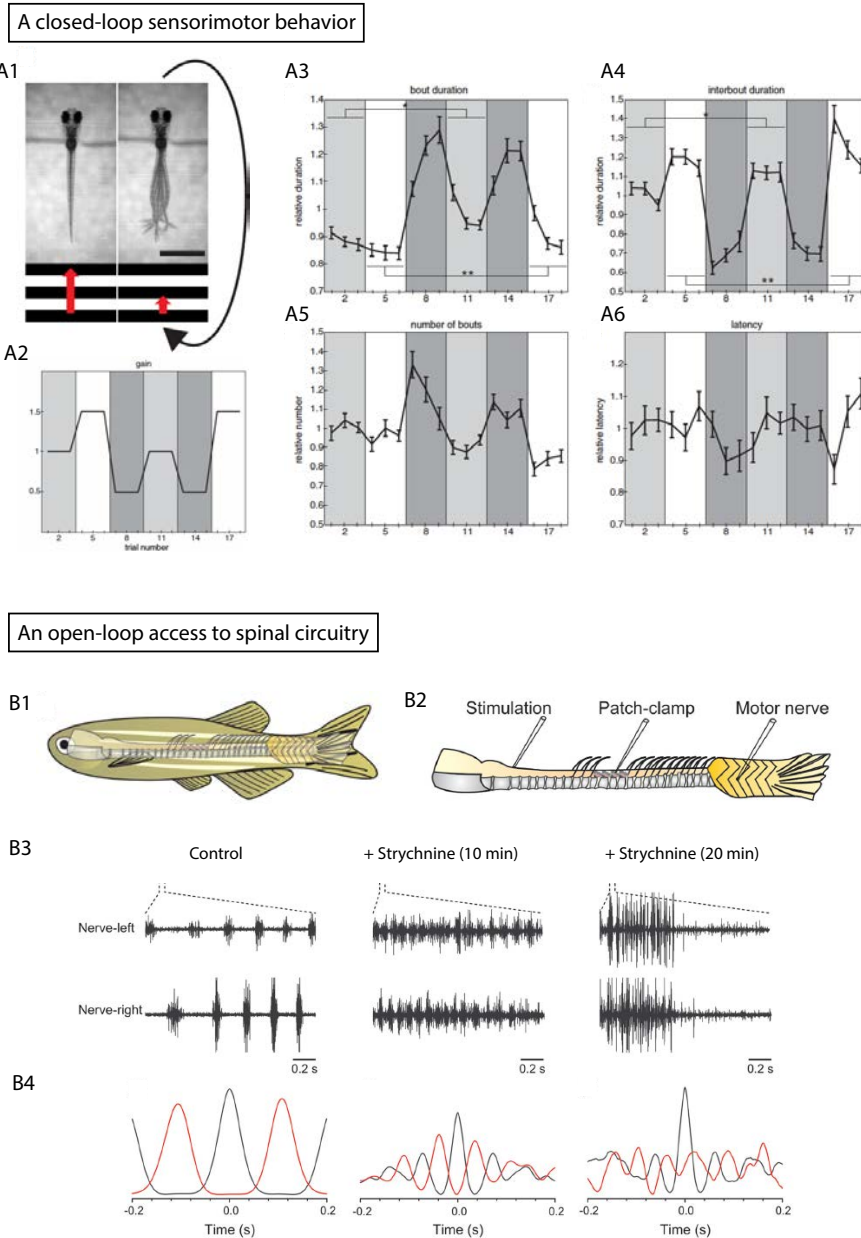


Figure 1. Closed-loop sensorimotor behaviors versus open-loop access to neural circuitry

A. A closed-loop virtual reality paradigm in the zebrafish larva. A moving visual stimulus is showed to a head-embedded larva (aged 6-7 days post-fertilization) while its behavior is monitored and its speed (red arrow) is modified by the swimming speed of the larva (A1). In this virtual closed-loop environment, a “gain” is used as a constant factor to adjust the grating speed to the larval swimming speed (A2). For 3 different gains, several kinematics parameters of the larvae locomotor output are modified consistently: bout duration (A3), interbout duration (A4), number of bouts (A5) and latency (A6). *Adapted from Portugues et al. 2011.*

B. An open-loop experimental fictive preparation for accessing spinal circuits. To record from spinal neurons in a juvenile zebrafish (aged 8-15 weeks), the skin and muscles are dissected out to expose the isolated spinal cord (B1), and a stimulating electrode (1s, 40Hz) is placed at the junction with brainstem to elicit episodes of “fictive” swimming, while the motor output can be recorded from the ventral nerve root or from patched-clamp spinal neurons (B2). Bath application of pharmacological substances, such as the glycinergic antagonist strychnine, is used to modify the fictive motor output on the ventral nerve root recordings (B3). Short (10 minutes) application of strychnine results in increased swimming burst frequency, while longer application (20 minutes) leads to a decreased duration of the swimming episode as well as disruption of the left-right alternation (B4). *Adapted from* (Kyriakatos et al., 2011).

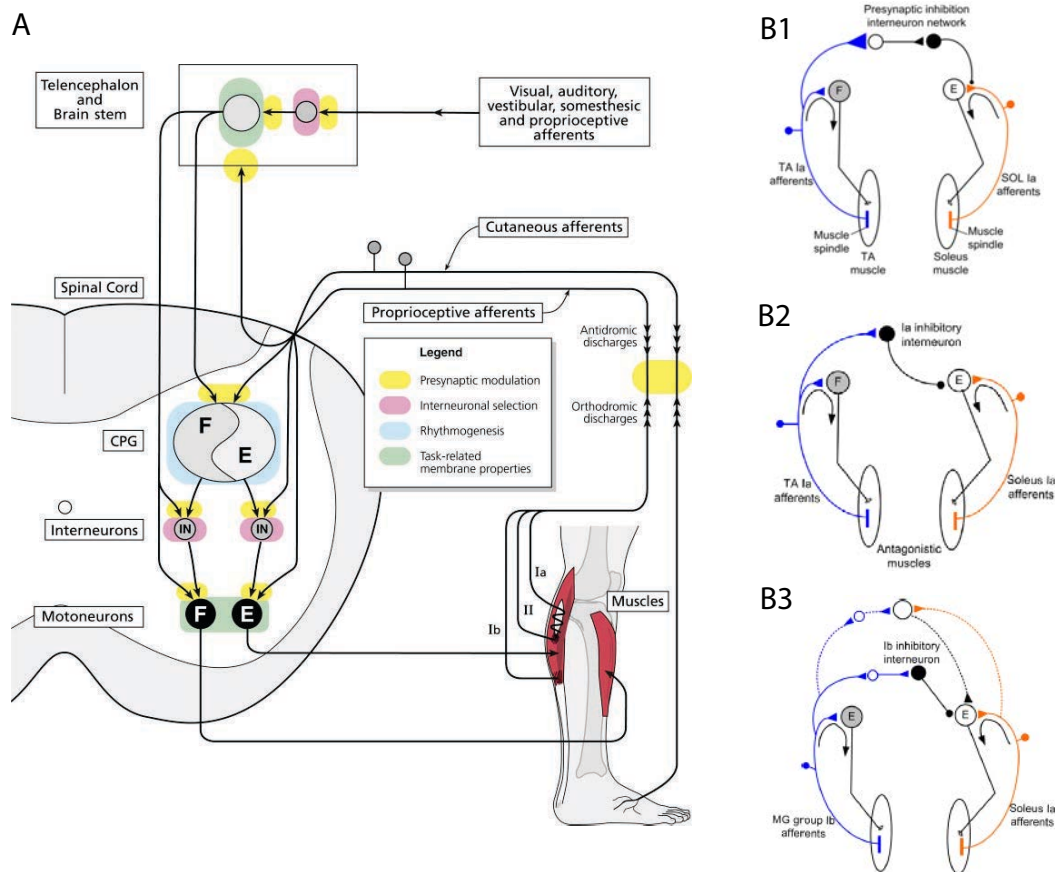


Figure 2. Descending and ascending inputs to spinal circuits involved in sensorimotor reflexes

A. Motor and sensory inputs to spinal neurons and sites for sensorimotor integration. Descending motor control from the corticospinal and rubrospinal tracts (in the dorsolateral funiculus) and reticulospinal and vestibulospinal tracts (in the the ventrolateral funiculus) are integrated with ascending sensory inputs from proprioceptive afferents Ia and II (from muscle spindles) and Ib (from Golgi tendon organs) at various premotor locations. *Adapted from Rossignol et al. 2006*

B. Some spinal sensorimotor reflexes and underlying interneuronal networks. Presynaptic inhibition of sensory afferents by GABAergic premotor interneurons in the intermediate laminae of the spinal cord is a common control mechanism for filtering sensory inputs (B1). Reciprocal Ia inhibition by glycinergic interneurons allows for antagonist muscles inhibition during a flexion movement (B2). Non-reciprocal Ib inhibition facilitates synergist muscle contraction though polysynaptic pathways (B3).

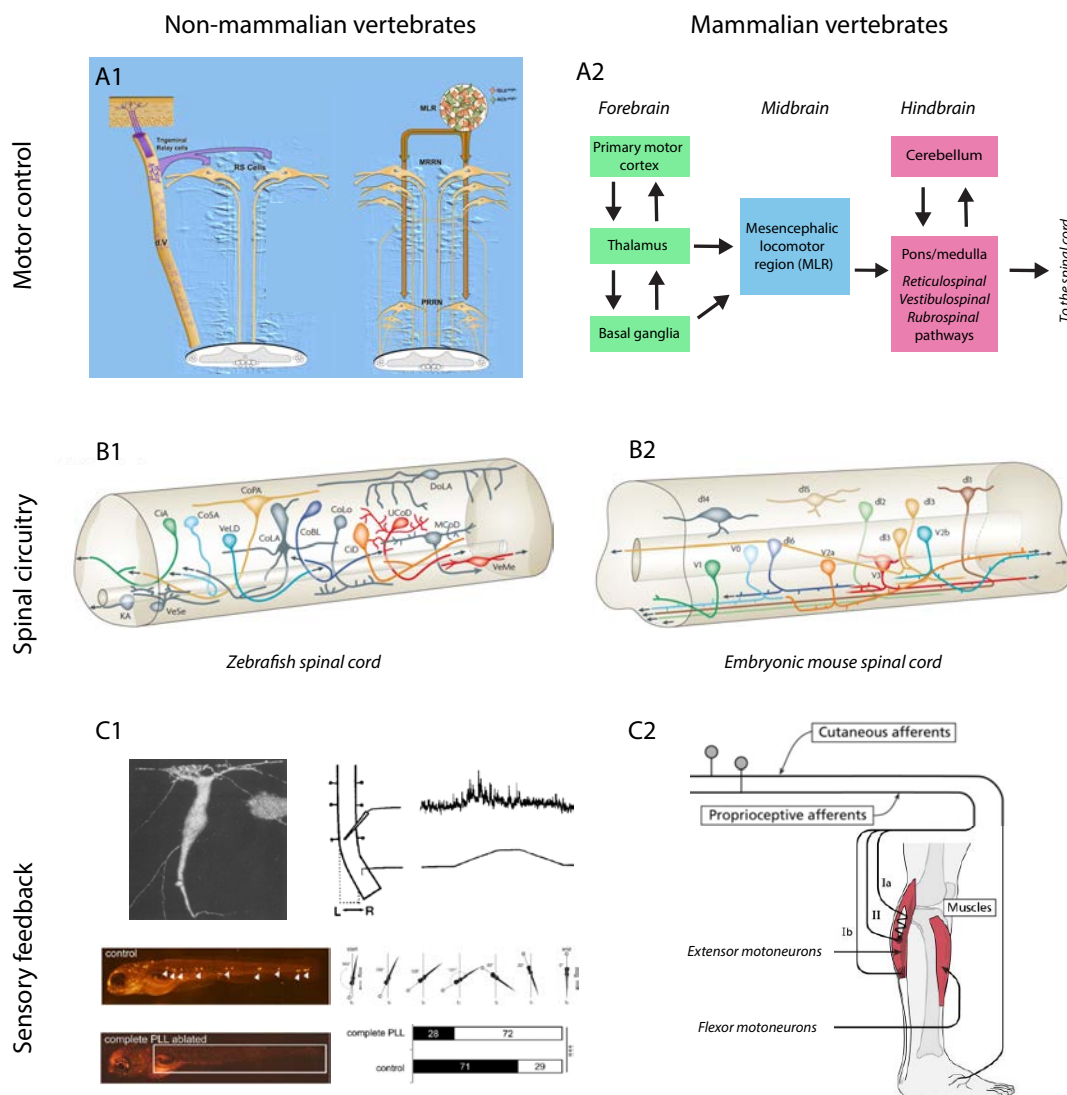


Figure 3. Neural substrates of spinal sensorimotor integration across vertebrates

A. Descending motor control. In the lamprey, a mechanical stimulation to the head activates reticulospinal neurons through the trigeminal nerve, eliciting escapes responses in an all-or-nothing fashion (A1 left). Swimming episodes can also be elicited by stimulating the Mesencephalic Locomotor Region (MLR), which projects onto reticulospinal neurons in the middle and posterior rhombencephalic reticular nuclei with a graded synaptic input (A1, right) *Adapted from Dubuc et al. 2008.* In mammalian vertebrates, forebrain regions such as the primary motor cortex can initiate locomotion by projection on the MLR, which in turn activate descending motor pathways that modulate the spinal circuitry (A2). *Adapted from Goulding, 2009.*

B. Intraspinal circuitry. Based on this molecular homology, similar neuronal cell types can be identified in the zebrafish (B1) and mouse (B2) spinal cords, as indicated by the same color in the schematic. Zebrafish homologs of the mouse interneurons are: CoSA/MCoD (V0), CiA (V1), CiD (V2a), VeLD (V2b), UCoD/VeMe (V3). *Adapted from Goulding, 2009*

C. Ascending sensory feedback. In the lamprey, intraspinal stretch receptors called the “edge cells” are activated upon mechanical bending of the spinal cord and could serve as mechanoreceptor during swimming (C1, top. *Adapted from Grillner et al. 1984 and Di Prisco et al. 1990*). In the zebrafish, the lateral line can be used to sense the water flow and provide feedback for rheotaxis behavior. (C1, bottom. *Adapted from Olszewski et al. 2012*). In mammalian vertebrates, cutaneous and proprioceptive muscle receptors provide sensory feedback to the spinal circuitry and can modulate the motor output in a phase and state-dependent manner (C2. *Adapted from Rossignol et al. 2006*).

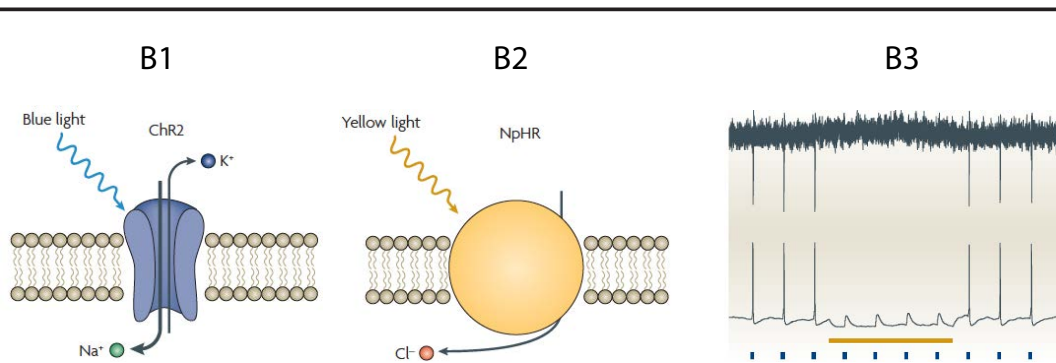
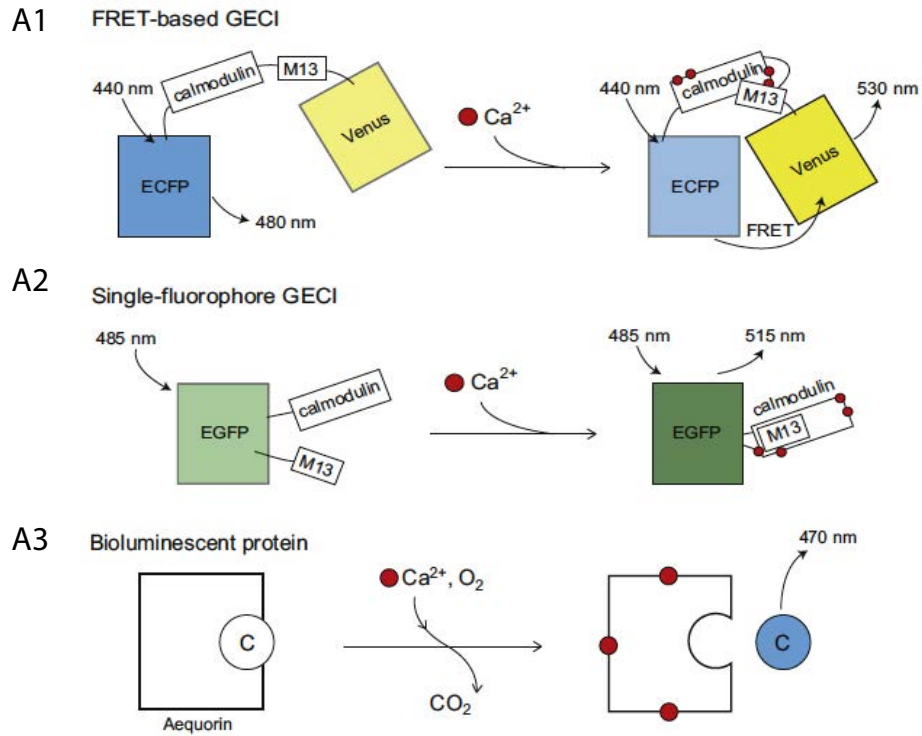


Figure 4. Monitoring and breaking neural circuits with genetically encoded reporters and actuators

A. Calcium indicators. Genetically encoded calcium indicators (GECIs) allows for monitoring neural activity through changes in intracellular calcium concentration. In a FRET-based GECI (A1), such as *Cameleon*, a conformational change occurs after calcium ions binding between the two fluorescent proteins, leading to Förster resonance energy transfer, with a decrease in the 480 nm fluorescence and an increase in the 530 nm fluorescence. In a single-fluorophore GECI (A2), such as *GCaMP*, conformational modification upon calcium binding is intra-molecular, leading to an increase in the emitted fluorescence (515 nm). Bioluminescent GECIs, such as *aequorin*, binding of calcium ions leads to oxidation of coelenterazine. Chemiluminescence resonance energy transfer (CRET) between

aequorin and GFP is responsible for the emission of a green photon. *Adapted from Grienberger et al. 2012*

B. Optogenetic actuators. Following illumination with blue light (470 nm, blue pulses in B3), channelrhodopsin-2 allows the entry of cations into the cell (B1), triggering action potentials in whole-cell current-clamp (B3). Following illumination with yellow light (580 nm, yellow line in B3), halorhodopsin pumps chloride anions (B2), leading to neural silencing (B3). *Adapted from Zhang et al. 2007*

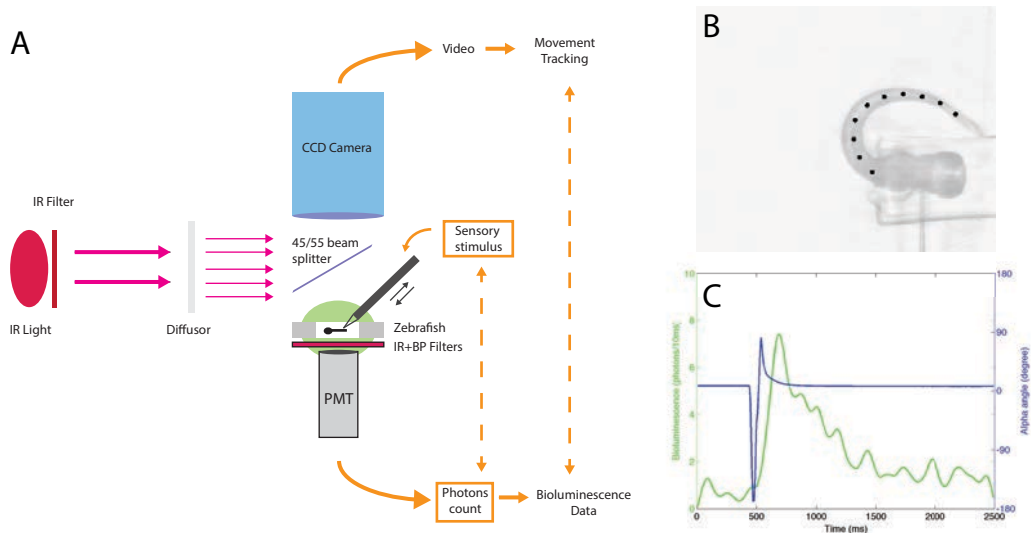


Figure 5. Monitoring the activity of spinal neurons during active escape responses in zebrafish

(A) A setup for simultaneously recording active locomotion using a high-speed camera and custom tracking software (B), while counting photons emitted by spinal motoneurons during escape responses in the transgenic line 1020;gal4/UAS:aequorin-GFP. (C) In blue: alpha angle (in degree) between the first and last points of the tail over time, superimposed with the bioluminescent signal in green (number of photons emitted /10 ms)

Part B.

Mechanosensory neurons enhance motor output in the zebrafish spinal cord during active locomotion

Abstract

Vertebrate locomotion relies on central pattern generators (CPGs) located in the spinal cord. Although there is converging evidence that mechanosensory feedback modulates the activity of CPGs, the mechanisms occurring at the circuit level are not well understood. One challenge lies in the fact that traditional electrophysiological techniques performed during so-called “fictive” locomotion do not allow the recording of identified neurons in the spinal cord of moving animals. Here we overcome this limitation by genetically targeting the bioluminescent sensor GFP-Aequorin to achieve selective and non-invasive monitoring of spinal motor and sensory neurons during active locomotion in larval zebrafish. By combining this technique with GCaMP imaging of individual neurons, we validate that the bioluminescence signal emitted by spinal motor neurons reflects the differential recruitment of motor pools during motion. We show a major reduction in bioluminescence signals recorded from spinal motor neurons in paralyzed animals and immotile mutants, demonstrating that mechanosensory feedback enhances the recruitment of motor neurons during active locomotion. Accordingly, we confirm using bioluminescence monitoring and GCaMP imaging that spinal mechanosensory neurons are recruited in moving larvae while silenced in paralyzed animals. Moreover, we also demonstrate that silencing mechanosensory neurons impairs escape responses in freely moving larvae. Altogether, these results shed light on the contribution of mechanosensory feedback to motor output during motion, and the resulting differences between active and fictive locomotion.

1. Introduction

Although the basic motor rhythm controlling flexion and extension can be produced by spinal central pattern generators in the absence of sensory inputs (Delcomyn, 1980), stimulation of peripheral afferents has the potential to control the amplitude and timing of motor output during ongoing locomotion (Grillner and Rossignol, 1978; Lundberg, 1979; Schomburg et al., 1998). However, electrophysiological investigation of spinal circuits typically rely on preparations where muscles are paralyzed or dissected out, thus abolishing the contribution of mechanosensory feedback caused by movement of the animal (Grillner, 2003). Although electromyogram recordings have been conducted in cats (Grillner and Rossignol, 1978), lampreys (Wallén and Williams, 1984), and rodents (Courtine et al., 2009a), recordings of identified motor and sensory neurons in the spinal cord have not been performed during active locomotion.

Recent advances in optogenetic sensors and actuators have enabled recording and stimulation of genetically identified neurons in freely behaving animals (Szabo et al., 2014). In particular, Aequorin is a bioluminescent calcium sensor derived from the jellyfish *Aequorea victoria* (Shimomura et al., 1962a). Upon neuronal activation, calcium binding leads to the oxidation of Aequorin substrate, coelenterazine, and subsequent chemiluminescence resonance energy transfer to a fused GFP results in the emission of a green photon (Baubet et al., 2000). Non-invasive bioluminescence neural monitoring has been conducted in restrained flies (Martin et al., 2007), mice (Rogers et al., 2007) and in freely swimming larval zebrafish (Naumann et al., 2010).

Here, we combined bioluminescence monitoring with genetic targeting of spinal neurons to investigate the recruitment of motor and mechanosensory neurons in motile and immotile zebrafish larvae. Non-invasive bioluminescence recording of spinal motor neurons during various locomotor behaviors and comparison with calcium imaging monitoring at the cellular level shows that the amplitudes of bioluminescence signals reflect the intensity and number of recruited cells. We tested whether the loss of mechanosensory feedback would affect spinal motor neuron recruitment and observed that bioluminescence signals were increased in motile

compared to paralyzed larvae and immotile mutants. Accordingly, using bioluminescence and GCaMP monitoring in moving animals, we showed that spinal mechanosensory neurons were recruited during active but not fictive locomotion. Altogether, our data suggest a mechanosensory loop enhancing motor neurons recruitment during active locomotion.

2. Results

2.1. *Bioluminescence signals reflect the level of recruitment of motor neurons during movement*

In *Tg(mnx1:Gal4, UAS:GFP-Aequorin-opt)* 4 dpf larvae we simultaneously recorded bioluminescence signals from the population of motor neurons and behavior during escapes elicited by an acoustic stimulus (see *Methods* and Fig. 1A, B). We observed three categories of behavioral responses: *i*) escapes ; *ii*) C-bends ; and *iii*) slow swims (Budick and O'Malley, 2000) (Fig. 1D ; Suppl. Table 1, n = 10 larvae). Each behavioral category was associated with different bioluminescence amplitudes (Fig. 1E), while the time-to-peak and the time decay of the signals remained approximately constant (Suppl. Fig. 1, A and B). Mean amplitude was higher for C-bends and escapes than slow swims (Fig. 1F). For all maneuvers, and within each category, bioluminescence signal amplitude correlated with the maximal angle of the tail bend (Fig. 1G). These data suggest greater recruitment of spinal motor neurons during behaviors with larger tail bends. However, bioluminescence monitoring lacks the single cell resolution to determine whether this increase in recruitment is due to a larger population of neurons being active.

We therefore performed calcium imaging in 4 dpf *Tg(mnx1:Gal4, UAS:GCaMP6f;cryaa:mCherry)* during fictive spontaneous slow swimming and fictive evoked escapes (Supp. Fig 2A, Supp. Fig. 2B). The locomotor burst frequency ranged between 20-30 Hz for slow swims (left panel, Fig 2A, (Masino and Fetcho, 2005)) and gradually decreased from 40-80 Hz to 20 Hz for escapes (right panel Fig. 2A). During slow swims, a small fraction of ventrally located motor neurons was active (Fig. 2, B and C, right panels). In contrast, the majority of the motor pool,

including large dorsal motor neurons, was recruited during escapes (Fig. 2, B and C, left panels). The dorsal motor neurons having larger calcium transients than ventral motor neurons (Fig. 2D), the mean $\Delta F/F$ amplitude was higher during escapes than slow swims across larvae (Fig. 2E) and within each larva (Supp. Fig. 2D). Calcium imaging in a fictive preparation demonstrates greater motor neuron recruitment during escapes than slow swims, resulting from a larger population of active cells and elevated calcium transients. The combination of these two phenomena could explain the increase in bioluminescence amplitudes for movements with larger tail bends.

2.2. Spinal motor neurons recruitment is enhanced in the presence of mechanosensory feedback

We next tested if the global recruitment of spinal motor neurons differed in actively moving versus immotile animals (Fig. 3A). In 4 dpf Tg(*mnx1:Gal4*, *UAS:GFP-Aequorin-opt*) larva, we performed the bioluminescence acoustic assay before and after paralysis induced by bath application of pancuronium bromide. Across all ten larvae, mean bioluminescence amplitude was markedly decreased in paralyzed compared to motile animals (Fig. 3, B and C). Within each larva, the mean normalized bioluminescence amplitude was decreased seven-fold (0.056 ± 0.08 versus 0.36 ± 0.18 , $p < 0.001$).

Since pancuronium bromide acts on the alpha 7 subunit of the acetylcholine receptor, we conducted additional experiments in immotile *Relaxed* (*cacnb1^{ts25}*) mutant zebrafish (Granato et al., 1996). Similarly to paralyzed larvae, the mean bioluminescence amplitude was markedly decreased in the triple transgenic Tg(*cacnb1^{ts25/ts25}*, *mnx1:Gal4*, *UAS:GFP-Aequorin-opt*) immotile larvae compared to control motile siblings Tg(*cacnb1^{+/+}* or *cacnb1^{ts25/+}*, *mnx1:Gal4*, *UAS:GFP-Aequorin-opt*) (Fig. 3, D and E). Altogether, these results demonstrate that spinal motor neurons recruitment is enhanced in active compared to fictive locomotion in the same experimental conditions.

2.3. Mechanosensory neurons are recruited during active but not fictive locomotion

We tested whether spinal mechanosensory neurons were recruited during active locomotion. We used the *Isl2b* promoter to target the expression of GFP-Aequorin to Rohon-Beard neurons and dorsal root ganglia in the spinal cord as well as trigeminal ganglia in the head (Fig. 4, A and B). We confirmed that there was no muscle expression by doing immunohistochemistry on GFP (Fig. 4B). In 4 dpf *Tg(Isl2b:Gal4, cmlc2:eGFP, UAS:GFP-Aequorin-opt)* we observed bioluminescence signals emitted by these mechanosensory neurons during active locomotion. Upon paralysis, the bioluminescence signals were abolished in all trials (Fig. 4, C and D). Moreover, the amplitude of bioluminescence signals emitted by mechanosensory neurons correlated with the amplitude of movements (Fig. 4E).

To determine which population of sensory neurons is active during locomotion we designed a calcium imaging setup to record from both trigeminal neurons in the agar-embedded head and Rohon-Beard neurons in the freely moving tail. We used 4 dpf *Tg(Isl2b:Gal4, cmlc2:eGFP, UAS:mRFP, UAS:GCaMP5)* larvae to record calcium activity in the green channel while correcting for shifts in the focal plane using the red channel to monitor cell position (Fig. 5, A and B, and *Methods*). We found that 32.5% of monitored spinal mechanosensory neurons, called Rohon-Beard neurons in zebrafish, were active ($\Delta F/F \geq 25\%$) during acoustic evoked escapes. Consistent with our bioluminescence results, most of the cells became silent after paralysis (4.3% of active cells in paralyzed larvae, Fig. 5, C and D). The mean $\Delta F/F$ amplitude in active Rohon-Beard neurons was also markedly reduced after paralysis (Fig. 5E). Similarly, trigeminal neurons showed activation only when the fish was actively moving, although significantly lower than in spinal Rohon-Beard neurons (23.2% of active cells, Supp. Fig. 3).

Altogether, these data demonstrate that spinal and trigeminal mechanosensory neurons are recruited during active but not fictive locomotion suggesting that they might underlie spinal motoneurons differential recruitment.

2.4. Silencing mechanosensory neurons impairs escape responses

Therefore, we finally tested whether silencing mechanosensory neurons could affect behavior in freely swimming larvae. In *Tg(Isl2b:Gal4, cmlc2:eGFP, UAS:BoTxLCB-GFP)* larvae, expression of botulinum toxin light chain B in mechanosensory neurons blocks vesicle release resulting in silencing their activity (see Methods). We found that several kinematic parameters of acoustic elicited escapes in 5 dpf *Tg(Isl2b:Gal4, cmlc2:eGFP, UAS:BoTxLCB-GFP)* larvae were decreased compared to *Tg(Isl2b:Gal4, cmlc2:eGFP)* siblings : mean escape speed, mean tail beat frequency and mean number of bends were lower in larvae where mechanosensory neurons were silenced (Fig. 4, A and B). Interestingly, while the mean initial C-bend angle was similar in both groups, the mean amplitude of the subsequent counter-bend was decreased in *Tg(Isl2b:Gal4, cmlc2:eGFP, UAS:BoTxLCB-GFP)* larvae (Fig. 4, C and D). These results suggest that mechanosensory neurons might enhance escapes efficiency by recruiting contralateral primary motor neurons through Commissural Primary Ascending (CoPA) interneurons in the moving spinal cord (Fig. 4, E and F).

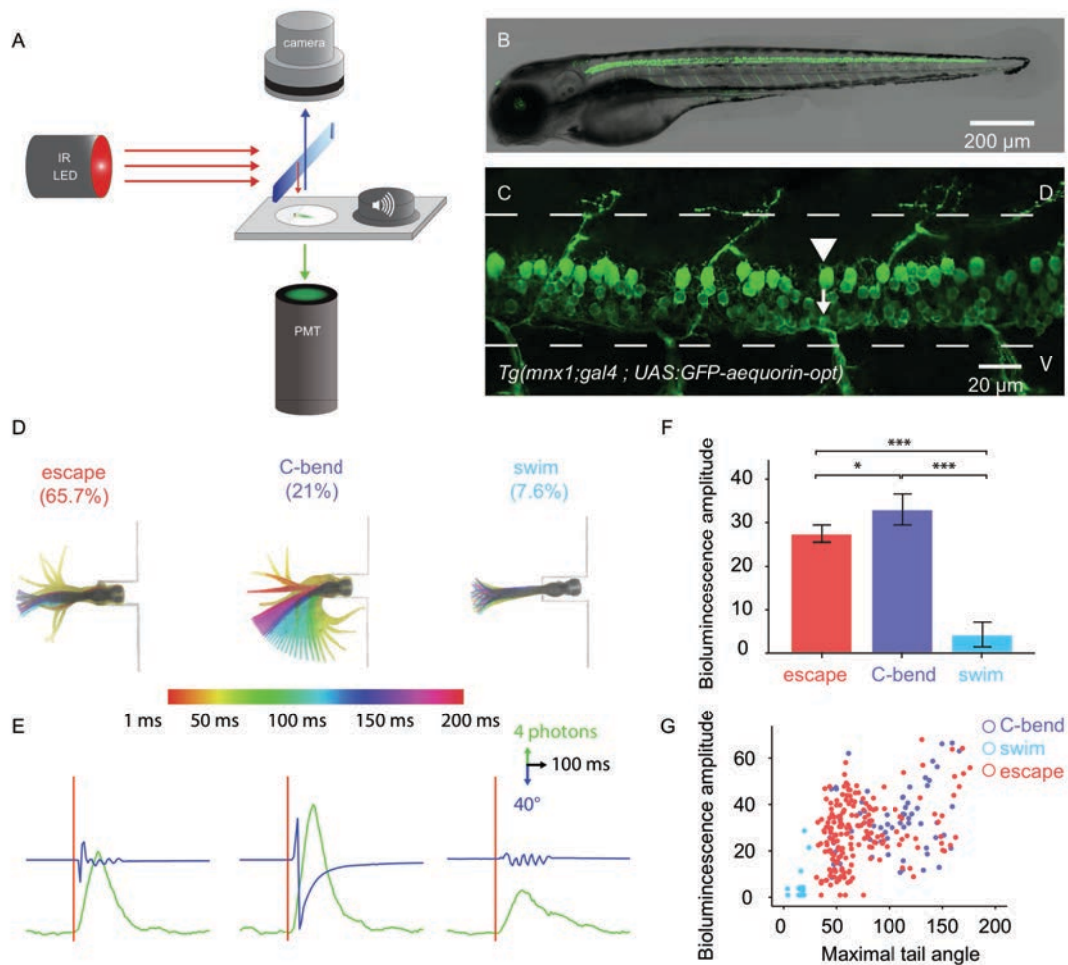


Figure 1. Bioluminescence monitoring of spinal motor neurons during active locomotion discriminates distinct behaviors

A. Design of the setup: upon acoustic stimulation (500 Hz, 10 ms), behavioral responses were recorded from above under infrared illumination using a high-speed (1000 Hz) camera, while photons emitted by GFP-Aequorin were simultaneously collected from below by a photomultiplier tube (PMT). **B.** *In vivo* fluorescent image and **C.** Immunostaining for GFP in 4 dpf *Tg(mnx1:Gal4, UAS:GFP-Aequorin-opt)* zebrafish larva show selective expression of GFP-Aequorin in all spinal motor neuron populations (arrowheads: dorsal primary motor neurons, arrows: ventral secondary motor neurons), with no expression in muscle fibers. **D.** Automated categorization based on maximum tail angle and number of cycles classified maneuvers into escapes (65.7%; $n = 197 / 300$), C-bends (21%; $n = 63 / 300$) and swims (7.7%; $n = 23 / 300$, $n = 10$ larvae with 30 trials each). **E.** Different bioluminescence signals and kinematic parameters were observed for each category. **F.** Mean bioluminescence amplitude was higher for C-bends (32.6 ± 1.8 photons / 10 ms; normalized amplitude per larva = 0.54 ± 0.04) and escapes (27.0 ± 1.0 photons / 10 ms; normalized amplitude = 0.36 ± 0.02) than slow swims ($3.9 \pm$

1.4 photons / 10 ms, $p = 0.002$; normalized amplitude = 0.06 ± 0.02 , $p = 0.014$). **G.** Correlation between bioluminescence signal amplitude and maximum tail angle amplitude ($R = 0.4$, $p < 0.001$) discriminate the three behavioral responses.

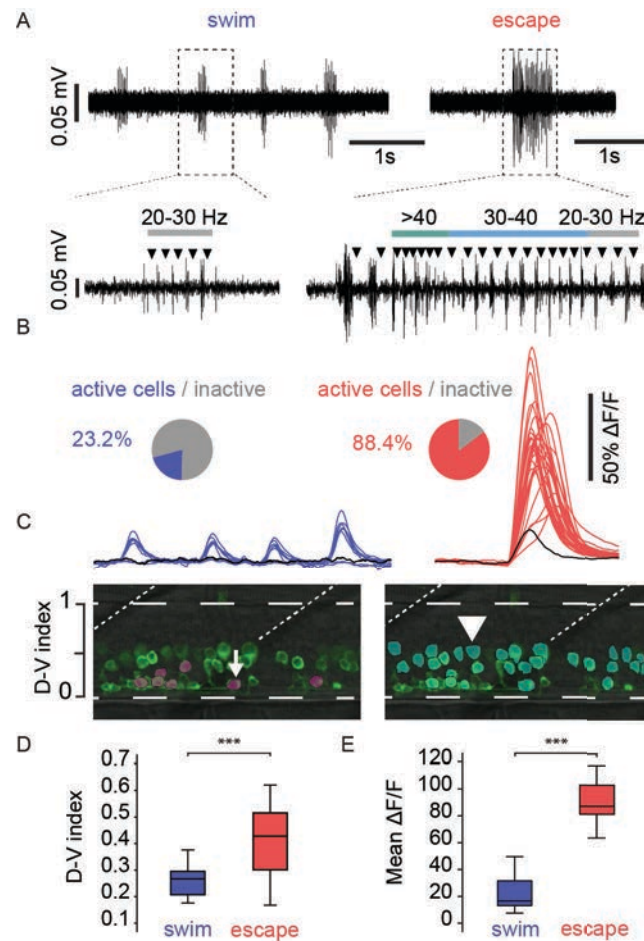


Figure 2. Calcium imaging of spinal motor neurons during fictive locomotion reveals specific patterns of recruitment for escape and slow swims

A. VNR traces for each behavior are enlarged to illustrate the different components during escapes and slow swims. Fictive locomotor frequencies ranged between 15 and 30 Hz for slow swims while they spanned from very slow (< 10 Hz) during the initial bends to very fast (> 40 Hz) gradually decaying to 15 Hz during the escapes. **B.** GCaMP6F signals from individual motor neurons aligned with VNR profile. Pie charts represent the proportion of active cells in each behavior: 16/69 cells across 27 swims versus 61/69 cells across 12 escapes, $n = 3$ larvae. **C.** Maps of motor neuron recruitment during fictive slow swimming and evoked escape. Active cells were highlighted with colors during each behavior (magenta for slow swimming, green for escapes). Black traces represent the spurious signals originating from light scattering in other planes and recorded in ventral and dorsal background regions for slow swimming and escapes respectively. **D.** Graph illustrating the D-V position of cells recruited during each behavior shows dorsal motor neurons are only recruited during escapes (mean D-V position for escapes = 0.41 ± 0.02 versus 0.25 ± 0.01 , $p < 0.001$, $n = 78$ cells in $n = 3$ larvae). **E.** The mean $\Delta F/F$ amplitude was higher during escapes compared to spontaneous fictive swims across larvae ($91.2 \pm 4.7\%$ versus $25.9 \pm 3.8\%$, $p < 0.001$, 12 escapes and 78 slow swims in $n = 3$ larvae).

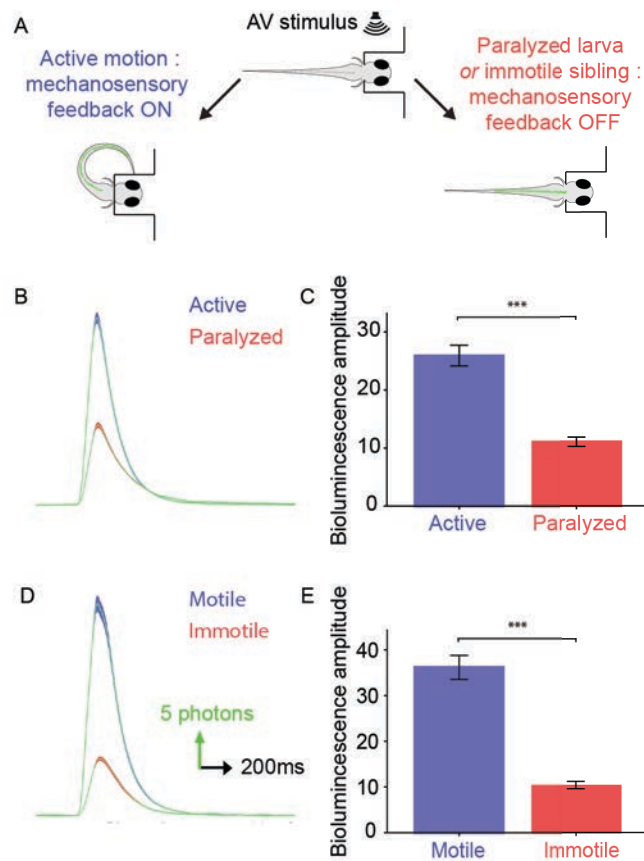


Figure 3. Spinal motor neurons recruitment is enhanced in the presence of mechanosensory feedback

A. To compare spinal motor neurons recruitment when mechanosensory feedback was present (“active locomotion”) or suppressed (“fictive locomotion”), we conducted bioluminescence assays before and after paralyzing the same animal with pancuronium bromide, and in immotile *Relaxed* (*cacnb1^{ts25/ts25}*) mutants compared to their motile siblings. **B.** Averaged bioluminescence signals traces in actively moving and paralyzed larvae revealed a marked decrease in bioluminescence amplitude after paralysis. **C.** Mean bioluminescence amplitude over 30 trials per larva in active versus fictive locomotion recorded in the same animals before and after paralysis (26.6 +/- 0.9 photons / 10 ms versus 11.1 +/- 0.4 photons / 10 ms, n = 10 larvae in each group, p < 0.001). **D.** Similarly, averaged bioluminescence signals were markedly decreased in immotile *Tg(cacnb1^{ts25/ts25}, mnx1:Gal4, UAS:GFP-Aequorin-opt)* mutant larvae when compared with the motile siblings. **E.** Mean bioluminescence amplitude in motile siblings (37.6 +/- 1.4 photons / 10 ms) and immotile mutants (9.8 +/- 0.4 photons / 10 ms, n = 300 trials in 10 larvae for each group, p = 0.001).

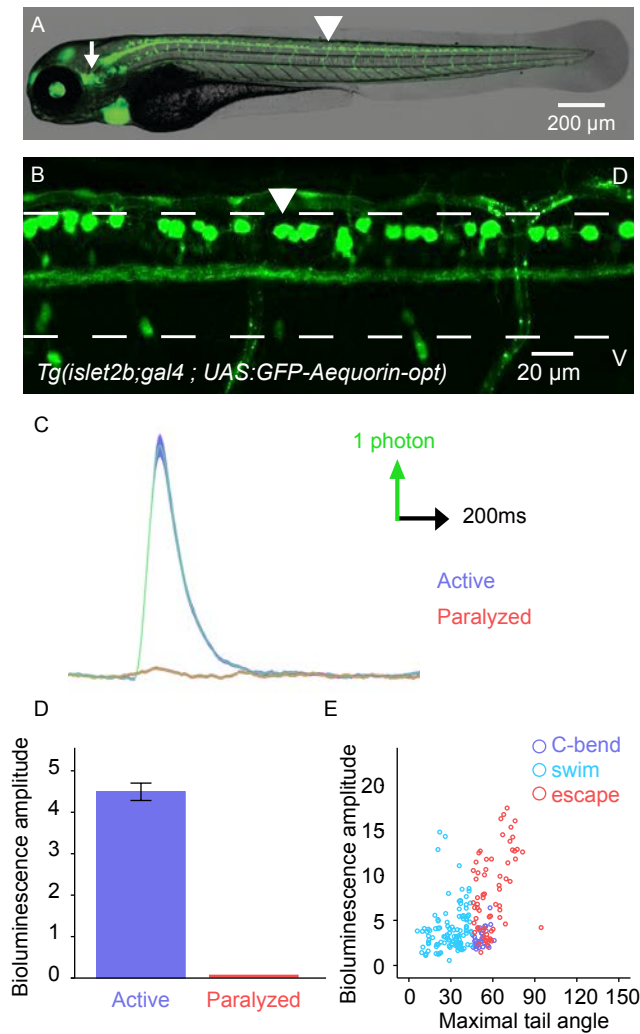


Figure 4. Mechanosensory neurons are recruited during active but not fictive locomotion

A, B. In vivo fluorescent image (A) and immunostaining (B) for GFP in 4 dpf *Tg(Isl2b:Gal4, cmlc2:eGFP, UAS:GFP-Aequorin-opt)* triple transgenic zebrafish larva show selective expression of GFP-Aequorin in mechanosensory neurons (trigeminal ganglia, Rohon-Beard spinal neurons and dorsal root ganglia), as well as expression in the retina and heart, with no expression in muscle fibers ($n = 4$). **C.** Averaged bioluminescence traces demonstrate that mechanosensory neurons are recruited during active motion but not in paralyzed larvae (mean amplitude in active trials = 4.53 ± 0.21 photons / 10 ms, no detected signal in paralyzed trials, $n = 10$ fish, $n = 600$ trials). **D.** Mean bioluminescence amplitude in active larvae was higher compared to freely swimming larvae (4.53 ± 0.21 versus 2.20 ± 0.10 photons / 10 ms, $n = 10$ fish, $n = 600$ trials, $p < 0.001$) and was completely suppressed in paralyzed larvae ($n = 10$ fish, $n = 300$ trials). **E.** Bioluminescence signals amplitude correlated with maximal tail angle during movements ($R = 0.44$, $p < 0.01$, $n = 9$ fish, $n = 248$ trials).

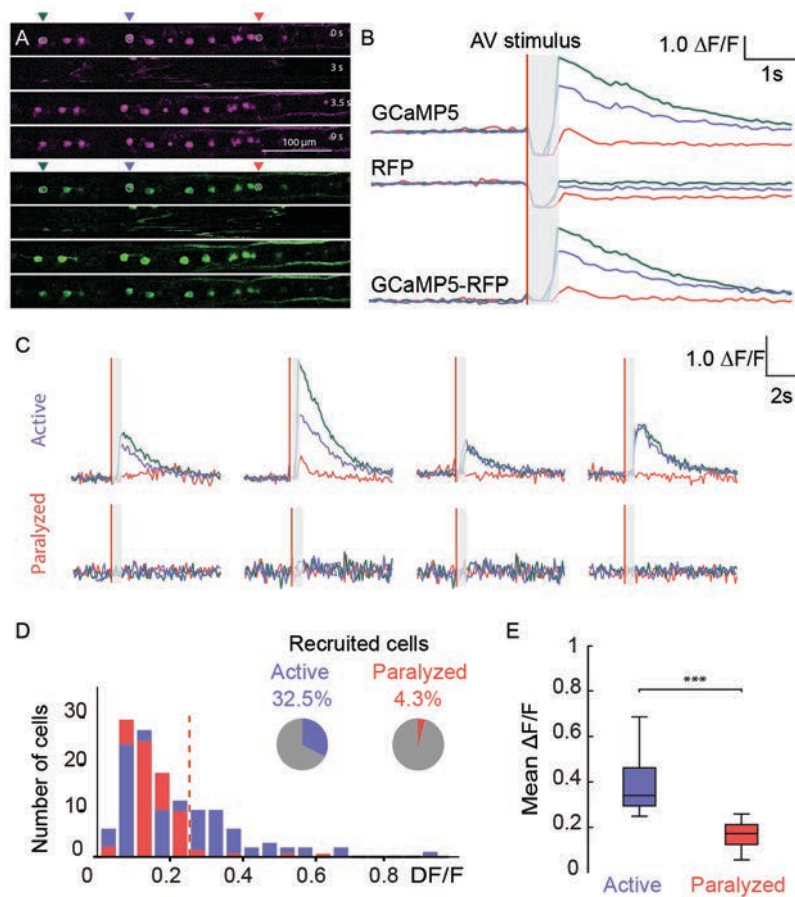


Figure 5. Calcium imaging of spinal mechanosensory neurons shows enhanced activation during motion

A. Monitoring of Rohon-Beard neurons at the cellular level in the spinal cord during motion of the tail was achieved using two-photon time-lapse microscopy of *Tg(Isl2b:Gal4, cmlc2:eGFP, UAS:mRFP, UAS:GCaMP5)* transgenic larvae at 4 dpf. **B.** Artifacts due to shift of the focal plane during motion of the tail were corrected by subtracting the red $\Delta F/F$ from the green $\Delta F/F$ signal. **C.** Rohon-Beard neurons reliably recruited upon repeated acoustic stimuli were silenced after the animals were paralyzed. **D.** Distribution of mean $\Delta F/F$ amplitude ($\Delta F/F$) of Rohon-Beard neurons during active locomotion (number of cells with $\Delta F/F \geq 25\%$ across fish = 32.5%, no significant difference between fish) and after paralysis (4.3%, $p = 0,038$, $n = 12$ fish, $n = 117$ cells). **E.** The mean $\Delta F/F$ amplitude in recruited Rohon-Beard neurons during active locomotion was markedly reduced after paralysis ($39.5 \pm 2.4\%$ versus $18.8 \pm 1.8\%$, $n = 12$ fish, $n = 38$ cells, $p < 0,001$).

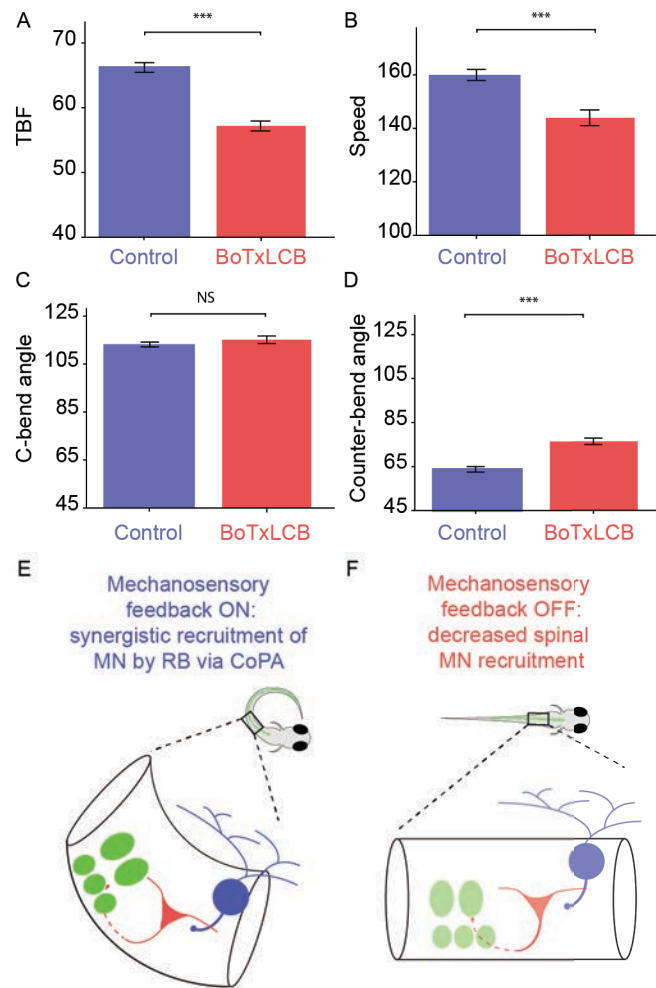
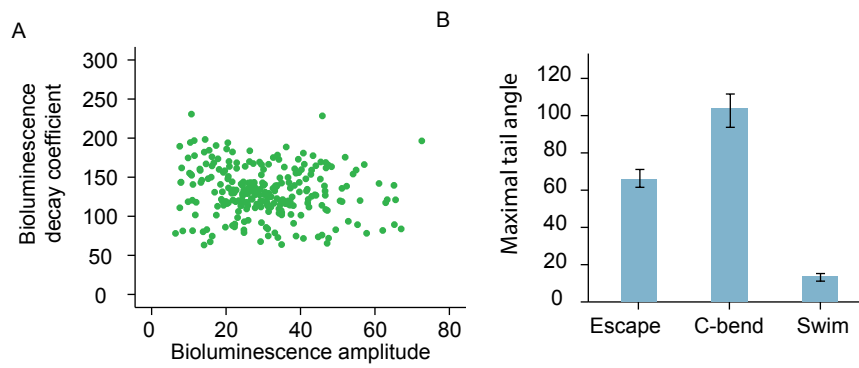


Figure 6. Silencing mechanosensory neurons impairs escape responses

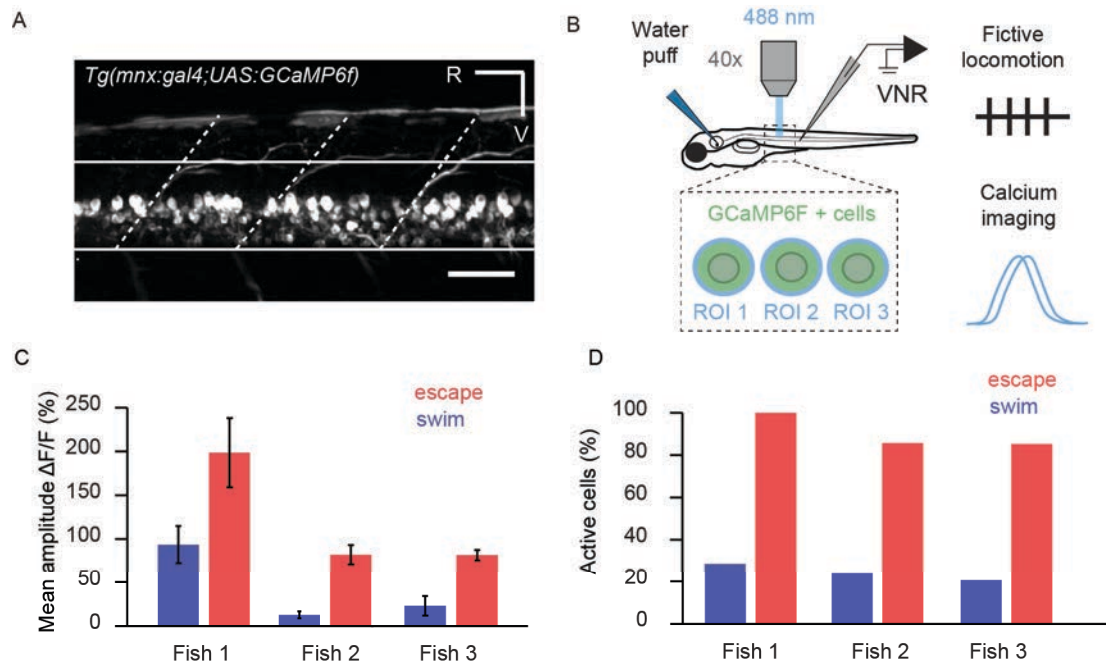
A. In freely swimming 5 dpf larvae, *Tg(Isl2b:Gal4, cmlc2:eGFP, UAS:BoTxLCB-GFP)* animals in which mechanosensory neurons are silenced showed a decreased tail-beat frequency (TBF, in Hz) during acoustic-elicited escapes compared to *Tg(Isl2b:Gal4, cmlc2:eGFP)* siblings (57.2 ± 7.7 versus 66.1 ± 7.4 Hz, $p < 0.001$) **B.** Similarly, the mean speed of escapes was decreased in silenced larvae (144 ± versus 159 ± 2.1 mm/s, $p < 0.001$). **C.** Mean initial C-bend bending of escapes was similar between the two groups (112.3 ± 1.0 versus 115.1 ± 1.6 degrees, $p = 0.1$). **D.** However, subsequent counter-bend was decreased in *Tg(Isl2b:Gal4, cmlc2:eGFP, UAS:BoTxLCB-GFP)* larvae compared to siblings (63.7 ± 1.2 versus 76.4 ± 1.5 degrees, $p < 0.001$); for all variables: $n = 356$ escapes in 131 larvae **E. F.** These results supports a closed-loop sensorimotor circuits within the spinal cord whereby mechanosensory Rohon-Beard neurons (in blue) would recruit Commissural Primary Ascending (CoPA) interneurons (in red), which in turn recruit contralateral spinal primary motor neurons (in green) during active (E) but not fictive (F) escapes.



Supp. Figure 1. Bioluminescence and kinematic parameters measured during active locomotion.

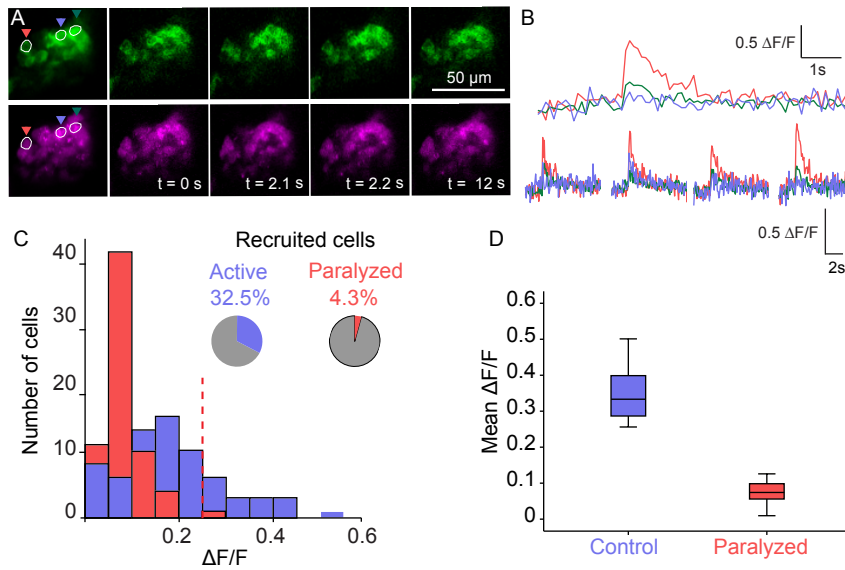
A. There was an absence of correlation between the time decay constant of the signal and bioluminescence amplitude, indicating that bioluminescence decay remained approximately constant.

B. Maximal tail angle were higher for C-bends compared to escapes and swims.



Supp. Figure 2. Calcium imaging of spinal motor neurons and fictive locomotion of ventral nerve root recording

A. Expression pattern in a *Tg(Mnx1:gal4;cry:mCherry-UAS:GCaMP6f)* double transgenic larva at 4 dpf imaged from the lateral side shows a specific targeting to motor neurons (white lines: ventral and dorsal limits of spinal cord; white dashed lines: axial segments limits; the dorso-ventral axis within the spinal cord is normalized to 0 at the ventral limit and 1 the dorsal limit; R is rostral, V is ventral; Scale bar is 50 μ m). **B.** Experimental setup. A paralyzed larva, mounted on its side in agarose is placed under a 40X objective. Motor neuron output is recorded at a ventral nerve root (VNR). Water is puffed onto the otic vesicle to induce fictive escape responses. A 488 nm laser is used on a spinning disk confocal microscope to record GCaMP6F signals at 20Hz. **C.** Mean signal amplitude ($\Delta F/F$) per fish for the active motor neuron population during each behavior (n=3 larvae). **D.** Proportion of active motor neurons per field of view during each behavior, plotted per fish (n = 12 escapes, 78 slow swims in N = 3 larvae).



Supp. Figure 3. Calcium imaging of trigeminal neurons in active and paralyzed *Tg(Isl2b:Gal4, cmlc2:eGFP, UAS:mRFP, UAS:GCaMP5)* larvae

A,B. Time-lapse images (A) and $\Delta F/F$ traces (B) of trigeminal ganglia neurons showing moderate activation upon repeated acoustic stimuli in 4 dpf *Tg(Isl2b:Gal4, cmlc2:eGFP, UAS:mRFP, UAS:GCaMP5)*. **B.** C. Trigeminal neurons also showed a response upon acoustic stimulus when the fish was actively moving but the mean $\Delta F/F$ per cell was significantly lower than in spinal Rohon-Beard neurons (mean $\Delta F/F = 18.0 \pm 1.4\%$, number of cells with $\Delta F/F \geq 25\%$ across fish = 16/69 (23.2%), $n = 6$ fish, $n = 69$ cells). **D.** All trigeminal neurons active in the control condition were silenced after addition of pancuronium bromide (mean $\Delta F/F$ amplitude in active trigeminal neurons = $34.5 \pm 7.3\%$ in active larvae and was reduced to $7.6 \pm 3.2\%$ after paralysis; $n = 6$ fish, $n = 16$ cells, $p < 0,001$).

Suppl. Movie 1: Bioluminescence and kinematics during escape.

Suppl. Movie 2: Bioluminescence and kinematics during C-bend.

Suppl. Movie 3: Bioluminescence and kinematics during slow swim.

Supp. Movie 4: Calcium imaging of spinal motor neurons during escape

Supp. Movie 5: Calcium imaging of spinal motor neurons during slow swim

Supp. Movie 6: Calcium imaging of spinal Rohon-Beard neurons during escape

3. Discussion

3.1. Investigating sensorimotor integration in the spinal cord during ongoing locomotion

The ability to record spinal sensorimotor circuits during locomotion is crucial to understanding the contribution of sensory feedback to motor output from CPGs. Previous investigations of mechanosensory integration in the spinal cord mainly relied on sensory perturbation of fictive locomotor rhythm (Rossignol et al., 2006). Studies in paralyzed decerebrate cats demonstrated phase-dependent reorganization of classical sensorimotor reflex pathways during ongoing fictive locomotion (McCrea, 2001). While stimulation of group Ib afferents at rest results in non-reciprocal inhibition of motor neurons projecting to synergist muscles, the same stimulation during ongoing fictive locomotion enhances ongoing motor neurons activity (Conway et al., 1987). Similarly, whereas stimulation of group II afferents inhibit extensors at rest, stimulation during ongoing fictive locomotion can reset the step cycle to flexion (Schomburg et al., 1998). Such experiments indicate that motor neuron activity can be strongly modulated by mechanosensory inputs during ongoing locomotion. However, because of the difficulty to record identified neurons in the moving spinal cord, the underlying cellular mechanisms remain elusive. Here, by taking advantage of the transparency and genetic accessibility of the zebrafish larva, we provide an innovative approach to achieve non-invasive recording of genetically targeted spinal motor and sensory neurons during active locomotion. By allowing monitoring of neural circuits in motion, this approach could be useful for revealing the contribution of spinal interneurons to active locomotion based on morphological and electrophysiological evidence accumulated in fictive preparations.

3.2. Non-invasive bioluminescence monitoring of genetically targeted neurons in motion

However, bioluminescence monitoring is technically challenging. Achieving GFP-Aequorin expression in a highly selective yet strong enough manner is key to obtain large signal-to-noise ratio allowing high-speed kinematics analysis. We

combined a codon-optimized version of GFP-Aequorin for zebrafish together with the GAL4/UAS amplification system to improve considerably the expression of the sensor. We carefully verified in live animals and after immunostaining for GFP that there was no expression in muscles. One practical limitation remains the ability to genetically identify neuronal populations of interest based on the expression of specific promoters. Continuously expanding sets of transgenic lines and recent refinement of genetic targeting techniques together with multiple color variants of Aequorin (Bakayan et al., 2011) should provide increasing options in the future.

The interpretation of bioluminescence signals *in vivo* is another challenge. *In vitro*, the onset rate of the signal and the total photons yield remaining relatively constant, an increase in bioluminescence amplitude is rather due to a shorter signal, i.e. a faster decay rate (Hastings et al., 1969). The fact that GFP-Aequorin decay rate is itself determined at the molecular level by the state of its three calcium binding sites leads to a calcium-dependent model for bioluminescence signals amplitude (Tricoire et al., 2006). Bioluminescence assays in single pyramidal neurons *ex vivo* also showed that the recorded number of photons increased exponentially with the number of action potentials elicited (Drobac et al., 2010). However, one major difficulty *in vivo* is that the bioluminescence signal integrates signals from many cells with different levels of expression and variable patterns of activity. One technique to resolve the overall signal at the cellular level is to compare bioluminescence and calcium imaging data in similar experimental conditions.

3.3. A closed-loop circuit within the spinal cord for mechanosensory integration

By combining bioluminescence with calcium imaging, we demonstrate that spinal motor neuron recruitment is enhanced in active compared to fictive locomotion. Within the spinal cord, several mechanosensory neurons could enhance the recruitment of spinal motor neurons during active locomotion. We show that Rohon-Beard neurons in the spinal cord as well as trigeminal neurons in the head were specifically recruited during active locomotion. In particular, Rohon-Beard neurons have been shown to activate contralateral primary motor neurons through Commissural Primary Ascending (CoPA) interneurons in response to tactile stimuli in

zebrafish embryos (24, 25). In *Xenopus*, a similar pathway involving Rohon-Beard neurons and dorsolateral commissural (dlc) sensorimotor interneurons has been described, which also involves inhibitory interneurons providing ipsilateral inhibition during swimming (26, 27). Our calcium imaging results obtained from moving animals suggest a closed-loop neural circuit in which Rohon-Beard neurons recruited upon tail bending during an escape would trigger a synergistic recruitment of contralateral motor neurons so as to enhance the efficiency of the escape. Our behavioral results showing impaired escapes when mechanosensory neurons are silenced, and in particular a decrease in counter-bend amplitude and tail beat frequency, support this hypothesis. Altogether, these results shed light on the contribution of mechanosensory feedback to motor output during motion, and the resulting differences between active and fictive locomotion.

4. Methods

4.1. Zebrafish care and strains

Adult AB and and Tüpfel long fin (TL) strains of *Danio rerio* were maintained and raised on a 14/ 10 hour light cycle and water was maintained at 28.5°C, conductivity at 500 μ S and pH at 7.4. Embryos were raised in blue water (3 g of Instant Ocean® salts and 2 mL of methylene blue at 1% in 10 L of osmosed water) at 28.5°C during the first 24 hours before screening for GFP expression. Selected embryos were subsequently dechorionated and soaked at 26°C in 100 μ L of blue water with a final concentration of 60 μ M of coelenterazine-h (Biotium, Hayward, USA). Coelenterazine-h was renewed at 2 days post-fertilization (dpf). Experiments were performed at 4 dpf unless otherwise stated. All procedures were approved by the Institutional Ethics Committee at the Institut du Cerveau et de la Moelle épinière (ICM), Paris, France, the Ethical Committee Charles Darwin and received subsequent approval from the EEC (2010/63/EU).

4.2. Generation of the transgenic lines

The *Tg(mnx1:Gal4)* line driving selective expression in spinal motor neurons was kindly provided by Dr. T. Auer and Dr. F. Del Bene (Institut Curie, Paris, France) based on the injection of the *mnx1* construct (Zelenchuk and Brusés, 2011). The original sequence for GFP-Aequorin was kindly provided by Dr. L. Tricoire (Université Pierre et Marie Curie, Paris, France) and was subsequently codon-optimized for expression in zebrafish and subcloned into a 14xUAS plasmid kindly provided by Pr. K. Kawakami (National Institute of Genetics, Mishima, Japan). Injection of this construct in the *Tg(mnx1:gal4)* allowed the generation of the *Tg(UAS:GFP-Aequorin-opt)^{icm09}* by selective expression of the GFP-Aequorin in all spinal motor neuron populations: more prominently primary dorsal motor neurons but also intermediate and ventral secondary motor neurons (Fig. 1A) without any expression in the muscles and only very limited expression in the brain and hindbrain.

Relaxed mutants (*cacnb1^{ts25/ts25}*) (Granato et al., 1996) were kindly provided by Pr. Paul Brehm (Oregon Health and Science University, Portland, USA). In homozygous *cacnb1* mutants, a mutation of the skeletal muscle dihydropyridine receptor β 1a subunit interferes with the calcium release and mutant larvae are immotile (Schredelseker et al., 2005).

The transgenic line *Tg(UAS:GCaMP6f;cryaa:mCherry)icm06* was generated by subcloning GCaMP6f (Chen et al., 2013) into pDONR221 and then assembled into the final expression vector in a three-fragment Gateway reaction using p5E-14XUAS, pME-GCaMP6f, p3E-poly(A) and pDest-CryAA:mCherry.

The *Tg(Isl2b:Gal4, cmlc2:eGFP)* line driving expression in trigeminal and Rohon-Beard neurons was kindly provided by V. Di Donato and Dr. F. Del Bene (Institut Curie, Paris, France) based on the injection of the *isl2b* construct (Auer et al., 2015). Crossing *Tg(Isl2b:Gal4, cmlc2:eGFP)* with *Tg(UAS:GFP-Aequorin-opt)icm09* animals allowed us to drive expression of GFP-Aequorin in sensory neurons (bilateral trigeminal ganglia, spinal Rohon-Beard neurons and dorsal root ganglia).

Immunohistochemistry on GFP confirmed that there was no expression in muscle fibers but GFP expression could also be seen in the retina, heart and blood vessels.

4.3. Immunohistochemistry for GFP-Aequorin and quantification of muscle fibers

The chicken anti-GFP primary antibody was used at 1:500 dilution (Abcam, Cambridge, UK). The secondary antibody used was the Alexa Fluor 488 donkey anti-chicken IgG (1:1000 dilution, Life Technologies). Immunostaining specificity was established by omitting the primary specific antibody, no immunoreactive signal was observed. Quantification of the number of muscle fibers expressing GFP-Aequorin was performed by counting the number of fibers in stacks of the whole *Tg(mnx1:Gal4, UAS:GFP-Aequorin-opt)* and *Tg(Isl2b:Gal4, cmlc2:eGFP, UAS:GFP-Aequorin-opt)* larvae imaged using a confocal spinning disk equipped with a 10X objective.

4.4. Monitoring of neuronal activity with GFP-Aequorin bioluminescence

All *GFP-Aequorin* expressing larvae were tested at 4 dpf (except 2 animals tested at 3 dpf for Fig. 2 and for which signals were comparable). In all experiments, one larva was head-embedded in 1.5% low melting agarose with the tail free to move in a circular (2 cm diameter) 3D-printed arena (Sculpteo, France). The arena was then placed in a lightproof box (Fig. 1A) and attached to a small speaker (2 Ohm). Each trial consisted of a 500 ms baseline followed by a 10 ms acoustic stimulus and 1990 ms subsequent recording. Assays consisted of 30 trials with 1-minute inter trial intervals to reduce habituation. Sinusoidal stimuli (5 cycles, 500Hz) were delivered through a wave generator (Agilent, 33210-A) and audio amplifier (Lepai, LP2020A). Intensity was adjusted to the lowest value that reliably elicited an escape response (between 0.5 and 5 Vpp).

The same larvae used for the active assay were subsequently paralyzed by bath application of pancuronium bromide (Sigma, P1918) at 0.6 mg/mL final concentration and stimulation intensity was adjusted to the lowest value that elicited a bioluminescent signal. For Fig. 4D-F *cacnb1^{ts25/ts25}* and control siblings were tested

alternatively on the same day and compared to each other. In non-moving animals (i.e. paralyzed or *cacnb1* mutants), the intensity was progressively increased until stimuli elicited fictive responses. A higher intensity of the acoustic stimulus was often needed after addition of pancuronium bromide, possibly due to modulation of cholinergic arousal brain circuitry (Yokogawa et al., 2007).

As negative controls, bioluminescence assays of wild type animals or *Tg(mnx1:GFP)* (Zelenchuk and Brusés, 2011) where motor neurons express GFP only revealed no signal (n = 3 wild type larvae with 30 trials each, n = 5 *Tg(mnx1:GFP)* larvae with 30 trials each). Animals deprived of GFP-Aequorin did not produce any signals above baseline noise level during escape responses.

4.5. High-speed behavior recording

Infrared light illumination for monitoring larval behavior was provided by an 850 nm LED (Effisharp, Effilux, France) mounted with 2 long-pass 780 and 810 filters (Asahi ZIL0780 and Asahi XIL0810, respectively) and a diffuser (Thorlabs, DG10-120B). Video acquisition was performed at 1000 Hz using a high-speed infrared sensitive camera (Eosens MC1362, Mikrotron, Germany; objective Nikkor 50 mm f/1.8D, Nikon, Japan) at 320x320 pixels resolution controlled by the software Hiris (RD Vision, France). Photons were counted with a PMT (Hamamatsu H7360-02) located under the larva arena and sent to an acquisition card (NI PCI 6602, National Instruments, USA). A band-pass filter (Carl Zeiss 525 nm / 50 nm, ref. 489038-8002) and a short-pass filter (Asahi 670 nm, XVS0670) were placed between the larva and the PMT. A custom application-programming interface developed in collaboration with R&D Vision synchronized the video acquisition with the photon count and the stimulus delivery using 30 trials batched TTL chronogram (EG Chrono, RD Vision).

4.6. Bioluminescence analysis

Photons were counted with a temporal resolution of 1 ms and then binned every 10 ms. The signal was filtered using a running average with a window size of 10, giving a typical signal-to-noise ratio (SNR) for active movements of 50 to 1. Noise

was extrapolated from a linear fit of the cumulative photon count before the stimulus and subtracted from the signal. The start and end of the bioluminescent signal were computed as the first time point followed by 3 points with a differential value above 0.4 photons / 10 ms and below 0.2 photons / 10 ms, respectively. The rising coefficient was calculated from a linear fit between the start and the peak of the bioluminescent signal while the decay coefficient was derived from the one-term exponential fit between the peak and the end of the signal.

4.7. Kinematics analysis

The rostral and caudal extremity of the tail were manually determined for each larva and the tail was subsequently automatically tracked with a custom Matlab algorithm (R2012b, Mathworks, USA). The tail angle (see Fig.1) was computed for each frame and filtered using median filtering (window size = 10). The start of the movement was determined as the first frame followed by 3 with a differential tail angle value above 0.08. The end was determined as the end of the 20 frames with a differential tail angle value below 0.1 degree. Local minimal and maximal values of the tail angle occurred at least 2 ms apart and 1 degree above the 5 ms preceding value (Fig. 1C). Only larvae with at least one tail bend above 45° were included in the final analysis. The number of cycles was determined by dividing the numbers of minima and maxima by two. Angular velocity was calculated by dividing the cumulative angle between the two extrema by the time between them. Automated movement categorization was determined as follows: Escapes for all movements with maximum values of tail angle > 45° and number of cycles > 1; C-bends for all movements with maximum values of tail angle > 45° and number of cycles ≤ 1; Swims for all movement with maximum values of tail angle < 25° and number of cycles > 1 (Fig. 1D).

4.8. Calcium imaging of spinal motor neurons

4 dpf *Tg(mnx1:Gal4, UAS:GCaMP6f;cryaa:mCherry)* double transgenic larvae were screened for dense labeling and good expression of GCaMP6f in spinal motor neurons under a dissecting microscope equipped with an epifluorescence lamp (Leica,

Germany). Larvae were anaesthetized in 0.02% Tricaine-Methiodide (MS-222, Sigma-Aldrich, St-Louis, USA) diluted in fish facility water and mounted on their lateral side in 1.5% low-melting point agarose in glass-bottom dishes filled with external solution ([NaCl]=134mM, [KCl]=2.9mM, [MgCl₂]=1.2mM, [HEPES]=10mM, [glucose]=10mM and [CaCl₂]=2.1mM; adjusted to pH 7.7-7.8 with NaOH and osmolarity 290mOsm). Larvae were immobilized by injecting 0.1-0.3 nL of 0.5mM α -Bungarotoxin (Tocris, UK) in the ventral axial musculature. A portion of agar was removed using a razor blade in order to expose 2 to 3 segments. To achieve a strong signal-to-noise ratio during fictive locomotion recordings, the skin overlying these segments was removed using suction glass pipettes. Zebrafish larvae were imaged using a custom spinning disk microscope (Intelligent Imaging Innovation, Denver, USA) equipped with a set of water-immersion objectives (Zeiss 20X, 40X, NA=1). Recordings were acquired using Slidebook® software at 20 Hz at 488nm. Gain and binning were optimized to maximize signal to noise ratio. Z projection stacks showed full pattern of expression using Fiji (Schindelin et al., 2012). Positions of cells along the D-V axis were computed using Fiji and MATLAB. Calcium signals were extracted online using custom scripts. Regions of interest (ROIs) were manually designed and calcium signals time series were extracted as the mean fluorescence from individual ROIs at each time point of the recording. We observed that out-of-focus signals varied between animals, from dorsal to ventral spinal cord regions in a behavior-dependent manner. To estimate the contribution of out-of-focus signals we systematically picked two background ROIs, one placed below the ventral limit of the spinal cord to capture out-of-focus signals at the level of ventral motor neurons during slow swimming, the second in the dorsal-most part of the spinal cord to capture out-of-focus signals in the dorsal spinal cord during the escape. We estimated the maximum out-of-focus signals observed during each behavior (see black traces in Fig 2D) and used this value as a threshold for discriminating active from silent motor neurons.

4.9. Ventral nerve root recording (VNR)

Thin-walled, borosilicate glass capillaries (Sutter Instruments, USA) were pulled and fire-polished from a Flaming/Brown pipette puller (Sutter Instruments, USA) to

obtain peripheral nerve recording micropipettes. Pipettes were filled with external solution and positioned next to the preparation using motorized micromanipulators under the microscope. Light suction was applied when the pipette reached the muscle region located at the vicinity of intermyotomal junctions, ventral to the axial musculature midline. VNR signals were acquired at 10kHz in current clamp IC=0 mode using a MultiClamp 700A amplifier (Molecular Devices–Axon Instruments, USA), a Digidata series 1322A digitizer (Axon Instruments, USA) and pClamp 8.2 software (Axon instruments, USA). Recordings were considered for analysis when the background noise did not exceed 0.05 mV amplitude and signal to noise ratio for fictive locomotor events detection was above three. VNR recordings were analyzed offline and aligned to calcium imaging data using custom-made MATLAB scripts.

4.10. Calcium imaging of spinal sensory neurons

Zebrafish larvae *Tg(Isl2b:Gal4, cmlc2:eGFP, UAS:mRFP;UAS:GCaMP5)* were screened at 3 dpf for nacre phenotype and selective expression of both GCaMP5 and mRFP in Rohon-Beard neurons and trigeminal ganglia under a dissecting microscope with an epifluorescence lamp (Leica, Germany). At 4 dpf larvae were embedded dorsally in 1.5% low melting agarose in a circular (2 cm diameter) 3D-printed arena (Sculpteo, France). The agar was cut at approximately the 10th segment of the tail so that the majority of the tail could move freely while also remaining stable enough to image. The arena was attached to a small speaker (2 Ohm) and mounted on the stage of a two-photon microscope (Intelligent Imaging Innovations, USA) with a 20x water-immersion objective (Zeiss, Germany). A 500 Hz acoustic stimulus was delivered for 10 ms with a one-minute interval between each trial for a total of 10-15 trials per region imaged. Rohon-Beard cells were imaged at least one segment outside and caudal to the agar cut and trigeminal ganglia were imaged through the agar. Two-photon time-lapse microscopy with an excitation wavelength of 900-1000 nm and an acquisition rate of 11 Hz was used to capture simultaneously both red (612/69 nm) and green (525/40 nm) channels in SlideBook 6 (Intelligent Imaging Innovations, USA) during the escape behavior elicited by the acoustic stimulus. Regions of interest (ROIs) were drawn with a graphics tablet (Wacom Co., Ltd., Japan) in Fiji (Schindelin et al., 2012). Calcium signals were extracted using custom-written scripts

in Matlab (2013a, Mathworks, USA). Cell positions were tracked over time and $\Delta F/F$ values were computed for both red and green channels with the background subtracted by $\Delta F/F=(F(t)-F_0)/(F_0-F_{bg})$. The red $\Delta F/F$ data was then subtracted from the green $\Delta F/F$ data to control for any shifts in the focal plane following the motion artifact. Changes in $\Delta F/F$ were computed by subtracting the average of the 10 frames before the stimulus from the maximum value during 10 frames following the stimulus.

4.11 Behavioral analysis of freely moving BoTxLCB larvae

Zebrafish larvae *Tg(Isl2b:Gal4, cmlc2:eGFP, UAS:BoTxLCB-GFP)* were screened at 3 dpf for expression. At 5 dpf, larvae were tested 4 by 4: each larva was positioned in a separate dish (2 cm diameter) with underneath illumination, freely moving. Escapes were elicited by delivering a 1 KHz stimulus for 1 ms using attached speakers. Each trial consisted of a 200 ms baseline followed by a 1 ms stimulus at 1 kHz and 800 ms subsequent recording. Assays consisted in 5 trials with 2 minutes inter-trial intervals. Behavior was recorded at 650 fps with a high-speed camera (Basler acA2000-340km) and analyzed using a tracking algorithm made in collaboration with R&D Vision and a custom Matlab script (R2012b, Mathworks, USA).

4.12 Statistical analysis

SPSS 20 (IBM, USA) was used to perform all statistical analyses. Comparisons of bioluminescence signals parameters was conducted using a t-test for paired samples for repeated measures within subjects (i.e. head-restrained versus free swimming or active versus paralyzed data). Mixed linear model analysis with repeated measures using an auto-regressive covariance structure was performed to compare the bioluminescence amplitude between movement categories in active assays, and between moving and immotile larvae in active versus fictive assays. Bioluminescence decay coefficients (τ) were included if the goodness of fit r-square value was > 0.95 . Normalized bioluminescence values were calculated as $[X(i)-\text{mean}(X)/(\text{max}(X)-\text{min}(X))]$. When comparing the exponential time decay, only trials

with a bioluminescence signal to noise ratio ≥ 5 were included, so as to obtain an r-square for goodness of fit $\geq 90\%$. A Pearson test was used to assess correlations for parametric data. Statistical significance is represented in the graphs as *** for $p < 0.001$, ** for $p < 0.01$, * for $p < 0.05$; all data are provided in the figures and text as means +/- standard error of the mean (SEM).

Acknowledgements

We would like to thank Dr. Ludovic Tricoire (University Pierre et Marie Curie, Paris, France) for providing the original GFP-Aequorin sequence, Dr. Michael Granato (University of Pennsylvania, USA) via Dr. Paul Brehm (Vollum Institute, USA) for providing the *Relaxed (cacnb1^{ts25})* mutants. We are indebted to RD Vision for developing the custom API to synchronize photon collection and video acquisition. We thank Dr. Thomas Auer and Dr. Filippo Del Bene for providing the *mnx1* construct, and to Sophie Nunes Figueiredo for injections and GFP immunostaining, Bogdan Buzurin and Natalia Maties for the excellent fish care. SK received a PhD fellowship from Inserm and Assistance Publique – Hôpitaux de Paris. AP received a postdoctoral fellowship from the Mairie de Paris Research in Paris programme and from the EMBO, KF from UPMC and UB from ENP. This work received financial support from the Institut du Cerveau et de la Moelle épinière with the French program “Investissements d’avenir” ANR-10-IAIHU-06, the network Ecole des Neurosciences de Paris (ENP), the Fondation Bettencourt Schueller (FBS), the City of Paris Emergence program, the Atip/Avenir junior program from INSERM and CNRS, the International Reintegration Grant from Marie Curie Actions Framework Program 6 #277200, the Human Frontier Science Program (HFSP) Research Grant RGP0063/2014 and the European Research Council (ERC) starter grant “OptoLoco” #311673.

Part C.

From spatial to genetic targeting: a paradigm shift for neurosurgery

Abstract

Genetic targeting has become a dominant approach in neurosciences over the last twenty years. Promoters have complemented morphological and spatial information to identify neurons, and numbers of genome editing techniques now allow the generation of an always-expanding library of transgenic lines in tractable animal models. Recently the development of optogenetics brought a toolbox of effectors to selectively monitor and manipulate the activity of neurons in space and time, opening new paths for dissecting neural circuits. While modern neurosciences rely heavily on genetically targeted approaches, neurosurgery has remained essentially based on spatial information (e.g. tumor location and morphology, deep brain stimulation target coordinates, etc.). However, spatial targeting might not be the most relevant approach for diseases with poor spatial resolution (e.g. diffuse gliomas, basal ganglia disorders, epilepsy) or when circuits are intrinsically mixed. Genetically targeted neurosurgery, consisting in selective expression of exogenous genes encoding effectors in identified cellular populations, could be a promising strategy for these conditions. Selectivity would be achieved through restricted gene expression by targeting cells rather than spatial selection by the surgeon's direct manipulation. However, to achieve this paradigm shift, several challenges must be overcome, such as the identification of selective genetic entry points into neurological diseases, safe gene delivery, efficient transduction and stimulation methods for clinical practice in humans.

1. Introduction

The formidable expansion of genetic tools and tractable animal models in the last decades has radically transformed basic neurosciences. Neuroscientists used to characterize neurons and circuits based on morphological and electrophysiological parameters in ex-vivo preparations. Nowadays, neurons can also be classified based on their genetic profile, which allows selective expression of tools to record and disrupt circuits at the cellular and population levels (Fink et al., 2015). Optogenetics, which is the convergence of optical tools and genetic targeting, is the best example, but not the only one, of this powerful combination (Miesenböck, 2009).

Similarly to the early days of neuroscience, neurosurgery is a field relying almost exclusively on spatial information. When a neurosurgeon is planning to remove a brain tumor, he needs to analyze its location relatively to anatomical landmarks and functional areas in order to choose the safest and most effective surgical approach. Hence, the recent development of advanced imaging tools, such as neuronavigation and peroperative imaging.

However, spatial targeting might not always be the most relevant approach to some neurosurgical conditions. For instance, gliomas are diffuse tumors that are known to spread far beyond their visible limits on magnetic resonance imaging. Deep brain stimulation has side effects due to non-selective electrical stimulation of mixed population of neurons in the vicinity of the electrode. Genetically targeted neurosurgery, that is achieving selectivity through genetic expression by the target rather than spatial selection by the surgeon, could provide some answers to these poorly spatially defined neurosurgical conditions.

2. How we moved to genetically targeted neurosciences

2.1. From morphological to genetic identification of neurons

Identification of neurons traditionally relies on spatial information: soma shape, dendritic branching, axonal projection, and localization within histological

structures. Based on morphological identification of neurons, traditional techniques of investigation such as microscopy and electrophysiology have built putative neuronal circuits. Making assumptions based on anatomical or electrophysiological observations in ex-vivo samples, neuroscientists drew “wiring diagrams” and extrapolated neuronal function.

However, because most experimental techniques based on spatial identification can only record neurons immobilized under a microscope objective, asserting the functional relevance in behaving animals of circuits identified ex-vivo is very difficult. Although such experiments have proved very valuable in characterizing neurons properties and proposing neuronal circuits, they are also subject to important limitations. For instance, different neuronal populations are intricate within the space of a single ex-vivo sample, and subtypes of neurons can share morphological or electrophysiological features without having a similar function.

Beyond morphological characteristics, several overlapping features can be used to classify neurons: developmental lineage, electrophysiological properties (firing patterns and currents), molecular markers (neurotransmitters and receptors), genes promoters and function (neurons performing the same function within a given circuit belong to the same class) (Masland, 2004). Ideally, these various classification methods should converge and define functionally relevant classes of neurons.

Among these classifying parameters, genetic profile is probably the best strategy to establish reliable experimental access to specific cell populations. Progress in developmental biology has brought the ability to use specific transcription factors to identify neuronal lineages (Siegert et al., 2012). Interestingly, these genetic signatures of neuronal populations can often be matched with topographic maps across species. In the spinal cord for instance, homologous neurons expressing the same transcription factors and sharing similar morphological features can be identified in tadpoles, larval zebrafish and embryonic mice (Goulding, 2009). Such homology across species makes it particularly relevant to study genetically targeted populations of neurons in less developed and more genetic model organisms.

2.2. Genetic targeting of neurons in tractable animal models

Genetic targeting is the selective expression of an exogenous gene of interest by a genetically identified cell population. Transgenesis can be achieved with various techniques at each step of the process: vector delivery (microinjection, electroporation or viral delivery), genome insertion (homologous recombination or transposition), gene transduction (endogenous expression or enhancer traps) and conditional expression (binary and inducible systems).

Vectors including the gene of interest can be delivered in embryonic stem cells or fertilized eggs through DNA microinjection or electroporation (Fig. 1A). If the construct gets inserted into germ cells genome, then the injected animal can transmit it to the next generation and establish a stable transgenic line. Viral delivery of vectors is an alternative that can be used to target cell types based on injection site, viral tropism and promoter-specific expression. Several viral vectors allowing long-term gene expression without cytotoxic effects are available, among which lentivirus (RNA virus), adeno-associated virus (single-stranded DNA) and herpes simplex virus (double-stranded DNA) (Verma and Weitzman, 2005).

Insertion of the gene of interest can either be directed to a specific locus in the host genome or random (Fig. 1B). Knock-in gene targeting uses homologous recombination at the targeted locus to insert the exogenous gene under an endogenous promoter whose expression is to be mimicked (Capecchi, 1989). However, this technique requires knowing the targeted locus DNA sequence, and disrupts expression of the endogenous gene. On the other hand, transposition relies on random insertion of the vector in the host genome by an enzyme called transposase. In zebrafish, the *Tol2*-mediated transposition relies on a donor plasmid containing a non-autonomous *Tol2*-construct delivered together with transposase mRNA. The *Tol2* construct contains specific sequences that are recognized by the transposase and allow upon excision its random insertion within the host genome (Kawakami et al., 2000).

Recent techniques such as TALEN (transcription activator-like effector nuclease) or CRISPR (clustered regularly interspaced short palindromic repeat) now

allow easy and efficient targeting of precise sequences in the host genome (Seruggia and Montoliu, 2014). Both TALEN and CRISPR systems have the ability to induce double-strand breaks at the targeted sequence using associated endonucleases FokI and Cas9 respectively. This double-strand DNA break can then generate two different outcomes: non-homologous end-joining in order to create a targeted mutation and gene disruption, or homologous-directed repair using an exogenous donor template in order to achieve gene correction or transgene insertion (Yin et al., 2014).

To drive the transduction of the inserted gene, one can either transfect the regulatory elements and promoter within the same construct or rely on the promoters and enhancers of the host genome (Fig. 1C). A bacterial artificial chromosome (BAC) can hold the promoter, the reporter gene and the target gene. If a BAC containing a specific promoter is inserted (even randomly) within the host genome, the enclosed reporter and exogenous gene will only be transduced in neurons where this promoter is expressed (Asakawa et al., 2013). Unlike BAC, enhancer traps take advantage of the random transposition into the genome of a given plasmid. In addition to the reporter gene, this plasmid contains a minimal promoter that is activated only when inserted close to an enhancer gene. Therefore, multiple transgenic lines labeling several neuronal populations can be rapidly generated and screened based on their fluorescence pattern of expression (Scott et al., 2007).

Lastly, combinatorial tools, such as the Gal4/UAS system in flies and fish, can optimize gene targeting (Fig. 1D). This bipartite system relies on the specific expression of the yeast Gal4 transcriptional activator to drive and increase the expression of the reporter gene placed under the control of repetitive Gal4-responsive upstream activator sequences (UAS) (Asakawa and Kawakami, 2009; Davison et al., 2007). Therefore, researchers can easily combine drivers and effectors by crossing animals with Gal4-attached promoters to others with UAS-attached gene of interest (Scott, 2009).

Another binary method for gene expression used in mammals is the Cre/LoxP system, in which expression of the *Cre* recombinase is driven by a specific promoter while the gene of interest is under the control of an ubiquitous promoter but is

interrupted by a stop-codon flanked by two recombinase target sites (*LoxP*). If the two transgenes are present in the same cell, the *LoxP* sites are excised by the *Cre* recombinase and the target gene is expressed (Huang and Zeng, 2013). Lastly, the expression of the transgene of interest can be controlled in time and space using inducible systems such as the tetracycline-dependent promoter: the tetracycline-regulated transactivator (*tTA*) is driven by the targeted promoter and can activate, only in the absence of doxycycline (a tetracycline analog), its operator sequence (*tetO*) controlling the gene of interest (Gossen and Bujard, 1992).

2.3. A toolbox for manipulating genetically identified neurons

Proteins expressed in the targeted population of neurons can either simply label the cells, e.g. fluorescent reporters such as the green fluorescent protein (GFP), monitor neuronal activity, e.g. genetically encoded calcium indicators (GECIs), activate or inhibit neuronal activity, e.g. optogenetic actuators, and even silence or ablate an entire neuronal population.

GECIs can indirectly monitor neural activity by measuring the intracellular calcium concentration (Grienberger and Konnerth, 2012) (Fig. 2A). Being the combination of a calcium-binding protein and a fluorescent protein, GECIs have the ability to modify their fluorescence properties when intracellular calcium levels increase. Calcium affinity, kinetics and dynamic range of some GECIs family such as GCaMP have been continuously improved through targeted mutagenesis and screening (Akerboom et al., 2012; Muto et al., 2011; Nakai et al., 2001; Tian et al., 2009). Expression of GCaMP under a specific promoter allows monitoring of genetically identified neurons at the population level in many animal models, from *Drosophila* to zebrafish (Akerboom et al., 2012). However, because fluorescent GECIs such as GCaMP need to be excited to emit photons, the sample must usually be immobilized under a microscope. Neural monitoring with GECI in freely behaving animals can however be achieved with either bioluminescence sensors that do not require light excitation to emit photons, such as GFP-Aequorin (Naumann et al., 2010; Shimomura et al., 1962b), or fiber optic apparatus tethered to the animal's head (Flusberg et al., 2008).

Optogenetic actuators are mainly light-activated ion channels that can depolarize (i.e. activate) or hyperpolarize (i.e. inhibit) genetically targeted neurons upon illumination with a specific wavelength (Fig. 2B). For instance, Channelrhodopsin-2 (ChR2) allows non-specific cation influx when illuminated with blue light, thus reversibly activating neurons with a millisecond-timescale precision (Boyden et al., 2005; Nagel et al., 2003). Similarly to the GCaMP family, the Channelrhodopsins family is continuously expanding with color shifted or improved kinetics and sensitivity variants (Klapoetke et al., 2014). Light-gated inhibition of genetically targeted neurons has been initially achieved using the chloride-pump Halorhodopsin (NpHR): being sensitive to yellow light, NpHR can be co-expressed with ChR2 to allow bidirectional optical stimulation of neurons (Zhang et al., 2007b). Following NpHR, genetically targeted optical inhibition of neurons has been achieved with proton pump Arch (*archaerhodopsin-3*) (Chow et al., 2010), a red-sensitive halorhodopsin called Jaws (Chuong et al., 2014), and ChloC, a variant of ChR2 modified to allow influx of chloride instead of sodium (Wietek et al., 2014).

Besides opsins-mediated optical control, silencing of an entire population of neurons can also be achieved with genetic targeting of toxins aiming for the SNARE proteins at the synapse (Fig. 2C). Expression of the tetanus toxin light chain (TeTxLc), which prevents neurotransmitter release by cleaving the synaptic vesicle protein synaptobrevin, has been successfully used in drosophila and zebrafish, in combination with the Gal4/UAS system, to silence neurons and affect behavior (Asakawa et al., 2008). Genetically targeted chemoablation of neurons can also be conducted using the expression of nitroreductase, a bacterial enzyme that catalyzes the innocuous prodrug metronidazole into a cytotoxic product leading to inducible and selective cell death (Curado et al., 2008).

3. Moving toward genetically targeted neurosurgery

3.1. Candidate diseases for genetically targeted neurosurgery

The rationale of genetically targeted (GT) neurosurgery is to achieve selectivity based on expression of effectors by genetically identified cells rather than manipulation of spatially identified targets by the surgeon.

Good candidate diseases for GT neurosurgery are therefore those having a poor spatial resolution, i.e. a diffuse cellular substrate mixed within healthy tissue, located within an individualized brain or spinal cord area. The aim can be to either monitor and/or modulate neuronal activity, as would be the case with Parkinson's disease and most current indications for electrical neuromodulation, or ablate targeted cells within a non-specific environment, as would be the case for gliomas. Conditions to which GT neurosurgery would typically not apply are those with diffuse or unidentified cellular substrates (e.g. Alzheimer's disease) or, on the other hand, well circumscribed lesions (e.g. meningiomas, metastases, etc.).

Neuromodulation is an obvious application of GT neurosurgery as most of the tools developed in GT neurosciences aim at selectively monitoring and manipulating neuronal activity. Parkinson's disease is currently the main indication for deep brain stimulation but its optimal target and the mechanisms underlying its efficacy remain a matter of debate (Rossi et al., 2015). Moreover, non-selective electrical stimulation within a few millimeters from the implantation site recruits many cells types belonging to distinct functional circuits, thereby producing side effects. By allowing selective and reversible control of basal ganglia circuitry in animal models of Parkinson's disease, optogenetics provided a new insight into the underlying mechanisms of the disease (Kravitz et al., 2010) but also of DBS itself (Gradinaru et al., 2009). The aim would be to achieve selective stimulation of genetically identified neuronal populations so as to maximize therapeutic effectiveness while avoiding side effects.

Gliomas are one of the most appealing disease candidates for GT neuroablation. Indeed, it is now documented that even low-grade gliomas (LGG) actually extend far beyond the visible boundaries on magnetic resonance imaging (Pallud et al., 2010). Since it has been demonstrated that the extent of resection was a key prognostic factor of LGG (Sanai and Berger, 2008), some authors proposed that “supratotal resection”, that is resection guided by intraoperative functional mapping rather than preoperative morphological evaluation, should be the goal whenever feasible (Yordanova et al., 2011). But even functionally guided resection makes sense only because it is currently impossible to remove malignant glial cells without removing surrounding neurons with them. Unfortunately, this intricacy between healthy brain and diffuse glioma is also a key limitation of brain radiation therapy. Moreover, the blood brain barrier hinders the penetration of systemically administered chemotherapy, making a new approach to treating gliomas all the more needed.

3.2. Genetic identification and cellular targeting in the human brain

Genetic targeting involves, among others, two critical parameters: the ability to identify the cell type of interest based on specific genetic expression and the ability to efficiently deliver the desired effector to the targeted genome.

Unlike tractable animal models in which stable transgenic lines can easily be generated and tested, genetic identification of neurons in humans must rely on a different approach to look for differential genetic expression in healthy and diseased tissues. Gene expression profiling (GEP) studies are mainly based on complementary DNA microarrays to monitor RNA levels of expression (i.e. “transcriptomes”) in a given sample. By allowing thousands of genes to be tested simultaneously, GEP has become a powerful tool to screen for specific genetic expression in various neurological disorders, ranging from Parkinson’s disease to gliomas (Cooper-Knock et al., 2012; Riddick and Fine, 2011).

Several GEP studies in post-mortem samples from patients with Parkinson’s disease have demonstrated genetic alterations in the protein processing machinery and mitochondrial pathways (Cooper-Knock et al., 2012). In particular, microarray

analysis of the substantia nigra of parkinsonian patients showed a down-regulation of the SKP1 gene, involved in the formation of several proteasome subunits, which may account for the abnormal accumulation of proteins such as Lewy bodies, a histological hallmark of PD (Mandel et al., 2005).

In high-grade gliomas (HGG), recent studies based on transcriptome-wide profiling of tumors have revealed genetically distinct subtypes, among which “proneural” HGG, whose molecular signature is global DNA methylation and mutations in the IDH1 gene, and “mesenchymal” HGG, harboring non-methylated DNA and NF1 gene mutations (Nakano, 2015). Interestingly, these two genetic profiles are also associated with different clinical prognoses, proneural gliomas being less aggressive than mesenchymal ones (Phillips et al., 2006). Since gliomas are thought to arise from a small population of “glioma stem cells” (GSCs) able to initiate and propagate the tumor (Singh et al., 2004), targeting these GSCs could prove to be a powerful therapeutic approach. Interestingly, distinct genetic markers of GSCs have also been described for specific HGG subtypes (Mao et al., 2013), making GSCs an ideal target for genetically targeted therapies.

However, identification of genetic alterations in neurological diseases has not yet provided a reliable genetic entry point for targeted expression of exogenous effectors. Until now, and in stark contrast to basic neurosciences, delivery of gene therapy relies essentially on spatial targeting, through either viral or non-viral techniques.

The majority of gene therapy preclinical and clinical trials conducted so far have used viral delivery to achieve exogenous gene insertion into spatially targeted cells. For instance, in a recent phase 1/2 clinical trial of gene therapy for Parkinson’s disease, a lentiviral vector carrying genes encoding dopamine biosynthetic enzymes (tyrosine hydroxylase, aminoacid decarboxylase, cyclohydrolase) was bilaterally injected in the striatum of parkinsonian patients (Palfi et al., 2014). The aim was to use striatal cells, which do not degenerate in PD, as a source for dopamine production. At 12-months follow-up, all 15 patients who received the gene therapy showed motor improvement. In preclinical trials for gliomas, modified adenovirus (HAd5 serotype)

or Herpes-Simplex Virus-1 (HSV-1) have been used to deliver genes encoding cytotoxic proteins or even anti-angiogenic angiostatin (Kane et al., 2015). Even if some vectors can be engineered to achieve a higher infection rate in glioma cells (Had5 expressing an improved receptor-binding motif for instance), inoculation of viruses was always spatially targeted to the tumor site in order to achieve transfection.

Non-viral synthetic vectors include liposomes, polymers, peptides and inorganic nanoparticles (Yin et al., 2014). These delivery techniques have several advantages over viruses: lower immunogenicity, larger DNA loading capacity and easier and cheaper synthesis methods. Until now, lower delivery efficiency has limited their use in clinical studies. However, recently developed non-viral vectors were used to deliver various exogenous materials such as DNA but also mRNA, small interfering RNA or microRNA (Yin et al., 2014). Owing to their better safety and cost-efficiency profiles, non-viral delivery techniques might represent a viable alternative to viral vectors in clinical applications.

3.3. Genetically targeted neuromodulation and neuroablation in patients

Most of optogenetic studies so far have been conducted tractable animal models such as rodents, zebrafish or drosophila. But successful translation of genetically targeted neuromodulation to humans will also require non-human primates studies. Indeed, delivery strategy (vector-based versus transgenic lines), genetic targeting (efficiency and selectivity of promoters), and effectors expression are quite different between rodents and non-human primates. So are neural circuitry and mechanisms of diseases. Two initial optogenetic studies in non-human primates (Diester et al., 2011) (Han et al., 2009) have relied on viral delivery (lentiviral and AAV-based) of opsins (excitatory ChR2 and inhibitory NpHR) under the control of ubiquitous neural promoters (CaMKII α , hThy1, hSyn) to achieve genetically targeted neuromodulation of neural activity in the frontal eye field and motor cortex respectively. However, these initial optogenetic studies in non-human primates failed to induce a behavioral effect, and even tough subsequent studies achieved changes in behavior (Afraz et al., 2015), their relatively low number in comparison with other animal models underscores their technical difficulty. Besides limitation of gene

transduction efficiency inherent to viral delivery, another issue is the ability to deliver enough light to neurons located further away: in the brain, 99% of the intensity of the blue light used to activate channelrhodopsin (480 nm) is lost 1 mm away from the fiber optic (2012). Increasing light wavelength could allow larger volume of tissue being activated, hence the interest in red-shifted opsins (Chuong et al., 2014). It is therefore not surprising that the retina, being easily accessible to both gene delivery and light, is a promising target for translational optogenetics (Busskamp et al., 2010). Moreover, since most experiments involving non-human primates are chronic, tissue damage from devices insertion and heat is also another major concern, requiring the development of specific tools (Han, 2012).

However, non-human and human optogenetics could benefit from the experience of chronically implanted electrophysiological devices. Combining optical and electrophysiological devices would indeed allow closed-loop neuromodulation, i.e. simultaneous electrical recording and optical stimulation of neuronal activity (Laxpati et al., 2014). To this end, high-density microelectrode arrays incorporating integrated fiber optics, or “optrodes”, could be chronically implanted for chronic closed-loop neuromodulation (Buzsáki et al., 2015).

Genetically targeted neuroablation for high-grade gliomas has been achieved in animal models and clinical trials using the “suicide gene therapy” strategy. It relies on the introduction in the tumor cells genome of an exogenous gene encoding an enzyme capable of converting a non-toxic prodrug into a lethal molecule. Systemic administration of this non-toxic prodrug therefore induces cell death selectively in transduced tumors cells (Kane et al., 2015). Two main systems have been used for suicide gene therapy in HGG: the herpes simplex virus type 1 thymidine kinase / ganciclovir (HSV-tk / GCV) system and the cytosine deaminase / 5-fluorocytosine (CD / 5-FC) system. In both systems, the non-toxic prodrug (GCV and 5-FC) is converted into a toxic compound (5-FU and GCV-3P respectively) by the genetically targeted enzyme (tk and CD) (Fischer et al., 2005). In addition to the direct toxicity, gene suicide therapy involves a so-called “bystander” effect in which toxicity is transferred from infected cells to surrounding cells, thereby enhancing its efficiency. Several clinical trials tested the safety and efficiency of HSV-1/tk gene therapy in

HGG: in the largest randomized phase III trial, involving 248 with newly diagnosed glioblastoma, HSV-1/tk proved to be safe but did not lead to a significant difference in median survival nor tumor progression (Rainov, 2000). This disappointing result is attributed to the lack of efficiency in transfecting the tk gene into tumoral cells genome (Okura et al., 2014), emphasizing the need for improved delivery and transduction strategies in humans.

Another technique to achieve genetically targeted neuroablation in HGG is “oncolytic” gene therapy, which relies on the introduction of replication competent viral vectors having a lytic cycle, thereby selectively killing the host cells while spreading to adjacent cells. Selectivity to tumor cells in oncolytic gene therapy can be achieved by genetically engineering a HSV-1 mutant (G207) carrying a mutation in the gene (UL39) encoding an enzyme (ribonucleotide reductase, RR) that is required for viral replication and expressed in dividing cells only. Although, oncolytic G207 HSV-1 cannot replicate in non-dividing cells, mitotic glioma cells can provide cellular RR and rescue HSV-1 lytic replication. However, only 5 to 15% of glioma cells being in mitotic phase at a given moment, the majority of tumor cells can actually escape this strategy (Okura et al., 2014).

4. Two challenges for a paradigm shift

Genetically targeted techniques have revolutionized neurosciences over the last twenty years. Relying on genetic rather than spatial identification of neurons, selective expression of effectors to manipulate neuronal activity has proved to be a very powerful tool to dissect neuronal circuits. Tractable animal models, continuous innovation in genome editing and an always-expanding library of transgenic lines made genetic targeting a predominant approach in modern neurosciences.

Translating this genetic approach to neurosurgery would imply three key steps: 1) being able to genetically identify cells that are involved in neurological diseases; 2) achieve selective delivery and transduction of exogenous effector genes in this cell population; 3) deliver, without spatial selectivity, the appropriate stimulation to activate the transduced effector.

Therefore, genetic targeting can be considered as a paradigm shift for neurosurgery: selectivity is not in the surgeon's hands anymore but in the neurons DNA instead. Although GT neurosurgery would not be, of course, always appropriate, it could represent a more rational approach to diseases that are poorly spatially defined such as high-grade gliomas or basal ganglia disorders. However, to achieve in the clinics this transformation from spatial to genetic targeting, two important challenges must be overcome.

The first challenge is a technical one. At each key step involved in GT neurosurgery, techniques from basic sciences would need to be modified or even reinvented to fit a clinical application. For instance, gene delivery will need improved viral or non-viral vectors, gene insertion and transduction techniques will require very efficient and safe tools, stimulation hardware must be improved to deliver more energy for longer durations without injuring the brain, etc. But these are foremost technical issues. And the speed of technical innovation in basic neurosciences in recent years gives an optimistic indication in this regard.

The second challenge is a biological one. The core assumption of GT neurosurgery is the knowledge of a specific genetic entry point into diseases. This entry point is key to a selective expression of the effector by targeted cells, and therefore the efficiency of the approach. Recent genetic expression profiling studies have provided evidence for a number of mutations involved in pathogenic processes, but have also shed light on the genetic heterogeneity of most neurological diseases. Therefore, it is likely that there won't be a single genetic entry point into a given condition, but rather a combination of them for each patient.

The paradigm shift behind genetic targeting might actually lie in the fact that these two challenges are driving each other: technical innovations are driving genetic dissection of diseases; genetic identification of target cells is paving the way for new treatments.

Figures

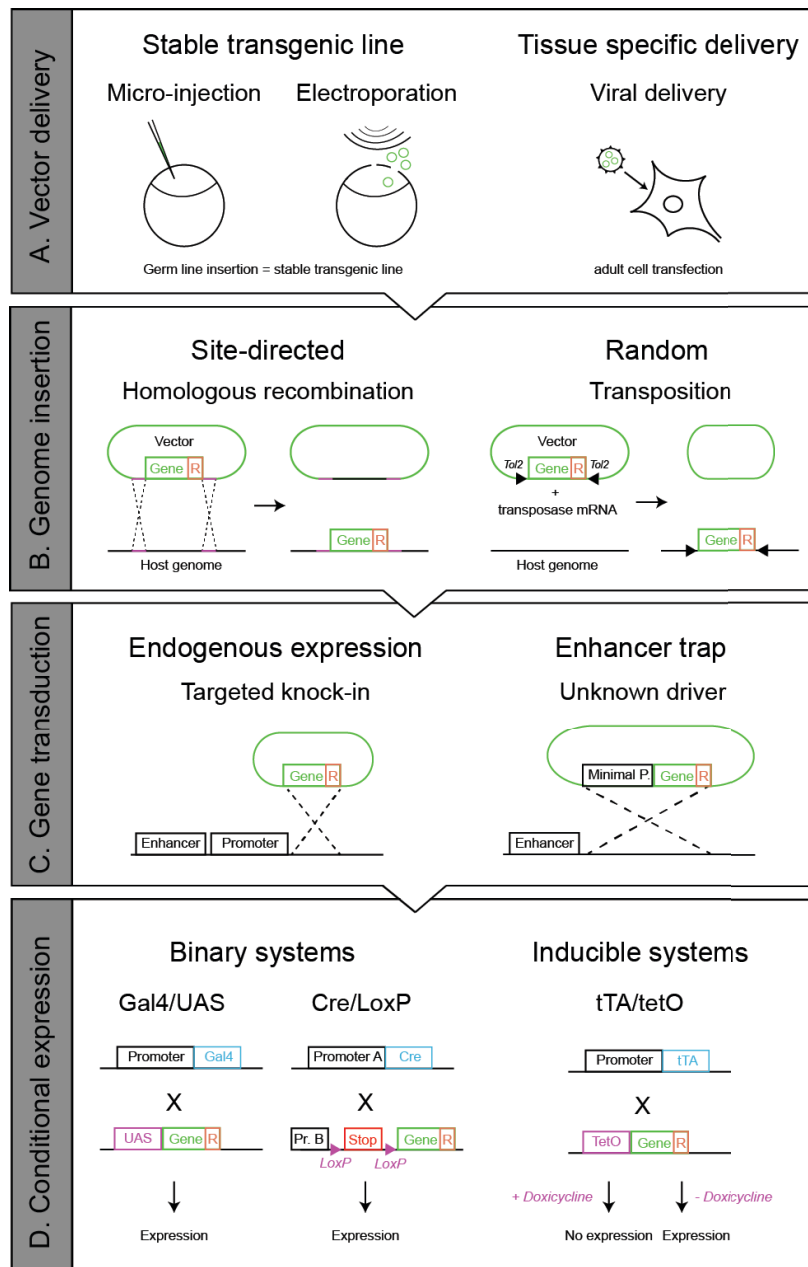


Figure 1. Genetic targeting of neurons in tractable animal models

A) In tractable animal models, such as zebrafish or mice, the vector carrying the exogenous gene can be delivered at embryonic stage to generate stable transgenic lines or using viral vector injection in targeted tissue. B) Insertion of the exogenous gene into the host genome can be achieved via homologous recombination if the targeted sequence is known or with random insertion with transposition. C) Gene transduction can rely on the control by an endogenous promoter (“targeted

knock-in”) or an unknown enhancer if the insertion was random (“enhancer trap”). D) Expression of the targeted gene can be restricted using condition expression systems such as the Gal4/UAS or the Cre/LoxP systems, and even induced by drug administration such as in the tTA/tetO system.

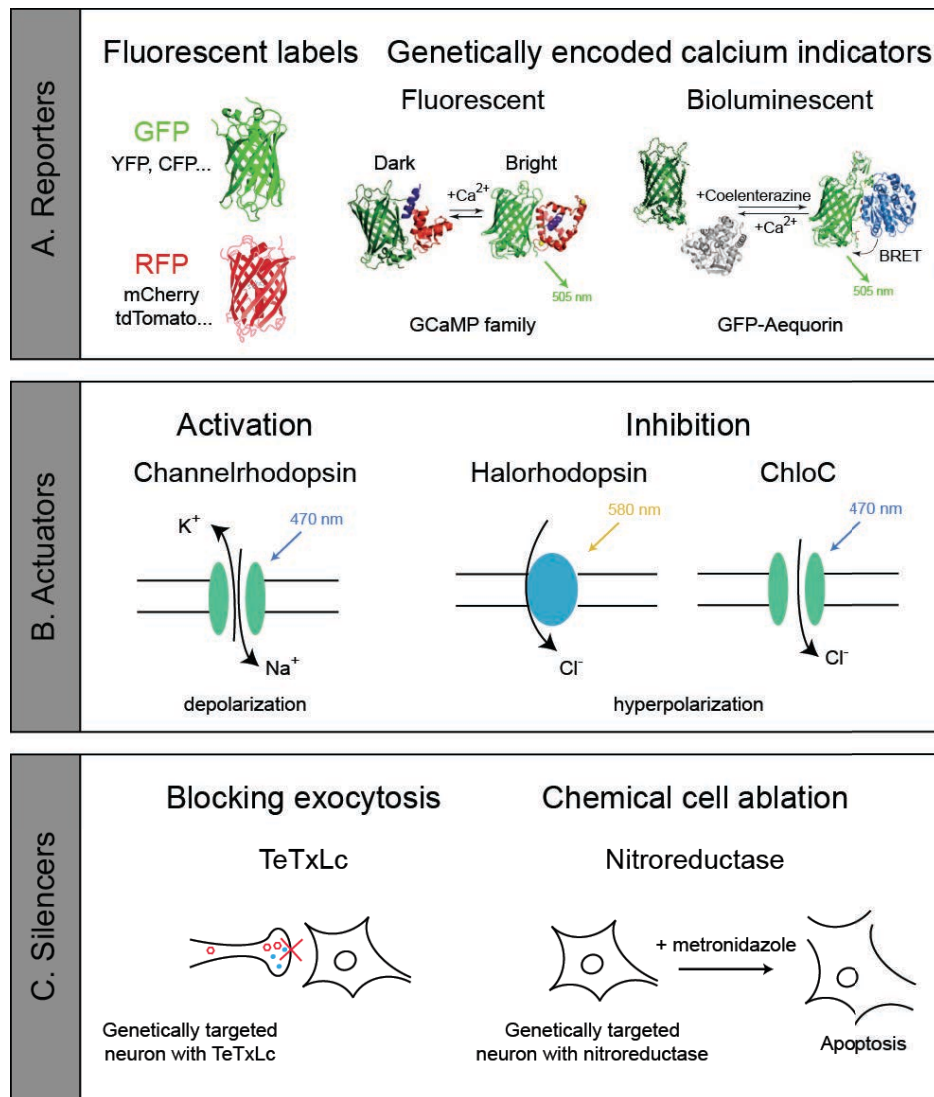


Figure 2. A toolbox for manipulating genetically identified neurons

A) Genetically targeted reporters allow fluorescent labeling of targeted cells using green or red fluorescent proteins and their variants. Neural activity can be monitored using genetically encoded calcium indicators (GECIs). Fluorescent GECIs, such as GCaMP, modify their fluorescence properties upon calcium binding, while bioluminescent GECIs, such as GFP-Aequorin, can transfer the energy upon oxidation of their substrate coelenterazine to an attached fluorescent protein in order to emit photons without the need for light excitation. B). Genetically targeted actuators are light-gated opsins that can dynamically activate (as with the cationic channel channelrhodopsin) or inhibit (as with the

chloride pump halorhodopsin) neurons in which they are expressed. C) Definitive neural silencing can also be achieved using vesicle release blockers, such as tetanus toxin light chain (TeTxLc), or chemically induced apoptosis with nitroreductase.

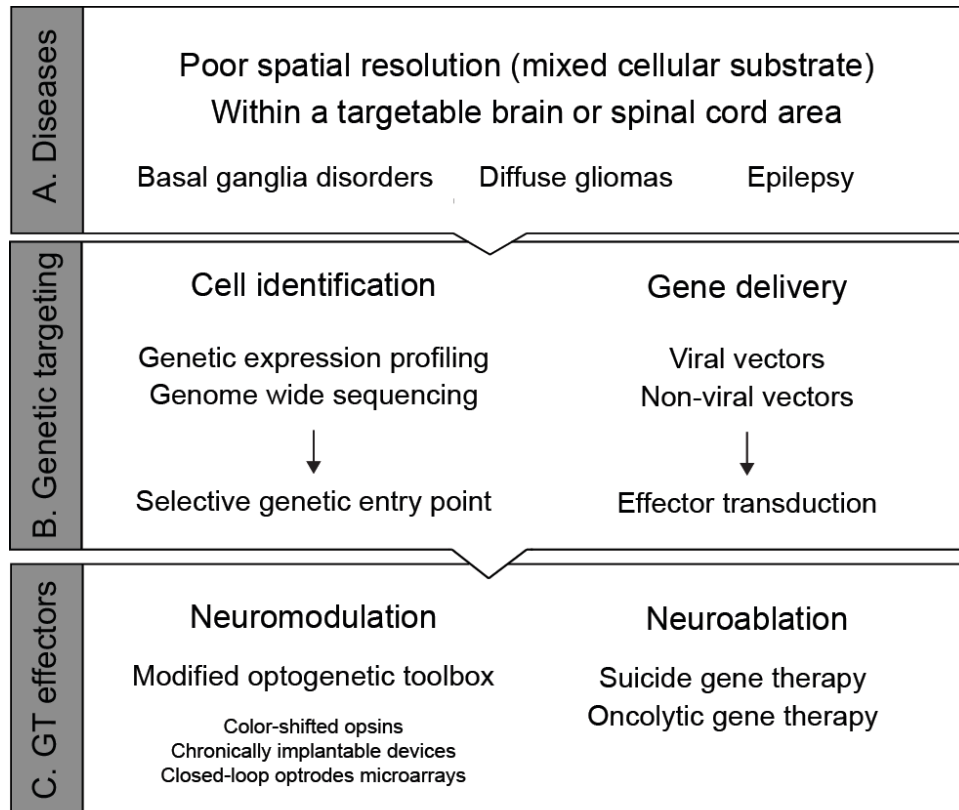


Figure 3. Moving toward genetically targeted neurosurgery

A) Ideal candidate diseases for genetically targeted neurosurgery involve a cellular substrate having a poor spatial resolution, e.g. the causative cells are mixed with healthy tissue, while still being in an individualized brain or spinal cord region. B) Genetic targeting faces a double challenge: being able to identify a genetic entry point that will be selective of the cell population of interest, and being able to deliver the vector into the host genome in order to achieve successful transduction. C) Genetically targeted effectors can achieve therapeutic results through either neuromodulation, using modified optogenetic tools, or neuroablation, using improved gene therapy techniques.

References

Abe, G., Suster, M.L., and Kawakami, K. (2011). Tol2-mediated Transgenesis, Gene Trapping, Enhancer Trapping, and the Gal4-UAS System (Elsevier Inc.).

Afraz, A., Boyden, E.S., and DiCarlo, J.J. (2015). Optogenetic and pharmacological suppression of spatial clusters of face neurons reveal their causal role in face gender discrimination. *Proceedings of the National Academy of Sciences* *112*, 6730–6735.

Ahrens, M.B., Li, J.M., Orger, M.B., Robson, D.N., Schier, A.F., Engert, F., and Portugues, R. (2012). Brain-wide neuronal dynamics during motor adaptation in zebrafish. *Nature* *485*, 471–477.

Akerboom, J., Chen, T.W., Wardill, T.J., Tian, L., Marvin, J.S., Mutlu, S., Calderon, N.C., Esposti, F., Borghuis, B.G., Sun, X.R., et al. (2012). Optimization of a GCaMP Calcium Indicator for Neural Activity Imaging. *J Neurosci* *32*, 13819–13840.

Akerboom, J., Carreras Calderón, N., Tian, L., Wabnig, S., Prigge, M., Tolö, J., Gordus, A., Orger, M.B., Severi, K.E., Macklin, J.J., et al. (2013). Genetically encoded calcium indicators for multi-color neural activity imaging and combination with optogenetics. *Front Mol Neurosci* *6*, 2.

Ampatzis, K., Song, J., Ausborn, J., and Manira, El, A. (2013). Pattern of Innervation and Recruitment of Different Classes of Motoneurons in Adult Zebrafish. *J Neurosci* *33*, 10875–10886.

Andersen, R.A., Essick, G.K., and Siegel, R.M. (1985). Encoding of spatial location by posterior parietal neurons. *Science* *230*, 456–458.

Arrenberg, A.B., Del Bene, F., and Baier, H. (2009). Optical control of zebrafish behavior with halorhodopsin. *Proceedings of the National Academy of Sciences* *106*, 17968–17973.

Asakawa, K., and Kawakami, K. (2009). The Tol2-mediated Gal4-UAS method for gene and enhancer trapping in zebrafish. *Methods* *49*, 275–281.

Asakawa, K., Abe, G., and Kawakami, K. (2013). Cellular dissection of the spinal cord motor column by BAC transgenesis and gene trapping in zebrafish. *Front. Neural Circuits* *7*, 100.

Asakawa, K., Suster, M.L., Mizusawa, K., Nagayoshi, S., Kotani, T., Urasaki, A., Kishimoto, Y., Hibi, M., and Kawakami, K. (2008). Genetic dissection of neural circuits by Tol2 transposon-mediated Gal4 gene and enhancer trapping in zebrafish. *Proc Natl Acad Sci USA* *105*, 1255–1260.

Auer, T.O., Xiao, T., Bercier, V., Gebhardt, C., Duroure, K., Concordet, J.-P., Wyart, C., Suster, M., Kawakami, K., Wittbrodt, J., et al. (2015). Deletion of a kinesin I motor unmasks a mechanism of homeostatic branching control by neurotrophin-3. *Elife* *4*.

Baek, J.-H., Cosman, P., Feng, Z., Silver, J., and Schafer, W.R. (2002). Using machine vision to analyze and classify *Caenorhabditis elegans* behavioral phenotypes quantitatively. *Journal of Neuroscience Methods* 118, 9–21.

Bagnall, M.W., and McLean, D.L. (2014). Modular organization of axial microcircuits in zebrafish. *Science* 343, 197–200.

Bakayan, A., Vaquero, C.F., Picazo, F., and Llopis, J. (2011). Red Fluorescent Protein-Aequorin Fusions as Improved Bioluminescent Ca²⁺ Reporters in Single Cells and Mice. *PLoS ONE* 6, e19520.

Bannatyne, B.A., Liu, T.T., Hammar, I., Stecina, K., Jankowska, E., and Maxwell, D.J. (2009). Excitatory and inhibitory intermediate zone interneurons in pathways from feline group I and II afferents: differences in axonal projections and input. *J. Physiol. (Lond.)* 587, 379–399.

Barrière, G., Leblond, H., Provencher, J., and Rossignol, S. (2008). Prominent Role of the Spinal Central Pattern Generator in the Recovery of Locomotion after Partial Spinal Cord Injuries. *J Neurosci* 28, 3976–3987.

Baubet, V.V., Le Mouellic, H.H., Campbell, A.K.A., Lucas-Meunier, E.E., Fossier, P.P., and Brûlet, P.P. (2000). Chimeric green fluorescent protein-aequorin as bioluminescent Ca²⁺ reporters at the single-cell level. *Proc Natl Acad Sci USA* 97, 7260–7265.

Bhatt, D.H., Mclean, D.L., Hale, M.E., and Fetcho, J.R. (2007). Grading movement strength by changes in firing intensity versus recruitment of spinal interneurons. *Neuron* 53, 91–102.

Bhatt, D.H., Otto, S.J., Depoister, B., and Fetcho, J.R. (2004). Cyclic AMP-induced repair of zebrafish spinal circuits. *Science* 305, 254–258.

Bican, O., Minagar, A., and Pruitt, A.A. (2013). The spinal cord: a review of functional neuroanatomy. *Neurol Clin* 31, 1–18.

Blitz, D.M., and Nusbaum, M.P. (2011). Neural circuit flexibility in a small sensorimotor system. *Current Opinion in Neurobiology* 21, 544–552.

Blumhagen, F., Zhu, P., Shum, J., Schärer, Y.-P.Z., Yaksi, E., Deisseroth, K., and Friedrich, R.W. (2012). Neuronal filtering of multiplexed odour representations. *Nature* 479, 493–498.

Bonnot, A., Whelan, P.J., Mentis, G.Z., and O'Donovan, M.J. (2002). Locomotor-like activity generated by the neonatal mouse spinal cord. *Brain Res. Brain Res. Rev.* 40, 141–151.

Boussaoud, D., Barth, T.M., and Wise, S.P. (1993). Effects of gaze on apparent visual responses of frontal cortex neurons. *Exp Brain Res* 93, 423–434.

Boyden, E.S., Zhang, F., Bamberg, E., Nagel, G., and Deisseroth, K. (2005). Millisecond-timescale, genetically targeted optical control of neural activity. *Nat Neurosci* 8, 1263–1268.

- Brand, R.V.D., Heutschi, J., Barraud, Q., DiGiovanna, J., Bartholdi, K., Huerlimann, M., Friedli, L., Vollenweider, I., Moraud, E.M., Duis, S., et al. (2012). Restoring voluntary control of locomotion after paralyzing spinal cord injury. *Science* 336, 1182–1185.
- Branson, K., Robie, A.A., Bender, J., Pietro Perona, and Dickinson, M.H. (2009). High-throughput ethomics in large groups of *Drosophila*. *Nat Meth* 6, 451–457.
- Briggman, K.L., and Kristan, W.B. (2008). Multifunctional pattern-generating circuits. *Annu Rev Neurosci* 31, 271–294.
- Briggman, K.L., Abarbanel, H.D.I., and Kristan, W.B. (2006). From crawling to cognition: analyzing the dynamical interactions among populations of neurons. *Current Opinion in Neurobiology* 16, 135–144.
- Brown, T.G. (1911). The Intrinsic Factors in the Act of Progression in the Mammal. *Proceedings of the Royal Society B: Biological Sciences* 84, 308–319.
- Brustein, E., and Rossignol, S. (1998). Recovery of locomotion after ventral and ventrolateral spinal lesions in the cat. I. Deficits and adaptive mechanisms. *Journal of Neurophysiology* 80, 1245–1267.
- Budick, S.A., and O'Malley, D.M. (2000). Locomotor repertoire of the larval zebrafish: swimming, turning and prey capture. *J Exp Biol* 203, 2565–2579.
- Budick, S.A., and Dickinson, M.H. (2006). Free-flight responses of *Drosophila melanogaster* to attractive odors. *J Exp Biol* 209, 3001–3017.
- Bundschuh, S.T., Zhu, P., Schärer, Y.-P.Z., and Friedrich, R.W. (2012). Dopaminergic modulation of mitral cells and odor responses in the zebrafish olfactory bulb. *J Neurosci* 32, 6830–6840.
- Bussièrès, N., and Dubuc, R. (1992). Phasic modulation of transmission from vestibular inputs to reticulospinal neurons during fictive locomotion in lampreys. *Brain Res* 582, 147–153.
- Busskamp, V., Duebel, J., Balya, D., Fradot, M., Viney, T.J., Siebert, S., Groner, A.C., Cabuy, E., Forster, V., Seeliger, M., et al. (2010). Genetic reactivation of cone photoreceptors restores visual responses in retinitis pigmentosa. *Science* 329, 413–417.
- Buzsáki, G., Stark, E., Berényi, A., Khodagholy, D., Kipke, D.R., Yoon, E., and Wise, K.D. (2015). Tools for Probing Local Circuits: High-Density Silicon Probes Combined with Optogenetics. *Neuron* 86, 92–105.
- Cangiano, L. (2005). Mechanisms of Rhythm Generation in a Spinal Locomotor Network Deprived of Crossed Connections: The Lamprey Hemicord. *J Neurosci* 25, 923–935.
- Capecchi, M.R. (1989). Altering the genome by homologous recombination. *Science* 244, 1288–1292.

Card, G.M. (2012). Escape behaviors in insects. *Current Opinion in Neurobiology* 22, 180–186.

Carmena, J.M., Lebedev, M.A., Crist, R.E., O’Doherty, J.E., Santucci, D.M., Dimitrov, D.F., Patil, P.G., Henriquez, C.S., and Nicolelis, M.A.L. (2003). Learning to Control a Brain–Machine Interface for Reaching and Grasping by Primates. *Plos Biol* 1, e2.

Chen, T.-W., Wardill, T.J., Sun, Y., Pulver, S.R., Renninger, S.L., Baohan, A., Schreiter, E.R., Kerr, R.A., Orger, M.B., Jayaraman, V., et al. (2013). Ultrasensitive fluorescent proteins for imaging neuronal activity. *Nature* 499, 295–300.

Chow, B.Y., Han, X., Dobry, A.S., Qian, X., Chuong, A.S., Li, M., Henninger, M.A., Belfort, G.M., Lin, Y., Monahan, P.E., et al. (2010). High-performance genetically targetable optical neural silencing by light-driven proton pumps. *Nature* 463, 98–102.

Chuong, A.S., Miri, M.L., Busskamp, V., Matthews, G.A.C., Acker, L.C., Sørensen, A.T., Young, A., Klapoetke, N.C., Henninger, M.A., Kodandaramaiah, S.B., et al. (2014). Noninvasive optical inhibition with a red-shifted microbial rhodopsin. *Nat Neurosci*.

Clark, D.A., Freifeld, L., and Clandinin, T.R. (2013). Mapping and Cracking Sensorimotor Circuits in Genetic Model Organisms. *Neuron* 78, 583–595.

Conway, B.A., Hultborn, H., and Kiehn, O. (1987). Proprioceptive input resets central locomotor rhythm in the spinal cat. *Exp Brain Res* 68, 643–656.

Cooper-Knock, J., Kirby, J., Ferraiuolo, L., Heath, P.R., Rattray, M., and Shaw, P.J. (2012). Gene expression profiling in human neurodegenerative disease. *Nature Reviews Neurology* 8, 518–530.

Courtine, G., Gerasimenko, Y., Brand, R.V.D., Yew, A., Musienko, P., Zhong, H., Song, B., Ao, Y., Ichiyama, R.M., Lavrov, I., et al. (2009a). Transformation of nonfunctional spinal circuits into functional states after the loss of brain input. *Nat Neurosci* 12, 1333–1342.

Courtine, G., Gerasimenko, Y., Brand, R.V.D., Yew, A., Musienko, P., Zhong, H., Song, B., Ao, Y., Ichiyama, R.M., Lavrov, I., et al. (2009b). Transformation of nonfunctional spinal circuits into functional states after the loss of brain input. *Nat Neurosci* 12, 1333–1342.

Curado, S., Stainier, D.Y.R., and Anderson, R.M. (2008). Nitroreductase-mediated cell/tissue ablation in zebrafish: a spatially and temporally controlled ablation method with applications in developmental and regeneration studies. *Nature Protocols* 3, 948–954.

Currie, S.N. (1991). Vibration-evoked startle behavior in larval lampreys. *Brain Behav Evol* 37, 260–271.

Davison, J.M., Akitake, C.M., Goll, M.G., Rhee, J.M., Gosse, N., Baier, H., Halpern, M.E., Leach, S.D., and Parsons, M.J. (2007). Transactivation from Gal4-VP16

- transgenic insertions for tissue-specific cell labeling and ablation in zebrafish. *Developmental Biology* 304, 811–824.
- Del Bene, F., Wyart, C., Robles, E., Tran, A., Looger, L., Scott, E.K., Isacoff, E.Y., and Baier, H. (2010). Filtering of Visual Information in the Tectum by an Identified Neural Circuit. *Science* 330, 669–673.
- Del Bene, F., and Wyart, C. (2012). Optogenetics: a new enlightenment age for zebrafish neurobiology. *Devel Neurobio* 72, 404–414.
- Delcomyn, F. (1980). Neural basis of rhythmic behavior in animals. *Science* 210, 492–498.
- Di Prisco, G.V., Wallén, P., and Grillner, S. (1990). Synaptic effects of intraspinal stretch receptor neurons mediating movement-related feedback during locomotion. *Brain Res* 530, 161–166.
- Dickinson, M., and Moss, C.F. (2012). Neuroethology. *Current Opinion in Neurobiology* 22, 177–179.
- Diester, I., Kaufman, M.T., Mogri, M., Pashaie, R., Goo, W., Yizhar, O., Ramakrishnan, C., Deisseroth, K., and Shenoy, K.V. (2011). An optogenetic toolbox designed for primates. *Nat Neurosci* 1–13.
- Dombeck, D.A., and Reiser, M.B. (2012). Real neuroscience in virtual worlds. *Current Opinion in Neurobiology* 22, 3–10.
- Douglass, A.D.A., Kraves, S.S., Deisseroth, K.K., Schier, A.F.A., and Engert, F.F. (2008). Escape Behavior Elicited by Single, Channelrhodopsin-2-Evoked Spikes in Zebrafish Somatosensory Neurons. *Curr Biol* 18, 5–5.
- Drobac, E., Tricoire, L., Chaffotte, A.-F., Guiot, E., and Lambolez, B. (2010). Calcium imaging in single neurons from brain slices using bioluminescent reporters. *J Neurosci Res* 88, 695–711.
- Dubuc, R., Brocard, F., Antri, M., Fénelon, K., Gariépy, J.-F., Smetana, R., Ménard, A., Le Ray, D., Viana Di Prisco, G., Pearlstein, É., et al. (2008). Initiation of locomotion in lampreys. *Brain Research Reviews* 57, 172–182.
- Eaton, R.C., Bombardieri, R.A., and Meyer, D.L. (1977). The Mauthner-initiated startle response in teleost fish. *J Exp Biol* 66, 65–81.
- Eaton, R.C., Lee, R.K., and Foreman, M.B. (2001). The Mauthner cell and other identified neurons of the brainstem escape network of fish. *Prog Neurobiol* 63, 467–485.
- Eccles, J.C., Eccles, D.M., and Fatt, P. (1956). Pharmacological investigations on a central synapse operated by acetylcholine. *J Physiol* 131, 154–169.
- Eccles, J.C., Eccles, R.M., and Lundberg, A. (1957a). The convergence of monosynaptic excitatory afferents on to many different species of alpha motoneurons. *J Physiol* 137, 22–50.

- Eccles, J.C., Eccles, R.M., and Lundberg, A. (1957b). Synaptic actions on motoneurons caused by impulses in Golgi tendon organ afferents. *J Physiol* 138, 227–252.
- Eccles, R.M., and Lundberg, A. (1958). Significance of supraspinal control of reflex actions by impulses in muscle afferents. *Experientia* 14, 197–199.
- Edgerton, V.R., Courtine, G., Gerasimenko, Y.P., Lavrov, I., Ichiyama, R.M., Fong, A.J., Cai, L.L., Otoshi, C.K., Tillakaratne, N.J.K., Burdick, J.W., et al. (2008). Training locomotor networks. *Brain Research Reviews* 57, 241–254.
- Eidelberg, E., Walden, J.G., and Nguyen, L.H. (1981). Locomotor control in macaque monkeys. *Brain* 104, 647–663.
- Fetcho, J.R., and Mclean, D.L. (2010). Some principles of organization of spinal neurons underlying locomotion in zebrafish and their implications. *Annals of the New York Academy of Sciences* 1198, 94–104.
- Fetz, E.E., Jankowska, E., Johannisson, T., and Lipski, J. (1979). Autogenetic inhibition of motoneurons by impulses in group Ia muscle spindle afferents. *J Physiol* 293, 173–195.
- Fink, A.J.P., Croce, K.R., Huang, Z.J., Abbott, L.F., Jessell, T.M., and Azim, E. (2015). Presynaptic inhibition of spinal sensory feedback ensures smooth movement. *Nature* 508, 43–48.
- Fischer, U., Steffens, S., Frank, S., Rainov, N.G., Schulze-Osthoff, K., and Kramm, C.M. (2005). Mechanisms of thymidine kinase/ganciclovir and cytosine deaminase/5-fluorocytosine suicide gene therapy-induced cell death in glioma cells. *Oncogene* 24, 1231–1243.
- Flusberg, B.A., Nimmerjahn, A., Cocker, E.D., Mukamel, E.A., Barretto, R.P.J., Ko, T.H., Burns, L.D., Jung, J.C., and Schnitzer, M.J. (2008). High-speed, miniaturized fluorescence microscopy in freely moving mice. *Nat Meth* 5, 935–938.
- Frank, K., and Fuortes, M. (1959). Presynaptic and postsynaptic inhibition of monosynaptic reflexes. *Fed Proc* 16, 39–40.
- Franklin, D.W., and Wolpert, D.M. (2011). Computational Mechanisms of Sensorimotor Control. *Neuron* 72, 425–442.
- Fry, S.N., Rohrseitz, N., Straw, A.D., and Dickinson, M.H. (2008). TrackFly: Virtual reality for a behavioral system analysis in free-flying fruit flies. *Journal of Neuroscience Methods* 171, 110–117.
- Frye, M.A. (2010). Multisensory systems integration for high-performance motor control in flies. *Current Opinion in Neurobiology* 20, 347–352.
- Gabriel, J.P., Ausborn, J., Ampatzis, K., Mahmood, R., Eklöf-Ljunggren, E., and Manira, El, A. (2011). Principles governing recruitment of motoneurons during

swimming in zebrafish. *Nature Publishing Group 14*, 93–99.

Gao, X.J., Potter, C.J., Gohl, D.M., Silies, M., Katsov, A.Y., Clandinin, T.R., and Luo, L. (2013). Specific kinematics and motor-related neurons for aversive chemotaxis in *Drosophila*. *Curr Biol 23*, 1163–1172.

Garcia-Rill, E., Kinjo, N., Atsuta, Y., Ishikawa, Y., Webber, M., and Skinner, R.D. (1990). Posterior midbrain-induced locomotion. *Brain Research Bulletin 24*, 499–508.

Ghazanfar, A.A., and Schroeder, C.E. (2006). Is neocortex essentially multisensory? *Trends Cogn. Sci. (Regul. Ed.) 10*, 278–285.

Ghysen, A.A., and Dambly-Chaudière, C.C. (2007). The lateral line microcosmos. *Genes Dev 21*, 2118–2130.

Gorostiza, P., Volgraf, M., Numano, R., Szobota, S., Trauner, D., and Isacoff, E.Y. (2007). Mechanisms of photoswitch conjugation and light activation of an ionotropic glutamate receptor. *Proc Natl Acad Sci USA 104*, 10865–10870.

Gosgnach, S., Lanuza, G.M., Butt, S.J.B., Saueressig, H., Zhang, Y., Velasquez, T., Riethmacher, D., Callaway, E.M., Kiehn, O., and Goulding, M. (2006). V1 spinal neurons regulate the speed of vertebrate locomotor outputs. *Nature 440*, 215–219.

Gossen, M., and Bujard, H. (1992). Tight control of gene expression in mammalian cells by tetracycline-responsive promoters. *Proc Natl Acad Sci USA 89*, 5547–5551.

Goulding, M. (2009). Circuits controlling vertebrate locomotion: moving in a new direction. *Nat Rev Neurosci 10*, 507–518.

Gradinaru, V., Mogri, M., Thompson, K.R., Henderson, J.M., and Deisseroth, K. (2009). Optical deconstruction of parkinsonian neural circuitry. *Science 324*, 354–359.

Gradinaru, V., Thompson, K.R., and Deisseroth, K. (2008). eNpHR: a *Natronomonas* halorhodopsin enhanced for optogenetic applications. *Brain Cell Bio 36*, 129–139.

Granato, M., van Eeden, F.J., Schach, U., Trowe, T., Brand, M., Furutani-Seiki, M., Haffter, P., Hammerschmidt, M., Heisenberg, C.P., Jiang, Y.J., et al. (1996). Genes controlling and mediating locomotion behavior of the zebrafish embryo and larva. *Development 123*, 399–413.

Green, A.M., and Angelaki, D.E. (2010). Multisensory integration: resolving sensory ambiguities to build novel representations. *Current Opinion in Neurobiology 20*, 353–360.

Grienberger, C., and Konnerth, A. (2012). Imaging Calcium in Neurons. *Neuron 73*, 862–885.

Grillner, S., and Rossignol, S. (1978). On the initiation of the swing phase of locomotion in chronic spinal cats. *Brain Res 146*, 269–277.

Grillner, S., Williams, T., and Lagerbäck, P.A. (1984). The edge cell, a possible

intraspinal mechanoreceptor. *Science* 223, 500–503.

Grillner, S. (2003). The motor infrastructure: from ion channels to neuronal networks. *Nat Rev Neurosci* 4, 573–586.

Grillner, S., Manira, El, A., Kiehn, O., Rossignol, S., and S G Stein, P. (2008). Networks in Motion. *Brain Research Reviews* 57, 1.

Guertin, P., Angel, M.J., Perreault, M.C., and McCrea, D.A. (1995). Ankle extensor group I afferents excite extensors throughout the hindlimb during fictive locomotion in the cat. *J Physiol* 487 (Pt 1), 197–209.

Guertin, P.A. (2013). Central pattern generator for locomotion: anatomical, physiological, and pathophysiological considerations. 1–15.

Hale, M.E.M., Ritter, D.A.D., and Fetcho, J.R.J. (2001). A confocal study of spinal interneurons in living larval zebrafish. *J Comp Neurol* 437, 1–16.

Han, X. (2012). Optogenetics in the nonhuman primate. In *Optogenetics: Tools for Controlling and Monitoring Neuronal Activity*, (Elsevier), pp. 215–233.

Harkema, S., Gerasimenko, Y., Hodes, J., Burdick, J., Angeli, C., Chen, Y., Ferreira, C., Willhite, A., Rejc, E., Grossman, R.G., et al. (2011). Effect of epidural stimulation of the lumbosacral spinal cord on voluntary movement, standing, and assisted stepping after motor complete paraplegia: a case study. *Lancet* 377, 1938–1947.

Harvey, C.D., Collman, F., Dombeck, D.A., and Tank, D.W. (2010). Intracellular dynamics of hippocampal place cells during virtual navigation. *Nature* 461, 941–946.

Hastings, J.W., Mitchell, G., Mattingly, P.H., Blinks, J.R., and Van Leeuwen, M. (1969). Response of aequorin bioluminescence to rapid changes in calcium concentration. *Nature* 222, 1047–1050.

Häggglund, M., Borgius, L., Dougherty, K.J., and Kiehn, O. (2010). Activation of groups of excitatory neurons in the mammalian spinal cord or hindbrain evokes locomotion. *Nat Neurosci* 13, 246–252.

Higashijima, S., Hotta, Y., and Okamoto, H. (2000). Visualization of cranial motor neurons in live transgenic zebrafish expressing green fluorescent protein under the control of the islet-1 promoter/enhancer. *J Neurosci* 20, 206–218.

Higashijima, S.-I., Masino, M.A., Mandel, G., and Fetcho, J.R. (2003). Imaging neuronal activity during zebrafish behavior with a genetically encoded calcium indicator. *Journal of Neurophysiology* 90, 3986–3997.

Higashijima, S.-I., Masino, M.A., Mandel, G., and Fetcho, J.R. (2004). Engrailed-1 expression marks a primitive class of inhibitory spinal interneuron. *J Neurosci* 24, 5827–5839.

Huang, Z.J., and Zeng, H. (2013). Genetic approaches to neural circuits in the mouse. *Annu Rev Neurosci* 36, 183–215.

- Hultborn, H. (1972). Convergence on interneurons in the reciprocal Ia inhibitory pathway to motoneurons. *Acta Physiol Scand Suppl* 375, 1–42.
- Hultborn, H. (2006). Spinal reflexes, mechanisms and concepts: From Eccles to Lundberg and beyond. *Prog Neurobiol* 78, 215–232.
- Issa, F.A.F., O'Brien, G.G., Kettunen, P.P., Sagasti, A.A., Glanzman, D.L.D., and Papazian, D.M.D. (2011). Neural circuit activity in freely behaving zebrafish (*Danio rerio*). *J Exp Biol* 214, 1028–1038.
- Jalalvand, E., Robertson, B., Wallén, P., Hill, R.H., and Grillner, S. (2014). Laterally projecting cerebrospinal fluid-contacting cells in the lamprey spinal cord are of two distinct types. *J Comp Neurol*.
- Jankowska, E. (1992). Interneuronal relay in spinal pathways from proprioceptors. *Prog Neurobiol* 38, 335–378.
- Jankowska, E., and Edgley, S.A. (2010). Functional subdivision of feline spinal interneurons in reflex pathways from group Ib and II muscle afferents; an update. *European Journal of Neuroscience* 32, 881–893.
- Jiang, W., and Drew, T. (1996). Effects of bilateral lesions of the dorsolateral funiculi and dorsal columns at the level of the low thoracic spinal cord on the control of locomotion in the adult cat. I. Treadmill walking. *Journal of Neurophysiology* 76, 849–866.
- Jordan, L.M., Liu, J., Hedlund, P.B., Akay, T., and Pearson, K.G. (2008a). Descending command systems for the initiation of locomotion in mammals. *Brain Research Reviews* 57, 183–191.
- Jordan, L.M., Liu, J., Hedlund, P.B., Akay, T., and Pearson, K.G. (2008b). Descending command systems for the initiation of locomotion in mammals. *Brain Research Reviews* 57, 183–191.
- Kane, J.R., Miska, J., Young, J.S., Kanojia, D., Kim, J.W., and Lesniak, M.S. (2015). Sui generis: gene therapy and delivery systems for the treatment of glioblastoma. *Neuro-Oncology* 17 Suppl 2, ii24–ii36.
- Kato, M. (1987). Motoneuronal activity of cat lumbar spinal cord following separation from descending or contralateral impulses. *Cent Nerv Syst Trauma* 4, 239–248.
- Kawakami, K., Shima, A., and Kawakami, N. (2000). Identification of a functional transposase of the Tol2 element, an Ac-like element from the Japanese medaka fish, and its transposition in the zebrafish germ lineage. *Proc Natl Acad Sci USA* 97, 11403–11408.
- Kiehn, O. (2006). Locomotor circuits in the mammalian spinal cord. *Annu Rev Neurosci* 29, 279–306.
- Kiehn, O. (2011). Development and functional organization of spinal locomotor circuits. *Current Opinion in Neurobiology* 21, 100–109.

- Kiehn, O., Quinlan, K.A., Restrepo, C.E., Lundfald, L., Borgius, L., Talpalar, A.E., and Endo, T. (2008). Excitatory components of the mammalian locomotor CPG. *Brain Research Reviews* 57, 56–63.
- Kimmel, C.B., Warga, R.M., and Kane, D.A. (1994). Cell cycles and clonal strings during formation of the zebrafish central nervous system. *Development* 120, 265–276.
- Kimura, Y. (2006). *alx*, a Zebrafish Homolog of Chx10, Marks Ipsilateral Descending Excitatory Interneurons That Participate in the Regulation of Spinal Locomotor Circuits. *J Neurosci* 26, 5684–5697.
- Kimura, Y., Satou, C., Fujioka, S., Shoji, W., Umeda, K., Ishizuka, T., Yawo, H., and Higashijima, S.-I. (2013). Hindbrain V2a Neurons in the Excitation of Spinal Locomotor Circuits during Zebrafish Swimming. *Current Biology* 23, 843–849.
- Klapoetke, N.C., Murata, Y., Kim, S.S., Pulver, S.R., Birdsey-Benson, A., Cho, Y.K., Morimoto, T.K., Chuong, A.S., Carpenter, E.J., Tian, Z., et al. (2014). Independent optical excitation of distinct neural populations. *Nat Meth* 11, 338–346.
- Knikou, M. (2008). The H-reflex as a probe: Pathways and pitfalls. *Journal of Neuroscience Methods* 171, 1–12.
- Knogler, L.D., and Drapeau, P. (2014). Sensory gating of an embryonic zebrafish interneuron during spontaneous motor behaviors. *Front. Neural Circuits* 1–36.
- Kohashi, T., and Oda, Y. (2008). Initiation of Mauthner- or non-Mauthner-mediated fast escape evoked by different modes of sensory input. *J Neurosci* 28, 10641–10653.
- Kohashi, T.T., Nakata, N.N., and Oda, Y.Y. (2012). Effective sensory modality activating an escape triggering neuron switches during early development in zebrafish. *J Neurosci* 32, 5810–5820.
- Korn, H., and Faber, D.S. (2005). The Mauthner Cell Half a Century Later: A Neurobiological Model for Decision-Making? *Neuron* 47, 13–28.
- Koster, R.W., and Fraser, S.E. (2001). Tracing transgene expression in living zebrafish embryos. *Developmental Biology* 233, 329–346.
- Körding, K.P., and Wolpert, D.M. (2004). Bayesian integration in sensorimotor learning. *Nature* 427, 244–247.
- Körding, K.P., and Wolpert, D.M. (2006). Bayesian decision theory in sensorimotor control. *Trends Cogn. Sci. (Regul. Ed.)* 10, 319–326.
- Kravitz, A.V., Freeze, B.S., Parker, P.R.L., Kay, K., Thwin, M.T., Deisseroth, K., and Kreitzer, A.C. (2010). Regulation of parkinsonian motor behaviours by optogenetic control of basal ganglia circuitry. *Nature* 466, 622–626.
- Kyriakatos, A.A., Mahmood, R.R., Ausborn, J.J., Porres, C.P.C., Büschges, A.A., and Manira, El, A.A. (2011). Initiation of locomotion in adult zebrafish. *J Neurosci* 31, 8422–8431.

- Lanuza, G.M., Gosgnach, S., Pierani, A., Jessell, T.M., and Goulding, M. (2004). Genetic identification of spinal interneurons that coordinate left-right locomotor activity necessary for walking movements. *Neuron* 42, 375–386.
- Latorre, R., Levi, R., and Varona, P. (2013). Transformation of Context-dependent Sensory Dynamics into Motor Behavior. *PLOS Computational Biology*.
- Lavrov, I., Courtine, G., Dy, C.J., Brand, R.V.D., Fong, A.J., Gerasimenko, Y., Zhong, H., Roy, R.R., and Edgerton, V.R. (2008). Facilitation of stepping with epidural stimulation in spinal rats: role of sensory input. *J Neurosci* 28, 7774–7780.
- Laxpati, N.G., Mahmoudi, B., Gutekunst, C.-A., Newman, J.P., Zeller-Townson, R., and Gross, R.E. (2014). Real-time in vivo optogenetic neuromodulation and multielectrode electrophysiologic recording with NeuroRighter. *Front. Neuroeng.* 7, 40.
- Levitz, J., Pantoja, C., Gaub, B., Janovjak, H., Reiner, A., Hoagland, A., Schoppik, D., Kane, B., Stawski, P., Schier, A.F., et al. (2013). Optical control of metabotropic glutamate receptors. *Nat Neurosci* 16, 507–516.
- Lewis, K.E., and Eisen, J.S. (2003). From cells to circuits: development of the zebrafish spinal cord. *Prog Neurobiol* 69, 419–449.
- Li, W.-C., Soffe, S.R., and Roberts, A. (2002). Spinal inhibitory neurons that modulate cutaneous sensory pathways during locomotion in a simple vertebrate. *J Neurosci* 22, 10924–10934.
- Li, W.-C., Soffe, S.R., and Roberts, A. (2004). Dorsal spinal interneurons forming a primitive, cutaneous sensory pathway. *Journal of Neurophysiology* 92, 895–904.
- Li, W.-C.W., Roberts, A.A., and Soffe, S.R.S. (2010). Specific brainstem neurons switch each other into pacemaker mode to drive movement by activating NMDA receptors. *J Neurosci* 30, 16609–16620.
- Li, X., Gutierrez, D.V., Hanson, M.G., Han, J., Mark, M.D., Chiel, H., Hegemann, P., Landmesser, L.T., and Herlitze, S. (2005). Fast noninvasive activation and inhibition of neural and network activity by vertebrate rhodopsin and green algae channelrhodopsin. *Proc Natl Acad Sci USA* 102, 17816–17821.
- Liao, J.C., and Fetcho, J.R. (2008). Shared versus Specialized Glycinergic Spinal Interneurons in Axial Motor Circuits of Larval Zebrafish. *J Neurosci* 28, 12982–12992.
- Liu, K.S., and Fetcho, J.R. (1999). Laser ablations reveal functional relationships of segmental hindbrain neurons in zebrafish. *Neuron* 23, 325–335.
- Liu, K.S., and Sternberg, P.W. (1994). Sensory regulation of male mating behavior in *Caenorhabditis elegans*. *Neuron* 14, 79–89.
- Loquet, G. (2013). Multisensory integration in non-human primates during a sensory-motor task. 1–15.

Lundberg, A. (1979). Multisensory control of spinal reflex pathways. *Prog Brain Res* 50, 11–28.

Mandel, S., Grunblatt, E., Riederer, P., Amariglio, N., Jacob-Hirsch, J., Rechavi, G., and Youdim, M.B.H. (2005). Gene expression profiling of sporadic Parkinson's disease substantia nigra pars compacta reveals impairment of ubiquitin-proteasome subunits, SKP1A, aldehyde dehydrogenase, and chaperone HSC-70. *Annals of the New York Academy of Sciences* 1053, 356–375.

Mao, P., Joshi, K., Li, J., Kim, S.-H., Li, P., Santana-Santos, L., Luthra, S., Chandran, U.R., Benos, P.V., Smith, L., et al. (2013). Mesenchymal glioma stem cells are maintained by activated glycolytic metabolism involving aldehyde dehydrogenase 1A3. *Proceedings of the National Academy of Sciences* 110, 8644–8649.

Marder, E. (2011). Variability, compensation, and modulation in neurons and circuits. *Proc Natl Acad Sci USA* 108, 15542–15548.

Marder, E. (2012). Neuromodulation of Neuronal Circuits: Back to the Future. *Neuron* 76, 1–11.

Marder, E., and Taylor, A.L. (2011). Multiple models to capture the variability in biological neurons and networks. *Nat Neurosci* 14, 133–138.

Martial, F.P., and Hartell, N.A. (2012). Programmable Illumination and High-Speed, Multi-Wavelength, Confocal Microscopy Using a Digital Micromirror. *PLoS ONE* 7, e43942.

Martin, J.-R., Rogers, K.L., Chagneau, C., and Brûlet, P. (2007). In vivo Bioluminescence Imaging of Ca²⁺ Signalling in the Brain of *Drosophila*. *PLoS ONE* 2, e275.

Martinez, M., Delivet-Mongrain, H., Leblond, H., and Rossignol, S. (2012). Incomplete spinal cord injury promotes durable functional changes within the spinal locomotor circuitry. *Journal of Neurophysiology* 108, 124–134.

Martinez, M., and Rossignol, S. (2013). A dual spinal cord lesion paradigm to study spinal locomotor plasticity in the cat. *Annals of the New York Academy of Sciences* 1279, 127–134.

Masino, M.A., and Fetcho, J.R. (2005). Fictive swimming motor patterns in wild type and mutant larval zebrafish. *Journal of Neurophysiology* 93, 3177–3188.

Masland, R.H. (2004). Neuronal cell types. *Current Biology* 14, R497–R500.

McClellan, A.D., and Grillner, S. (1984). Activation of “fictive swimming” by electrical microstimulation of brainstem locomotor regions in an in vitro preparation of the lamprey central nervous system. *Brain Res* 300, 357–361.

McCrea, D.A. (2001). Spinal circuitry of sensorimotor control of locomotion. *J Physiol* 533, 41–50.

McCrea, D.A., Pratt, C.A., and Jordan, L.M. (1980). Renshaw cell activity and

- recurrent effects on motoneurons during fictive locomotion. *Journal of Neurophysiology* 44, 475–488.
- Mclean, D.L., Fan, J., Higashijima, S.-I., Hale, M.E., and Fetcho, J.R. (2007). A topographic map of recruitment in spinal cord. *Nature* 446, 71–75.
- Mclean, D.L., Masino, M.A., Koh, I.Y.Y., Lindquist, W.B., and Fetcho, J.R. (2008). Continuous shifts in the active set of spinal interneurons during changes in locomotor speed. *Nat Neurosci* 11, 1419–1429.
- Miesenböck, G. (2009). The optogenetic catechism. *Science* 326, 395–399.
- Mirat, O., Sternberg, J.R., and Severi, K.E. (2013). ZebraZoom: an automated program for high-throughput behavioral analysis and categorization. *Frontiers in Neural ...*
- Miyawaki, A., Llopis, J., Heim, R., McCaffery, J.M., Adams, J.A., Ikura, M., and Tsien, R.Y. (1997). Fluorescent indicators for Ca²⁺ based on green fluorescent proteins and calmodulin. *Nature* 388, 882–887.
- Moran-Rivard, L., Kagawa, T., Saueressig, H., Gross, M.K., Burrill, J., and Goulding, M. (2001). *Evx1* is a postmitotic determinant of v0 interneuron identity in the spinal cord. *Neuron* 29, 385–399.
- Musienko, P., Brand, R.V.D., Märzendorfer, O., Roy, R.R., Gerasimenko, Y., Edgerton, V.R., and Courtine, G. (2011). Controlling specific locomotor behaviors through multidimensional monoaminergic modulation of spinal circuitries. *J Neurosci* 31, 9264–9278.
- Muto, A., Ohkura, M., Kotani, T., Higashijima, S., Nakai, J., and Kawakami, K. (2011). Genetic visualization with an improved GCaMP calcium indicator reveals spatiotemporal activation of the spinal motor neurons in zebrafish. *Proc Natl Acad Sci USA* 108, 5425–5430.
- Nagai, T., Sawano, A., Park, E.S., and Miyawaki, A. (2001). Circularly permuted green fluorescent proteins engineered to sense Ca²⁺. *Proc Natl Acad Sci USA* 98, 3197–3202.
- Nagel, G., Szellas, T., Huhn, W., Kateriya, S., Adeishvili, N., Berthold, P., Ollig, D., Hegemann, P., and Bamberg, E. (2003). Channelrhodopsin-2, a directly light-gated cation-selective membrane channel. *Proc Natl Acad Sci USA* 100, 13940–13945.
- Nakai, J., Ohkura, M., and Imoto, K. (2001). A high signal-to-noise Ca(2+) probe composed of a single green fluorescent protein. *Nat Biotechnol* 19, 137–141.
- Nakano, I. (2015). Stem cell signature in glioblastoma: therapeutic development for a moving target. *J Neurosurg* 122, 324–330.
- Nakayama, H.H., and Oda, Y.Y. (2004). Common sensory inputs and differential excitability of segmentally homologous reticulospinal neurons in the hindbrain. *J Neurosci* 24, 3199–3209.

- Naumann, E.A., Kampff, A.R., Prober, D.A., Schier, A.F., and Engert, F. (2010). Monitoring neural activity with bioluminescence during natural behavior. *Nat Neurosci* 13, 513–520.
- O'Malley, D.M.D., Kao, Y.H.Y., and Fetcho, J.R.J. (1996). Imaging the functional organization of zebrafish hindbrain segments during escape behaviors. *Neuron* 17, 1145–1155.
- Okura, H., Smith, C.A., and Rutka, J.T. (2014). Gene therapy for malignant glioma. *Mol Cell Ther* 2, 21.
- Olszewski, J., Haehnel, M., Taguchi, M., and Liao, J.C. (2012). Zebrafish Larvae Exhibit Rheotaxis and Can Escape a Continuous Suction Source Using Their Lateral Line. *PLoS ONE* 7, e36661.
- Orger, M.B., Kampff, A.R., Severi, K.E., Bollmann, J.H., and Engert, F. (2008). Control of visually guided behavior by distinct populations of spinal projection neurons. *Nat Neurosci* 11, 327–333.
- Oron, D., Papagiakoumou, E., Anselmi, F., and Emiliani, V. (2012). Two-photon optogenetics. *Prog Brain Res* 196, 119–143.
- O'Doherty, J.E., Lebedev, M.A., Ifft, P.J., Zhuang, K.Z., Shokur, S., Bleuler, H., and Nicolelis, M.A.L. (2012). Active tactile exploration using a brain–machine–brain interface. *Nature* 479, 228–231.
- Palfi, S., Gurruchaga, J.M., Ralph, G.S., Lepetit, H., Lavis, S., Buttery, P.C., Watts, C., Miskin, J., Kelleher, M., Deeley, S., et al. (2014). Long-term safety and tolerability of ProSavin, a lentiviral vector-based gene therapy for Parkinson's disease: a dose escalation, open-label, phase 1/2 trial. *Lancet* 383, 1138–1146.
- Pallud, J., Varlet, P., Devaux, B., Geha, S., Badoual, M., Deroulers, C., Page, P., Dezamis, E., Daumas-Duport, C., and Roux, F.-X. (2010). Diffuse low-grade oligodendrogliomas extend beyond MRI-defined abnormalities. *Neurology* 74, 1724–1731.
- Papagiakoumou, E., Anselmi, F., Bègue, A., de Sars, V., Glückstad, J., Isacoff, E.Y., and Emiliani, V. (2010). Scanless two-photon excitation of channelrhodopsin-2. *Nat Meth* 7, 848–854.
- Phillips, H.S., Kharbanda, S., Chen, R., Forrest, W.F., Soriano, R.H., Wu, T.D., Misra, A., Nigro, J.M., Colman, H., Soroceanu, L., et al. (2006). Molecular subclasses of high-grade glioma predict prognosis, delineate a pattern of disease progression, and resemble stages in neurogenesis. *Cancer Cell* 9, 157–173.
- Pietri, T., Manalo, E., Ryan, J., Saint-Amant, L., and Washbourne, P. (2009). Glutamate drives the touch response through a rostral loop in the spinal cord of zebrafish embryos. *Devel Neurobio* 69, 780–795.
- Pirri, J.K., and Alkema, M.J. (2012). The neuroethology of *C. elegans* escape. *Current Opinion in Neurobiology* 22, 187–193.

- Portugues, R. (2011). Adaptive locomotor behavior in larval zebrafish. 1–11.
- Portugues, R., Severi, K.E., Wyart, C., and Ahrens, M.B. (2013). Optogenetics in a transparent animal: circuit function in the larval zebrafish. *Current Opinion in Neurobiology* 23, 119–126.
- Pouget, A., and Snyder, L.H. (2000). Computational approaches to sensorimotor transformations. *Nat Neurosci* 3 *Suppl*, 1192–1198.
- Pouget, A.A., Deneve, S.S., and Duhamel, J.-R.J. (2002). A computational perspective on the neural basis of multisensory spatial representations. *Nat Rev Neurosci* 3, 741–747.
- Quinlan, K.A., and Kiehn, O. (2007). Segmental, Synaptic Actions of Commissural Interneurons in the Mouse Spinal Cord. *J Neurosci* 27, 6521–6530.
- Rainov, N.G. (2000). A phase III clinical evaluation of herpes simplex virus type 1 thymidine kinase and ganciclovir gene therapy as an adjuvant to surgical resection and radiation in adults with previously untreated glioblastoma multiforme. *Human Gene Therapy* 11, 2389–2401.
- Renshaw, B. (1946). Central effects of centripetal impulses in axons of spinal ventral roots. *Journal of Neurophysiology* 9, 191–204.
- Reyes, R., Haendel, M., Grant, D., Melancon, E., and Eisen, J.S. (2003). Slow degeneration of zebrafish Rohon-Beard neurons during programmed cell death. *Dev Dyn* 229, 30–41.
- Riddick, G., and Fine, H.A. (2011). Integration and analysis of genome-scale data from gliomas. *Nature Reviews Neurology* 7, 439–450.
- Ritter, D.A., Bhatt, D.H., and Fetcho, J.R. (2001). In vivo imaging of zebrafish reveals differences in the spinal networks for escape and swimming movements. *J Neurosci* 21, 8956–8965.
- Roberts, A.A., Li, W.-C.W., and Soffe, S.R.S. (2009). How neurons generate behavior in a hatchling amphibian tadpole: an outline. *Front Behav Neurosci* 4, 16–16.
- Rogers, K.L., Picaud, S., Roncali, E., Boisgard, R., Colasante, C., Stinnakre, J., Tavitian, B., and Brûlet, P. (2007). Non-Invasive In Vivo Imaging of Calcium Signaling in Mice. *PLoS ONE* 2, e974.
- Rogers, K.L., Stinnakre, J., Agulhon, C., Jublot, D., Shorte, S.L., Kremer, E.J., and Brûlet, P. (2005). Visualization of local Ca²⁺ dynamics with genetically encoded bioluminescent reporters. *European Journal of Neuroscience* 21, 597–610.
- Rohrseitz, N., and Fry, S.N. (2010). Behavioural system identification of visual flight speed control in *Drosophila melanogaster*. *Journal of the Royal Society Interface* 8, 171–185.
- Rossi, M.A., Calakos, N., and Yin, H.H. (2015). Spotlight on movement disorders:

- What optogenetics has to offer. *Mov. Disord.* 30, 624–631.
- Rossignol, S. (1996). Visuomotor regulation of locomotion. *Can J Physiol Pharmacol* 74, 418–425.
- Rossignol, S., and Gauthier, L. (1980). An analysis of mechanisms controlling the reversal of crossed spinal reflexes. *Brain Res* 182, 31–45.
- Rossignol, S., and Frigon, A. (2011). Recovery of locomotion after spinal cord injury: some facts and mechanisms. *Annu Rev Neurosci* 34, 413–440.
- Rossignol, S., Dubuc, R., and Gossard, J.-P. (2006). Dynamic sensorimotor interactions in locomotion. *Physiol Rev* 86, 89–154.
- Rudomin, P., and Schmidt, R.F. (1999). Presynaptic inhibition in the vertebrate spinal cord revisited. *Exp Brain Res* 129, 1–37.
- Rudomin, P. (2009). In search of lost presynaptic inhibition. *Exp Brain Res* 196, 139–151.
- Sanai, N., and Berger, M.S. (2008). Glioma extent of resection and its impact on patient outcome. *Neurosurgery* 62, 753–64–discussion264–6.
- Sankrithi, N.S., and O'Malley, D.M. (2010). Activation of a multisensory, multifunctional nucleus in the zebrafish midbrain during diverse locomotor behaviors. *Neuroscience* 166, 970–993.
- Satou, C., Kimura, Y., Kohashi, T., Horikawa, K., Takeda, H., Oda, Y., and Higashijima, S.I. (2009). Functional Role of a Specialized Class of Spinal Commissural Inhibitory Neurons during Fast Escapes in Zebrafish. *J Neurosci* 29, 6780–6793.
- Satou, C., Kimura, Y., Hirata, H., Suster, M.L., Kawakami, K., and Higashijima, S.-I. (2013). Transgenic tools to characterize neuronal properties of discrete populations of zebrafish neurons. *Development* 140, 3927–3931.
- Schindelin, J., Arganda-Carreras, I., Frise, E., Kaynig, V., Longair, M., Pietzsch, T., Preibisch, S., Rueden, C., Saalfeld, S., Schmid, B., et al. (2012). Fiji: an open-source platform for biological-image analysis. *Nat Meth* 9, 676–682.
- Schobert, B., and Lanyi, J.K. (1982). Halorhodopsin is a light-driven chloride pump. *J Biol Chem* 257, 10306–10313.
- Schomburg, E.D., Petersen, N., Barajon, I., and Hultborn, H. (1998). Flexor reflex afferents reset the step cycle during fictive locomotion in the cat. *Exp Brain Res* 122, 339–350.
- Schoonheim, P.J., Arrenberg, A.B., Del Bene, F., and Baier, H. (2010). Optogenetic localization and genetic perturbation of saccade-generating neurons in zebrafish. *J Neurosci* 30, 7111–7120.
- Schredelseker, J., Di Biase, V., Obermair, G.J., Felder, E.T., Flucher, B.E., Franzini-

- Armstrong, C., and Grabner, M. (2005). The beta 1a subunit is essential for the assembly of dihydropyridine-receptor arrays in skeletal muscle. *Proc Natl Acad Sci USA* *102*, 17219–17224.
- Schroeder, C.E., and Foxe, J. (2005). Multisensory contributions to low-level, “unisensory” processing. *Current Opinion in Neurobiology* *15*, 454–458.
- Schuster, S. (2012). Fast-starts in hunting fish: decision-making in small networks of identified neurons. *Current Opinion in Neurobiology* *22*, 279–284.
- Scott, E.K. (2009). The Gal4/UAS toolbox in zebrafish: new approaches for defining behavioral circuits. *Journal of Neurochemistry* *110*, 441–456.
- Scott, E.K., Mason, L., Arrenberg, A.B., Ziv, L., Gosse, N.J., Xiao, T., Chi, N.C., Asakawa, K., Kawakami, K., and Baier, H. (2007). Targeting neural circuitry in zebrafish using GAL4 enhancer trapping. *Nat Meth* *4*, 323–326.
- Seelig, J.D., and Jayaraman, V. (2011). *Studying Sensorimotor Processing With Physiology in Behaving Drosophila* (Elsevier Inc.).
- Seelig, J.D., Chiappe, M.E., Lott, G.K., Dutta, A., Osborne, J.E., Reiser, M.B., and Jayaraman, V. (2010). Two-photon calcium imaging from head-fixed *Drosophila* during optomotor walking behavior. *Nat Meth* *7*, 535–540.
- Seruggia, D., and Montoliu, L. (2014). The new CRISPR-Cas system: RNA-guided genome engineering to efficiently produce any desired genetic alteration in animals. *Transgenic Res.* *23*, 707–716.
- Shik, M.L., Severin, F.V., and Orlovsky, G.N. (1969). Control of walking and running by means of electrical stimulation of the mesencephalon. *Electroencephalogr Clin Neurophysiol* *26*, 549.
- Shimomura, O., Johnson, F.H., and Saiga, Y. (1962a). Extraction, purification and properties of aequorin, a bioluminescent protein from the luminous hydromedusan, *Aequorea*. *J Cell Comp Physiol* *59*, 223–239.
- Shimomura, O., Johnson, F.H., and Saiga, Y. (1962b). Extraction, purification and properties of aequorin, a bioluminescent protein from the luminous hydromedusan, *Aequorea*. *J Cell Comp Physiol* *59*, 223–239.
- Siebert, S., Cabuy, E., Scherf, B.G., Kohler, H., Panda, S., Le, Y.-Z., Fehling, H.J., Gaidatzis, D., Stadler, M.B., and Roska, B. (2012). Transcriptional code and disease map for adult retinal cell types. *Nature Publishing Group* *15*, 487–95–S1–2.
- Sillar, K.T., Combes, D., Ramanathan, S., Molinari, M., and Simmers, J. (2008). Neuromodulation and developmental plasticity in the locomotor system of anuran amphibians during metamorphosis. *Brain Research Reviews* *57*, 94–102.
- Singh, S.K., Hawkins, C., Clarke, I.D., Squire, J.A., Bayani, J., Hide, T., Henkelman, R.M., Cusimano, M.D., and Dirks, P.B. (2004). Identification of human brain tumour initiating cells. *Nature* *432*, 396–401.

- Slimko, E.M., McKinney, S., Anderson, D.J., Davidson, N., and Lester, H.A. (2002). Selective electrical silencing of mammalian neurons in vitro by the use of invertebrate ligand-gated chloride channels. *J Neurosci* 22, 7373–7379.
- Suli, A., Watson, G.M., Rubel, E.W., and Raible, D.W. (2012). Rheotaxis in larval zebrafish is mediated by lateral line mechanosensory hair cells. *PLoS ONE* 7, e29727.
- Szabo, V., Ventalon, C., de Sars, V., Bradley, J., and Emiliani, V. (2014). Spatially Selective Holographic Photoactivation and Functional Fluorescence Imaging in Freely Behaving Mice with a Fiberscope. *Neuron* 84, 1157–1169.
- Szobota, S.S., Gorostiza, P.P., Del Bene, F.F., Wyart, C.C., Fortin, D.L.D., Kolstad, K.D.K., Tulyathan, O.O., Volgraf, M.M., Numano, R.R., Aaron, H.L.H., et al. (2007). Remote Control of Neuronal Activity with a Light-Gated Glutamate Receptor. *Neuron* 54, 11–11.
- Tabot, G.A., Dammann, J.F., and Berg, J.A. (2013). Restoring the sense of touch with a prosthetic hand through a brain interface.
- Talpalari, A.E., Bouvier, J., Borgius, L., Fortin, G., Pierani, A., and Kiehn, O. (2013). Dual-mode operation of neuronal networks involved in left-right alternation. *Nature* 500, 85–88.
- Tazerart, S., Vinay, L., and Brocard, F. (2008). The persistent sodium current generates pacemaker activities in the central pattern generator for locomotion and regulates the locomotor rhythm. *J Neurosci* 28, 8577–8589.
- Tian, L., Hires, S.A., Mao, T., Huber, D., Chiappe, M.E., Chalasani, S.H., Petreanu, L., Akerboom, J., McKinney, S.A., Schreiter, E.R., et al. (2009). Imaging neural activity in worms, flies and mice with improved GcamP calcium indicators. *Nat Meth* 6, 875–881.
- Tricoire, L., Tsuzuki, K., Courjean, O., Gibelin, N., Bourout, G., Rossier, J., and Lambolez, B. (2006). Calcium dependence of aequorin bioluminescence dissected by random mutagenesis. *Proc Natl Acad Sci USA* 103, 9500–9505.
- Trotter, Y., and Celebrini, S. (1999). Gaze direction controls response gain in primary visual-cortex neurons. *Nature* 398, 239–242.
- Verma, I.M., and Weitzman, M.D. (2005). Gene therapy: twenty-first century medicine. *Annu. Rev. Biochem.* 74, 711–738.
- Viana Di Prisco, G., Ohta, Y., Bongianni, F., Grillner, S., and Dubuc, R. (1995). Trigeminal inputs to reticulospinal neurones in lampreys are mediated by excitatory and inhibitory amino acids. *Brain Res* 695, 76–80.
- Wallén, P., and Williams, T.L. (1984). Fictive locomotion in the lamprey spinal cord in vitro compared with swimming in the intact and spinal animal. *J Physiol* 347, 225–239.
- Wannier, T., Deliagina, T.G., Orlovsky, G.N., and Grillner, S. (1998). Differential effects of the reticulospinal system on locomotion in lamprey. *Journal of*

Neurophysiology 80, 103–112.

Whelan, P.J. (1996). Control of locomotion in the decerebrate cat. *Prog Neurobiol* 49, 481–515.

Wietek, J., Wiegert, J.S., Adeishvili, N., Schneider, F., Watanabe, H., Tsunoda, S.P., Vogt, A., Elstner, M., Oertner, T.G., and Hegemann, P. (2014). Conversion of channelrhodopsin into a light-gated chloride channel. *Science* 344, 409–412.

Windhorst, U. (2007). Muscle proprioceptive feedback and spinal networks. *Brain Research Bulletin* 73, 155–202.

Wolpert, D.M. (2007). Probabilistic models in human sensorimotor control. *Human Movement Science* 26, 511–524.

Wyart, C., Del Bene, F., Warp, E., Scott, E.K., Trauner, D., Baier, H., and Isacoff, E.Y. (2009). Optogenetic dissection of a behavioural module in the vertebrate spinal cord. *Nature* 461, 407–410.

Ye, H., Morton, D.W., and Chiel, H.J. (2006). Neuromechanics of Multifunctionality during Rejection in *Aplysia californica*. *J Neurosci* 26, 10743–10755.

Yemini, E., Jucikas, T., Grundy, L.J., Brown, A.E.X., and Schafer, W.R. (2013). A database of *Caenorhabditis elegans* behavioral phenotypes. *Nat Meth* 10, 877–879.

Yin, H., Kanasty, R.L., Eltoukhy, A.A., Vegas, A.J., Dorkin, J.R., and Anderson, D.G. (2014). Non-viral vectors for gene-based therapy. *Nat Rev Genet* 15, 541–555.

Yokogawa, T., Marin, W., Faraco, J., Pézeron, G., Appelbaum, L., Zhang, J., Rosa, F., Mourrain, P., and Mignot, E. (2007). Characterization of sleep in zebrafish and insomnia in hypocretin receptor mutants. *Plos Biol* 5, e277.

Yordanova, Y.N., Moritz-Gasser, S., and Duffau, H. (2011). Awake surgery for WHO Grade II gliomas within "noneloquent" areas in the left dominant hemisphere: toward a "supratotal" resection. Clinical article. *J Neurosurg* 115, 232–239.

Zajac, F.E. (1989). Muscle and tendon: properties, models, scaling, and application to biomechanics and motor control. *Crit Rev Biomed Eng* 17, 359–411.

Zelenchuk, T.A., and Brusés, J.L. (2011). In vivo labeling of zebrafish motor neurons using an *mxn1* enhancer and Gal4/UAS. *Genesis* 49, 546–554.

Zhang, F., Aravanis, A.M., Adamantidis, A., de Lecea, L., and Deisseroth, K. (2007a). Circuit-breakers: optical technologies for probing neural signals and systems. *Nat Rev Neurosci* 8, 577–581.

Zhang, F., Wang, L.-P., Brauner, M., Liewald, J.F., Kay, K., Watzke, N., Wood, P.G., Bamberg, E., Nagel, G., Gottschalk, A., et al. (2007b). Multimodal fast optical interrogation of neural circuitry. *Nature* 446, 633–639.

Zhu, P., Narita, Y., Bundschuh, S.T., Fajardo, O., Schäfer, Y.-P.Z., Chattopadhyaya, B., Bouldoires, E.A., Stepien, A.E., Deisseroth, K., Arber, S., et al. (2009).

Optogenetic Dissection of Neuronal Circuits in Zebrafish using Viral Gene Transfer and the Tet System. *Front. Neural Circuits* 3, 21.

(2012). *Optogenetic Neuromodulation* (Elsevier Inc.).